Records from the Past, Lessons for the Future: What the Palaeorecord Implies about Mechanisms of Global Change

Sandy P. Harrison[a] and Pat Bartlein[b]

[a]*School of Biological Sciences, Macquarie University, Sydney, Australia,* [b]*Department of Geography, University of Oregon, Oregon, USA*
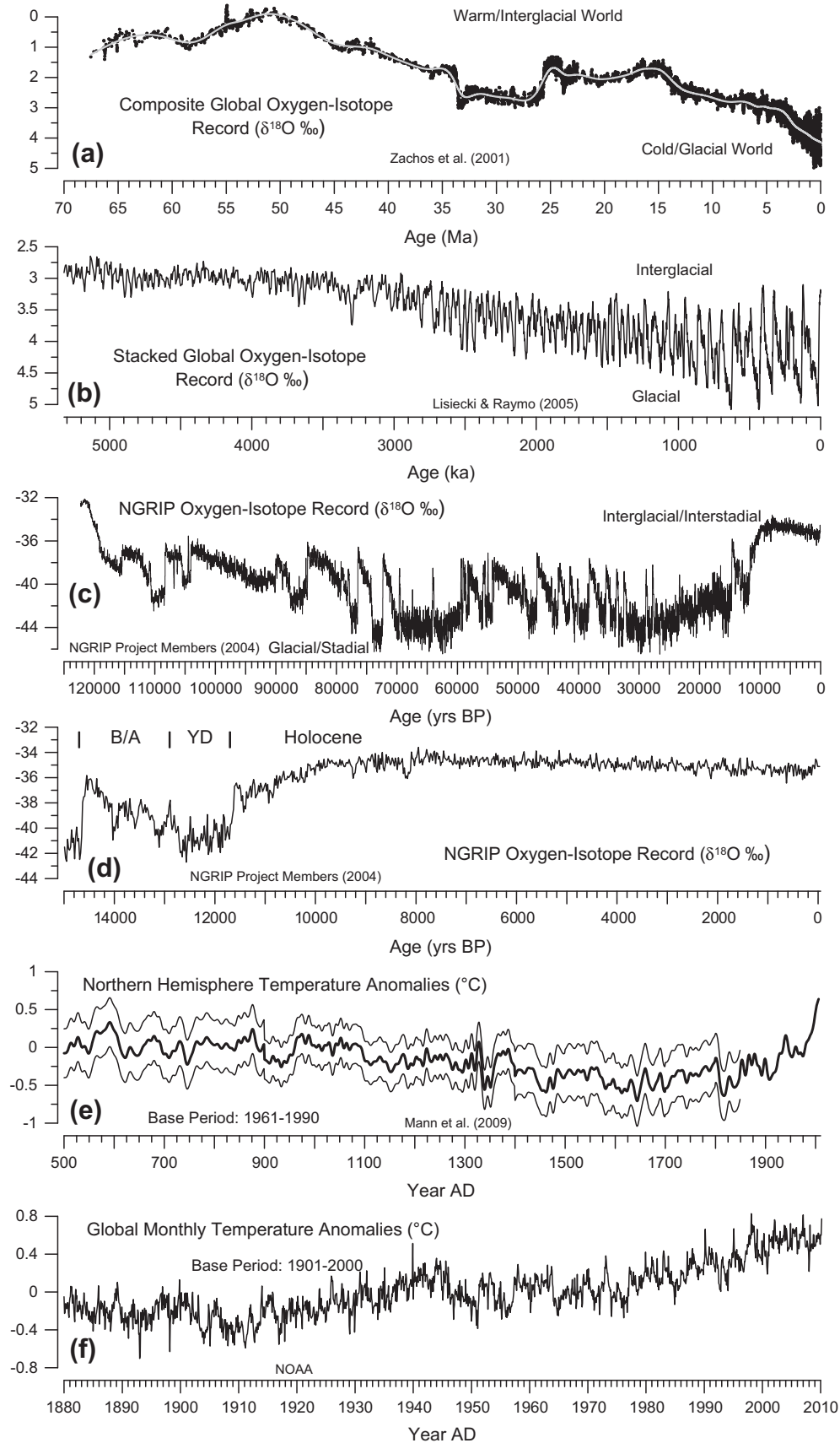
Chapter Outline

14.1. TIMESCALES OF CLIMATE CHANGE, THEIR CAUSATION, AND DETECTION

The climate of a region is most commonly expressed in terms of the 30-year average of key variables such as seasonal temperature, precipitation, and sea-level pressure. In this sense, climate could be considered as average weather conditions. However, this view does not work well with the perspective offered by the study of past climates, palaeoclimatology, which emphasizes climate variability on multiple timescales ranging from inter-annual to multimillennial. In this light, climate is not 'average weather', but rather the state of the Earth system at the particular timescale.

Over the past 70 million years (Figure 14.1a), $\delta^{18}O$ records (which can be regarded as a gross index of global temperature) show the Earth shifting from a warm, ice-free state to a predominantly cold state (Zachos et al., 2001). The long-term trend towards cooler conditions during the Cenozoic is marked by more rapid transitions, for example, around 35 Ma. On multimillennial timescales (Figure 14.1b), transitions between cold (glacial) and warmer (interglacial) climates show periodicity, but also variability in the amplitude of the transitions between warm and cold states, including a gradual increase in the amplitude of the temperature shifts after ~3 Ma (Lisiecki and Raymo, 2007). Both the periodicity and the variability are predictable consequences of the inherent variation in the Earth's energy budget caused by the superimposition of changes in the Earth's orbit on the configuration of the oceans and continents (Berger and Yin, 2012, this volume). Glacial intervals are characterized by pronounced, high-amplitude, millennial-scale variability (Figure 14.1c). These Dansgaard–Oeschger (D–O) cycles (Dansgaard

(a) Composite Global Oxygen-Isotope Record (δ¹⁸O ‰)
Zachos et al. (2001)
Warm/Interglacial World
Cold/Glacial World
Age (Ma)

(b) Stacked Global Oxygen-Isotope Record (δ¹⁸O ‰)
Lisiecki & Raymo (2005)
Interglacial
Glacial
Age (ka)

(c) NGRIP Oxygen-Isotope Record (δ¹⁸O ‰)
Interglacial/Interstadial
NGRIP Project Members (2004)   Glacial/Stadial
Age (yrs BP)

(d) B/A YD Holocene
NGRIP Project Members (2004)
NGRIP Oxygen-Isotope Record (δ¹⁸O ‰)
Age (yrs BP)

(e) Northern Hemisphere Temperature Anomalies (°C)
Base Period: 1961-1990   Mann et al. (2009)
Year AD

(f) Global Monthly Temperature Anomalies (°C)
Base Period: 1901-2000
NOAA
Year AD

et al., 1984) appear to be related to the behaviour of the meridional overturning circulation (MOC). The most recent of these events is the Younger Dryas climate reversal (Figure 14.1d). Similar millennial-scale variability, including Younger Dryas-like climate reversals, is a regular feature of glacial intervals and is not unique to the last 100,000 years (Martrat et al., 2007; Cheng et al., 2009).

Millennial-scale variability has also been recognized during interglacial intervals (see e.g., Marchant and Hooghiemstra, 2004; Booth et al., 2005; Rohling and Palike, 2005) but is generally of lower amplitude than during glacial intervals. The climate record from Greenland (Figure 14.1e) shows a progressive, but small, cooling trend during the recent (Holocene) interglacial interval. Climate variability is also evident on centennial timescales (Figure 14.1e) although, again, over the last two millennia, this is superimposed on a longer term cooling trend (Mann et al., 2009) that culminates in the so-called Little Ice Age and is followed by the comparatively rapid warming characteristic of the industrial era (post 1750 A.D.). Finally, in addition to the strong imprint of the seasonal cycle, the observational record of the last century (Figure 14.1f) shows variability at both inter-annual and inter-decadal timescales (cf. Latif and Park, 2012, this volume).

Thus, climate variability has considerable structure on a wide range of timescales. The available records show several styles of variability: periodicity, resulting from astronomical or 'orbital' forcing on multimillennial and seasonal timescales; progressive changes, such as the long-term cooling through the Cenozoic in response to changes in land−sea configuration and atmospheric composition (Zachos et al., 2001; Fletcher et al., 2007), or the more recent cooling trend of the last two millennia; and rapid climate shifts, for example, following re-organisation of the coupled atmospheric−oceanic circulation during the D−O cycles (Bond et al., 1993; Kageyama et al., 2010). At each timescale, the climate system is characterized by changes in both frequency and magnitude of its variations. However, the magnitude of climate shifts is not a simple function of the timescale. Large and rapid changes in climate occur both on multimillennial and much shorter timescales (Figure 14.1).

On any timescale, global climate can be seen to be continuously varying, never dwelling long at any one value and frequently crossing the mean, thereby further rendering the definition of climate as a long-term mean unworkable when considering the history of changes in the Earth system. However, over some timespans, such as the past million years (Figure 14.1b) and over the interval between 80,000 and 10,000 years ago (Figure 14.1c), the variations of climate remain within a 'corridor' of values, indicating that the climate system is not completely non-stationary, in the sense of having continuously varying statistical properties.

Variations in climate influence many other aspects of the Earth system, including atmospheric composition, the hydrological cycle, and marine and terrestrial biology. Records of these changes are preserved in natural archives (see Bradley, 1999): for example, variations in atmospheric composition are recorded by air trapped in bubbles in the slowly accumulating ice sheets, changes in the hydrological cycles are recorded by lake shorelines or fluvial deposits, while changes in vegetation cover are recorded through pollen and plant macrofossils trapped in anoxic lake or bog sediments. Provided that such records can be unambiguously dated, they can be used as 'sensors' of climate and environmental change. (We eschew the term 'proxy', used as an abbreviation for 'climate proxy', preferring to use the term 'sensor' because any environmental archive is a palimpsest of both direct and indirect climate and other influences − and the primary goal of palaeo-environmental research is to disentangle the multiple factors influencing the record at any one time.)

Since environmental conditions change as climate changes, it is unsurprising that a large number of environmental archives show similar scales and types of variability (Figure 14.2). As an example, Figure 14.2 shows the variability in the incidence of wildfire on different timescales. Wildfire is controlled both by the occurrence of suitable weather conditions (e.g., convective activity controls the frequency of lightning ignitions, while seasonal drought controls the dryness of fuels) and by the nature of the vegetation cover, and hence the availability of fuel to burn, which in itself is determined by climate (Dwyer et al., 2000; Harrison et al., 2010). Sedimentary charcoal records document variability in fire regimes over millions of years (Figure 14.2a) through multimillennial (Figure 14.2b), millennial (Figure 14.2c), centennial (Figure 14.2d), decadal (Figure 14.2e) to annual (Figure 14.2f) timescales, and show progressive, quasi-periodic and abrupt changes in fire regimes. Furthermore, as with more direct indicators of

FIGURE 14.1 Variability in temperature on multiple timescales. The record for the last 65 Myr (a) is based on a global compilation of ^{18}O isotope records on benthic foraminifera (Zachos et al., 2001), and that for last 5500 kyr (b) on 57 ^{18}O isotope records (Lisiecki and Raymo, 2007). The δ^{18}O record from the NGRIP ice core (c; North Greenland Ice Core Project Members, 2004) is based on 50-year mean values over the past 125 kyr. An expansion of the last part of this record (from 15 ka onwards) is also shown (d). The decadally-resolved record for the past 1500 years (e; from 500 AD onwards) is based on a synthesis of instrumental and historical documentary records with palaeo-data including tree-ring reconstructions (Mann et al., 2009). The data for the last century (f) is from the NOAA historical climatology (*http://www.ncdc.noaa.gov/ghcnm*). The curves illustrate that climate is always varying and has no particular average value (but often varies within a particular corridor). The curves also show the rich set of trends (a, b, c, d, e, and f), periodic and quasi-periodic (b and c) variations, and abrupt changes (a and c), that both require explanation and provide 'natural experiments' with which to test models.

FIGURE 14.2 Variability in global fire on multiple timescales, as an illustration of the variability of a particular set of environmental subsystems and processes (i.e., disturbance of terrestrial ecosystems by fire). The record for the past billion years (1 Gyr) (a) is a qualitative index of global fire based on discontinuous sedimentary charcoal records (Bowman et al., 2009). The record for the past 80 kyr (b) is a global composite of 30 sedimentary charcoal records (Daniau et al., 2010), that for the past 21 kyr (c) is a global composite of ~700 sedimentary charcoal records (Daniau et al., submitted) and that for the past 2 kyr is a global composite of ~400 sedimentary charcoal records (d; Marlon et al., 2008). Global area burnt over the twentieth century (e) is estimated by combining data from tree-ring, historical, and remotely-sensed sources (Mouillot and Field, 2005), while global area burnt from 1997 to 2006 (f) is derived from satellite-based remote sensing (GFED v3.1, Giglio et al., 2010). Like palaeoclimatic records in Figure 14.1, the palaeofire records show continuous variability, as well as similarly recurring patterns of variability and abrupt changes.
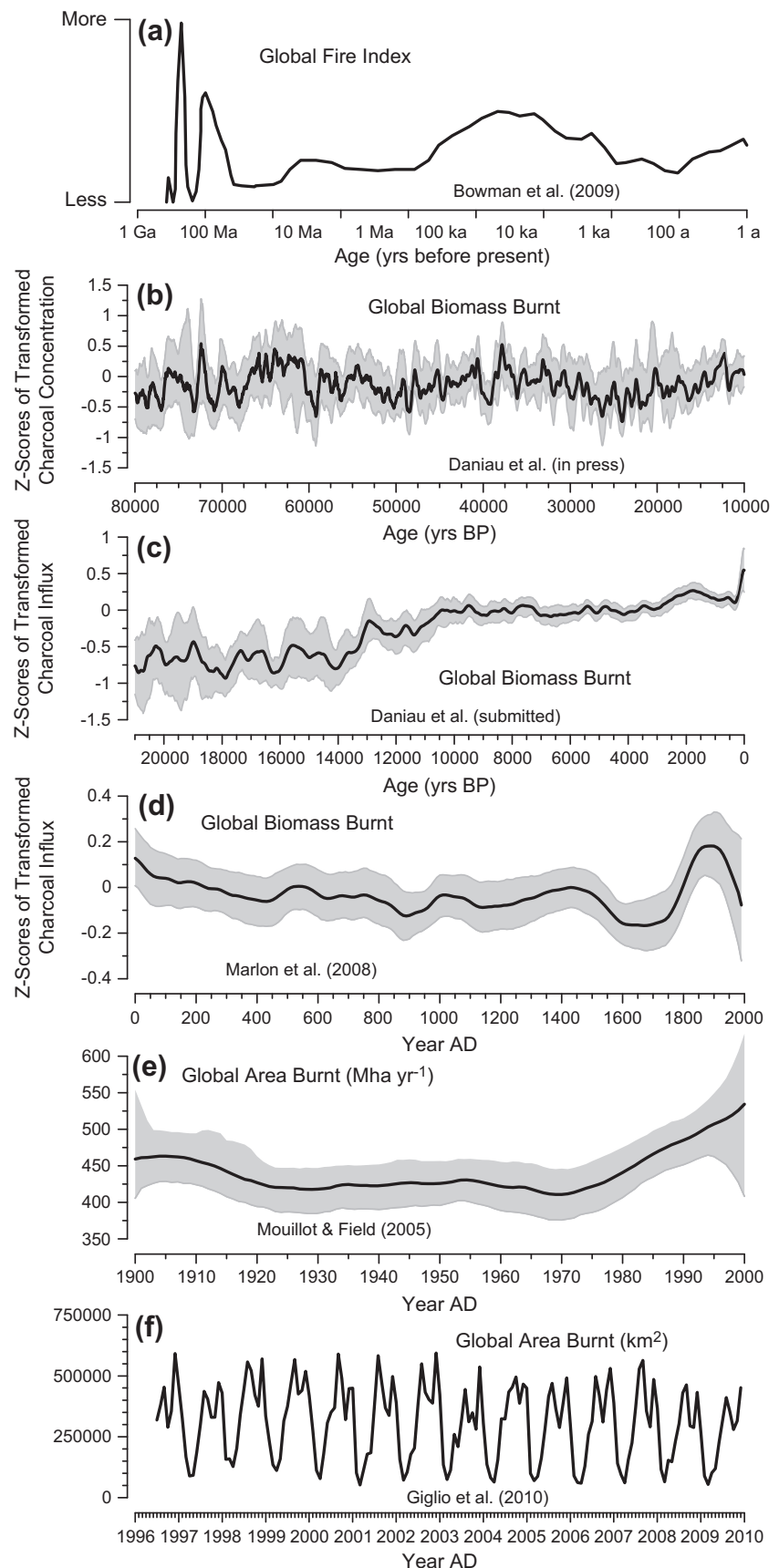
climate, the magnitude of the changes in fire regime is not necessarily related to the timescale or the frequency of variability.

Climatic variations on all timescales evoke responses in the terrestrial and marine biota that range from evolution and disappearance of species and genera on the longest of timescales, to wholesale re-organisations of the biosphere accompanying glacial−interglacial variations, to impacts on the phenology and growth of terrestrial plants and the distribution of short-lived or migratory organisms on the inter-annual timescale (Dickinson, 2012, this volume; Sen Gupta and McNeil, 2012, this volume). Re-organisations of climate and the biosphere on orbital timescales provide the most useful guide to the likely response of environmental systems related to climate during the coming centuries − not through exact analogy, but by revealing the mechanism and ways in which the climate system responds to changes in external forcing comparable in magnitude to those underway at present.

14.1.1. The Climate System and Timescales of Variability

The number of basic components of the climate system (atmosphere, ocean, biosphere, cryosphere) is small, but the number of variables that describe those components (e.g., regional seasonal temperatures, carbon stocks) is enormous. The many variables describing the climate system fall into one of three categories (Figure 14.3; after Saltzman, 2002): (i) those that describe the external forcing of the system (*boundary conditions*; e.g., insolation, volcanic aerosols, and a broad set of 'geodynamic' variables, including the configuration, topography and bathymetry of continents and ocean basins); (ii) those that describe the more slowly varying aspects of the system (*slow-response variables*; e.g., the ice sheets, bedrock, and mantle that are deformable by ice sheets; sea level and the temperature and salinity of the deep ocean, and the long-term state of its overturning and horizontal circulation; and the slowly varying reservoirs involved in biogeochemical cycling that ultimately determine atmospheric composition); and (iii) those that describe the internal variables that are ordinarily thought of as weather, but also include rapidly varying biophysical and biogeochemical processes (*fast-response variables*; e.g., precipitation, evapotranspiration, respiration, seasonally varying sea-ice extent, soil-moisture content, vegetation properties, the temperature, depth, and other physical and biological characteristics of the mixed layer of the ocean). A fourth category of variables, *subsystem variables*, describes the state and function of the many environmental subsystems that are governed by climate, and which, depending on context, include many of the fast-response variables. For example, evapotranspiration can be considered both as a fast-response variable that is
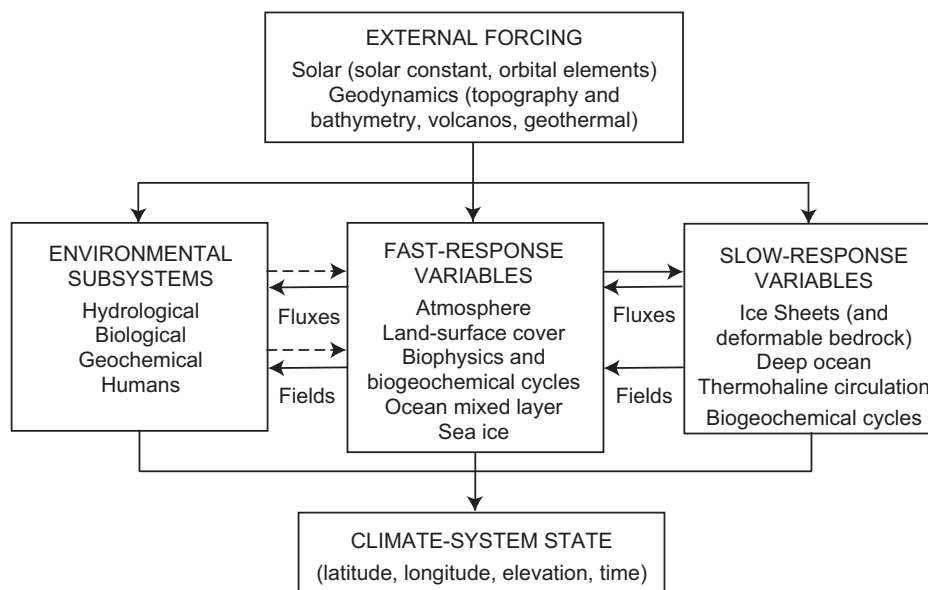

FIGURE 14.3 The climate system. The variables that describe the external forcing of the system (or boundary conditions) directly or indirectly influence the slow-response, fast-response, and environmental-subsystem variables; these, in turn, influence each other and determine the state of the climate system as a function of longitude, latitude, elevation, and time. The arrows labelled 'fields' indicate that one set of variables influences the other through patterns of atmospheric circulation, moisture, and heat, while those labelled 'fluxes' indicate that one set of variables influences another through the transfer of mass and energy. The dashed arrows indicate that the influence of the fast-response variable on environmental subsystem variables is currently unidirectional in climate models, but that eventually environmental subsystem variables will interact with the fast-response variables as climate models develop (after Saltzman, 2002: Bartlein and Hostetler, 2005). Many of the individual variables listed here leave evidence (i.e., palaeoclimatic data) of their variations over time.

a component of the surface water and energy balance, and as a subsystem variable when describing hydrological systems on scales from watershed to continents. Human activities such as fossil-fuel burning are often thought of as 'external' variables, but are more realistically considered as an environmental subsystem that both influences and is influenced by climate (i.e., as part of a 'coupled Earth system', e.g., Rice and Henderson-Sellers, 2012, this volume).

Many environmental systems respond to variations of climate. These systems are also characterized by a large number of variables, including some that play a role in the interaction and feedback between the atmosphere and the surface (and might therefore be thought of as fast-response variables), and some that are dependent on climate but do not feed back to the climate system except in limited ways. Human social and economic systems can also be considered as another environmental subsystem that responds to climate, but ultimately feeds back to it, as is illustrated by the current focus on the mitigation of anthropogenic climate change (Metz et al., 2007) and by the new approaches for developing emissions scenarios that include input from integrated assessment models of the coupled natural and human environment (Moss et al., 2008; Rice and Henderson-Sellers, 2012, this volume).

Some variables are not easily categorized. Vegetation plays a key role in the instantaneous coupling of the atmospheric boundary layer and land surface by controlling the exchanges of energy and moisture, and also plays an important role in biogeochemical cycles (e.g., Pitman and de Noblet-Ducoudré, 2012, this volume). The rates of these fast exchanges depend on the structure of the vegetation, and the states of the atmosphere and underlying soil (including atmospheric humidity, wind, net radiation at the surface and soil-moisture availability) that together influence plant physiology (e.g., stomatal conductance), while the role of vegetation in biogeochemical cycling is governed by vegetation structure and composition. It was formerly thought that vegetation structure responds slowly to climate changes (on the order of hundreds to thousands of years), placing it in the category of slow-response variables. It is now clear that vegetation structure can respond rapidly to climate changes over timespans of years to decades (Tinner and Lotter, 2001; Shuman et al., 2009). Soils are dependent on climate and vegetation, but also have strongly expressed geological and geomorphic controls (e.g., Harvey, 2012, this volume). Key attributes of the soil such as water-holding capacity may be dominated by parent material (as in arenaceous soils), and so this might be regarded as a boundary condition; in other situations water-holding capacity is dominantly controlled by soil morphology, and hence acts like a slow-response variable. The particular category a variable falls into is thus largely dependent on context, location, and scale.

14.1.2. Insolation Variations

The temporal-scales of variability in the climate system depend on the nature of the external forcing of the climate system and the response time of the internal components of the climate system to this forcing. On orbital timescales (Figure 14.1b and 14.1c), the ultimate cause of natural climate variability is changes in the latitudinal and seasonal distribution of incoming solar radiation (insolation) as a result of changes in the Earth's orbit (Berger, 1978, 1981, 1988; Berger and Yin, 2012, this volume). These insolation variations govern the principal mode of climate variability over the past several million years—the variations between glacial and interglacial states—and these variations therefore provide a perspective on the behaviour of the climate system to changes in its external controls, and on the resulting re-organisation of the terrestrial and marine biospheres and biogeochemical cycles, and on the mechanisms by which the climate system amplifies the external forcing.

Earth's orbit can be described by three parameters (Figure 14.4a): the shape of the orbit about the Sun (eccentricity), the tilt of the Earth's axis relative to the Sun (obliquity), and the time of the year when the Earth is closest to the Sun (precession). Strictly speaking, obliquity is an 'astronomical' parameter, not a characteristic of the Earth's orbit about the Sun, but we include it here in the collection of 'orbital' parameters that influence insolation. The shape of the Earth's orbit varies from nearly circular (low eccentricity of 0.005) to elliptical (high eccentricity of 0.058), with periodicities of roughly 100,000 and 400,000 years. The angle of the Earth's axial tilt (obliquity) with respect to the plane of the orbit varies between 22.1° and 24.5° with a periodicity of around 41,000 years. As obliquity increases, the amplitude of the seasonal cycle of insolation increases, with summers in both hemispheres receiving more insolation and winters less. Changes in obliquity also affect the latitudinal variations of annual mean insolation, with the high latitudes of both hemispheres receiving greater insolation during times of high obliquity and the tropics less. Astronomical precession refers to the change in the direction of the Earth's axis of rotation relative to the fixed stars (i.e., the 'wobble' of Earth's axis) while climatic precession, which depends on eccentricity and the time of year of perihelion (and hence varies with astronomical precession), governs the average solar irradiance on any given day (Loutre, 2009). Climatic precession varies with periodicities of 23,000 and 19,000 years (Berger, 1978; Crucifix et al., 2009), and leads to opposing variations in insolation between the Northern and Southern Hemispheres. From the perspective of one of the hemispheres, when the axis is aligned towards the Sun during the time when the Earth is closest to the Sun (perihelion), the seasonal difference in radiation receipt is
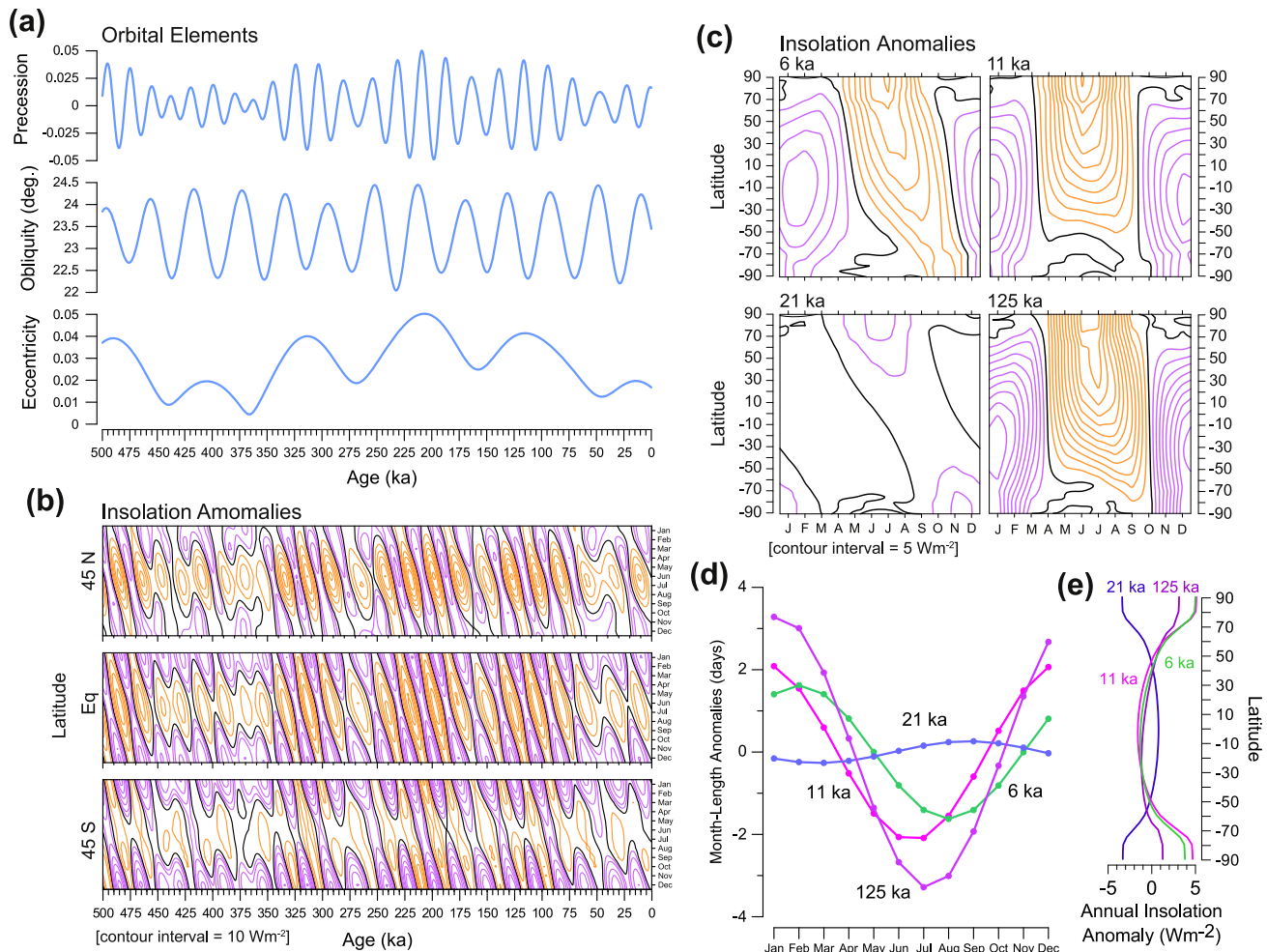
(a)

(b)

(c)

(d)

(e)

FIGURE 14.4   Effects of changes in orbital parameters on insolation. (a) Changes in climatic precession, obliquity, and eccentricity over the past 500 kyr (Berger, 1978). These changes in orbital configuration give rise to complex changes (b) in seasonal insolation through time (here represented as plots of mid-monthly insolation in W m^{-2} at 45°N, the equator, and 45°S over the past 500 kyr). The difference (relative to present) in seasonal insolation by latitude (in W m^{-2}) is shown for four iconic time periods (c): the mid-Holocene (6 ka), the early Holocene (11 ka), the Last Glacial Maximum (LGM; 21 ka), and the peak of the last interglacial (125 ka). The impact of changes in orbital configuration on (d) 'month length' anomalies (Kutzbach and Gallimore, 1988), or the difference in the time taken by the Earth to sweep through one-twelfth of its orbit, and (e) the latitudinal distribution of insolation is also shown for these iconic time periods. In panels (b), (c), and (d), months are labelled using their conventional names; strictly speaking 'months' are defined by the angular position of Earth relative to that at the vernal equinox. The first month of the year (labelled 'J' or 'Jan' is the interval between the time of Earth's angular location at −81° and −50° (before the vernal equinox). Along with the annual cycle, these insolation variations are the only controls of climate variations that vary in a strictly periodic, or cyclical, way.

enhanced in that hemisphere (the hemisphere experiencing 'summer' conditions) and reduced in the other hemisphere.

The superimposition of variations in these three parameters gives rise to remarkably complex patterns in the seasonal and latitudinal distribution of insolation through time (Figure 14.4b). Precessional variations produce the most obvious pattern in the variations of the annual cycle of insolation over time at all latitudes: the repeating pattern of positive and negative insolation anomalies at the precessional timescale. These translate into changes in seasonality within a single hemisphere, and to opposition in the sign of the anomaly between hemispheres during any

particular month and opposition of the magnitude of the anomaly during any particular season (i.e., positive summer anomalies in the north are accompanied by negative summer anomalies in the south). The amplitude of the precessional maxima and minima is related to eccentricity: times of high eccentricity produce larger differences between insolation maxima and minima (e.g., between 250,000 and 175,000 years ago), while times of low eccentricity produce smaller differences (e.g., between 450,000 and 350,000 years ago). Obliquity variations modify these variations by amplifying the summer insolation maxima, the winter minima, and seasonal contrast

when obliquity is high (such as during the maximum of the last precessional cycle, ~10,000 years ago), and damping it when low (as ~30,000 years ago). The precessional maxima and minima can also be seen to progress through the year, with the extremes occurring progressively later in the year during any given cycle.

The net effect of the variations in the different orbital elements can be seen in latitude by month anomalies in insolation at particular times (Figure 14.4c). At 6000 years ago, perihelion occurred at the end of the northern summer, while obliquity was slightly greater and eccentricity about the same as present (see Berger and Yin, 2012, this volume). Summer insolation was roughly 6% greater than present and winter 8% less in the mid-latitudes to high latitudes of the Northern Hemisphere, while in the Southern Hemisphere the anomalies were reversed. At 21,000 years ago, all three of the orbital elements were close to their present values, and so the insolation anomalies relative to present were small. The previous interglacial period, ~125,000 years ago, was characterized by perihelion during the northern summer (and at the boreal summer solstice at 127,000 years ago, Berger and Yin, 2012, this volume), high obliquity and high eccentricity. Consequently, the insolation anomalies were greater than those at 6000 years ago, and the seasonality of insolation in both hemispheres was high relative to both 6000 years ago and to present.

Eccentricity of the orbit also leads to differences in the length of the summer and winter seasons (Figure 14.4d), because the Earth moves more rapidly along its orbital track near perihelion and less rapidly near aphelion (Joussaume and Braconnot, 1997; Braconnot et al., 2008; Berger et al., 2010). This effect can oppose that of precession. For example, at both 6000 and 125,000 years ago, the effect of the climatic precession-related maximum in the Northern Hemisphere insolation is partly compensated by a reduction in the length of the summer months relative to today (Berger et al., 2010; Berger and Yin, 2012, this volume).

The time course of insolation at a specific latitude differs from that at adjacent latitudes, even in the same hemisphere. Consequently, while it is often convenient to refer to situations like 'Northern Hemisphere summer insolation maxima' or 'interglacials,' the regional and temporal expression of these situations vary. For example, the interglacials of the last million or so years are all different in terms of the particular sequence and spatial pattern of insolation variations that caused them, although some may be broadly similar (Berger and Yin, 2012, this volume). This fact severely limits the potential for constructing analogies between them, for example, specific sequences of variations in greenhouse gases or global ice volume (e.g., Ruddiman, 2008). There is no reason to expect that the sequence of events in one interglacial should be exactly similar to that in another, and indeed there is ample evidence that this is not the case.

Insolation variations can potentially be expressed as any number of sinusoidal curves; for example, one could produce a curve of April mid-month insolation anomalies at a particular latitude, or of the February−October difference in insolation integrated over a specific hemisphere. This situation creates a danger of finding spurious explanations for a particular palaeoclimatic time series, in the same way that any curve can be represented by a Fourier series. Consequently, the search for explanations of climatic variations in terms of a specific record of insolation forcing must be based on an underlying mechanistic or conceptual model that specifies why that particular linkage should occur and, furthermore, allows testing of explicit hypotheses about how it occurs.

14.1.3. Implications of Insolation Variations

The temporal variations in insolation are gradual, producing smoothly varying shifts in climate on orbital timescales and giving rise to alternations between globally cold, glacial states and globally warm, interglacial states. These changes in insolation affect other elements of the climate system: large ice sheets grow during cold states and decay during warm states, while changes in land−sea geography consequent on the growth and decay of these ice sheets affects ocean circulation. Vegetation responds to changes in global temperature, with increases in the area of forests during warm periods and decreases during cold periods. Likewise, major changes in the carbon cycle (see below) occur on orbital timescales.

However, each of these elements of the climate system has an inherent timescale of response to the initial orbital forcing. Ice sheets take many millennia to build up and decay, changes in ocean circulation take centuries to millennia, and vegetation migration takes decades to centuries. The timescale of interest determines whether each of these elements has to be considered as a dependent or independent variable in the climate system. On timescales of 10^4 to 10^6 years, ice sheets are dependent variables in the climate system, with their build-up and decay controlled by orbitally driven variations in insolation. At shorter timescales (10^3 to 10^4 years), ice sheets are independent variables that have an important impact on atmospheric circulation and global temperature. Similarly, at millennial timescales (10^3 years) vegetation changes are driven by climate changes, but on shorter timescales (10^2 to 10^3) changes in vegetation distribution affect climate through changing albedo and other land-surface characteristics, as well as through changing emissions of climatically important trace gases and aerosols (Arneth et al., 2010).

Changes in insolation provide the explanation for the first-order climate variation evident on orbital timescales. However, analysis of the response of the climate system to insolation forcing provides numerous insights into the

functioning of the Earth system, which under some circumstances responds to orbital forcing in extremely non-linear ways. The insolation variations provide what might be thought of as a continuous experiment with the global energy balance involving manipulations of all aspects of the incoming radiation at the top of the atmosphere, including weak variations of the annual average insolation integrated over the whole planet, as well as the large perturbations of its latitudinal and seasonal distribution. The transmission of these perturbations through the climate system can be used to understand the general linkages among different pathways of energy flow in the Earth—atmosphere energy balance, and to estimate the sensitivity of climate to such perturbations.

Although the insolation variations can be regarded as the 'pacemaker' of the glacial—interglacial variations of climate (Imbrie et al., 1984), they fail to fully explain those variations in several important ways: (i) the variations in annual insolation are small and insufficient by themselves to generate the glacial—interglacial variations; (ii) the main variations in insolation occur on the precessional timescale (Figure 14.4a and 14.4b), while the principal variations of global climate occur variously on the obliquity and eccentricity timescales (Figure 14.1b), and (iii) the expression of these timescales of variation in terms of global climate can change relatively abruptly (as for example around 1 million years ago, when 41-kyr variations gave way to 100-kyr variations). Often referred to as the 100-kyr or 41-kyr problems (Raymo and Nisancioglu, 2003; Lisiecki and Raymo, 2007), several ideas have been advanced that emphasize either variations in the mode of transmission of the 'signals' of the three orbital elements through the climate system (Imbrie et al., 1992; Ruddiman, 2006), or to specific features of one of the elements (e.g., obliquity and summer insolation, Huybers and Wunch, 2005), but as yet no consensus has emerged. Nevertheless, although the explanation is still incomplete, the empirical link between insolation and glacial—interglacial variations of climate attests to the role of mechanisms internal to the climate system that amplify the effects of externally forced perturbations of the energy balance. There is strong evidence that this amplification involves the effects of the ice sheets themselves on planetary albedo (along with that of changing vegetation distributions), global biogeochemical cycles (in particular those of the long-lived greenhouse gases: carbon dioxide and methane), and physically and/or biologically mediated changes in the dust and aerosol content of the atmosphere — all of which substantially modify the Earth—atmosphere energy balance (Hansen et al., 1984; Forster et al., 2007).

Several proposed explanations for the amplification of climate change on orbital timescales rest on a combination of geophysical and biological mechanisms. Some biological mechanisms operate at the level of the physiology of individual organisms; but large-scale re-organisations of the biosphere also involve geographical range shifts. Variations in climate on orbital timescales have been a constantly present feature in the evolution of life on Earth, and so it should not be surprising that species have developed strategies for dealing with large-scale re-organisations of the biosphere. Species persist for periods that are typically several orders of magnitude longer that the timescales of insolation variations (Bartlein and Prentice, 1989; Bennett, 2004). Because of the conservatism of species' environmental niches, range boundary shifts are a near-universal feature of species' responses to climate change (Huntley and Webb, 1989; Davis et al., 2005). The responses of species are individualistic, but species generally are capable of migration, allowing major biogeographical re-organisations to take place along with re-organisations of climate.

14.1.4. Co-variation of Climate and Biogeochemical Cycles Over the Past 800 kyr

The co-variation among components that describe the general state of the climate system, as represented, for example, by global ice volume and elements of biogeochemical cycles, can be seen through the perspective provided by polar ice cores (Figure 14.5). The longest and most comprehensively analysed record to date is the EPICA Dome C (EDC) record from Antarctica (Jouzel et al., 2007a; Barbante et al., 2010), which spans the past 800,000 years. In addition to chemical and physical measures (such as dust concentration), ice core records provide samples of the actual atmosphere at different times, and thereby (subject to synchronization of records derived from trapped air and records derived from the ice itself) provide an internally consistent record of climate and biogeochemical cycles. Atmospheric composition in terms of long-lived greenhouse gases (carbon dioxide, methane, nitrous oxide), dust and local temperature indicators (Figure 14.5) all show the signatures of insolation forcing (represented here by the often-used index of July insolation at 65°N), in common with the oxygen isotope record of global ice volume from marine sediments. Individual precessional peaks are evident to a greater (e.g., methane) or lesser (e.g., carbon dioxide, but see Ahn and Brook, 2008) extent and are modulated by the 100-kyr eccentricity cycle. Interglacials are characterized by high levels of greenhouse gases, relatively warm Antarctic conditions, and low dust concentrations, while glacials show the opposite features.

The specific contributions of both the external (insolation) and internal (the ice sheets, sea-ice, land cover, greenhouse gases, and dust) drivers to variations in the net radiative forcing over the past 800,000 years has been
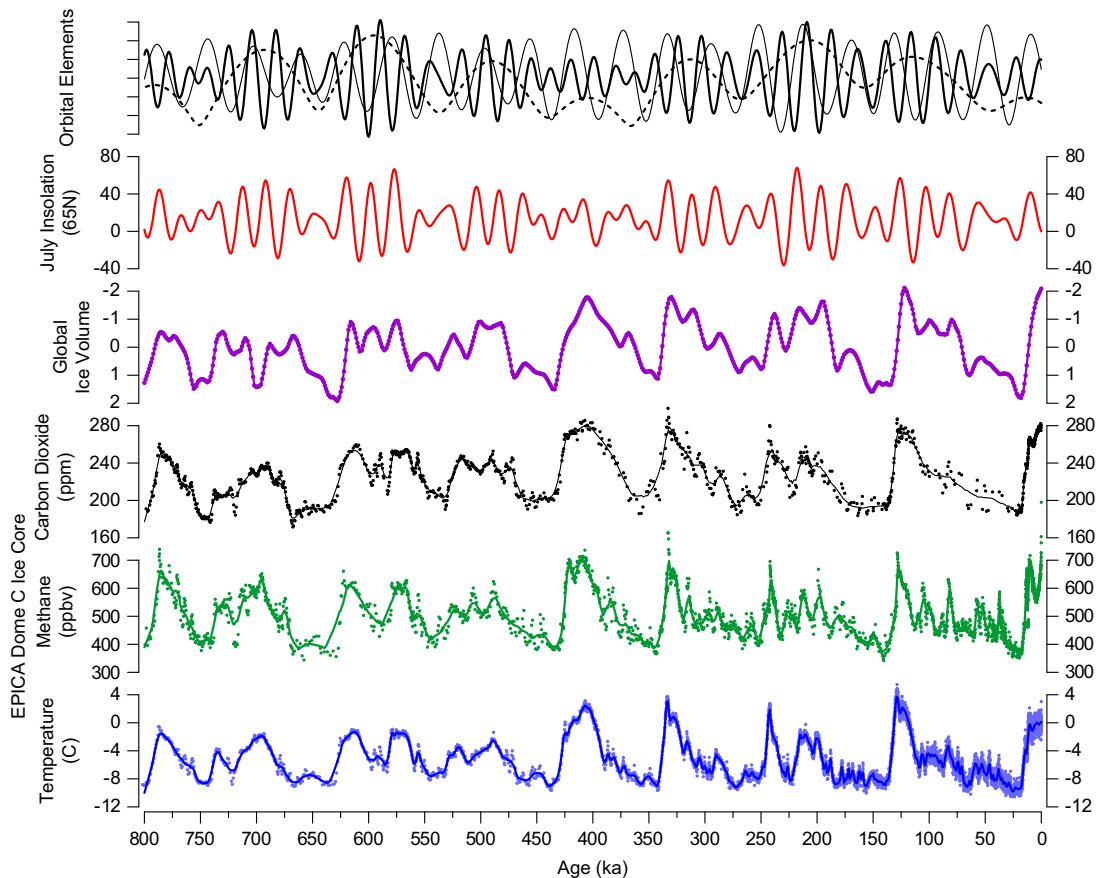
FIGURE 14.5　Co-variation of climate and biogeochemical cycles over the past 800 kyr. Changes in precession (black solid line), obliquity (grey line), and eccentricity (dotted line), and the resultant July insolation at 65°N are compared with global ice volume (Martinson et al., 1987), changes in CO_2 (Lüthi et al., 2008), and CH_4 (Loulergue et al., 2008) from the EPICA Dome C (EDC) ice core and with inferred temperature from the deuterium isotope record from EPICA (Jouzel et al., 2007a). The imprint of the insolation variations is clearly expressed in temperature and greenhouse gas records.

estimated by Köhler et al. (2010) using a combination of observations from the EDC records and other palaeo-climatic data and model-based interpretations of these records. 'Radiative forcing' is a way to express the impact of a heterogeneous set of potential controls (and feedbacks) on the global energy balance, and in turn on global average temperatures (e.g., Forster et al., 2007; Arneth et al., 2010). The analysis by Köhler et al. (2010) suggests that the ice sheets make the largest contribution to the overall radiative forcing variations over the past 800,000 years, followed by greenhouse gases and sea-ice, and dust and vegetation, with the feedbacks all much larger than the direct effects of insolation (see figure 7 in Köhler et al., 2010). They did not directly estimate the impacts of additional feedbacks from water vapour, clouds, and related changes in lapse rates (which are highly uncertain and model dependent), but these are roughly comparable to the others, and again exceed the direct effects of insolation. The feedbacks are all positive in the sense of driving the climate system towards colder conditions when Northern Hemisphere insolation

decreases, and towards warmer conditions when it increases. Although the specific mechanisms, pathways, and spatial variations in feedbacks remain to be disclosed, the overall potential of the climate system to amplify relatively weak changes in radiative forcing is clear (cf. Harvey, 2012, this volume).

On long timescales (e.g., over the full span of the EDC ice core), insolation, ice volume, and greenhouse gases co-vary. On shorter timescales, such as the interval since the Last Glacial Maximum (LGM, Figure 14.6), they are quasi-independent drivers of climate changes because of inherent time lags in their response to insolation changes. What is considered an internal component of the climate system and what is an external control is not arbitrary, but depends on the specific timescale of interest and the response time of a particular component relative to that timescale.

The LGM-to-present interval has been a major focus of palaeoclimate investigations because it provides a range of 'natural experiments' allowing differentiation of the role
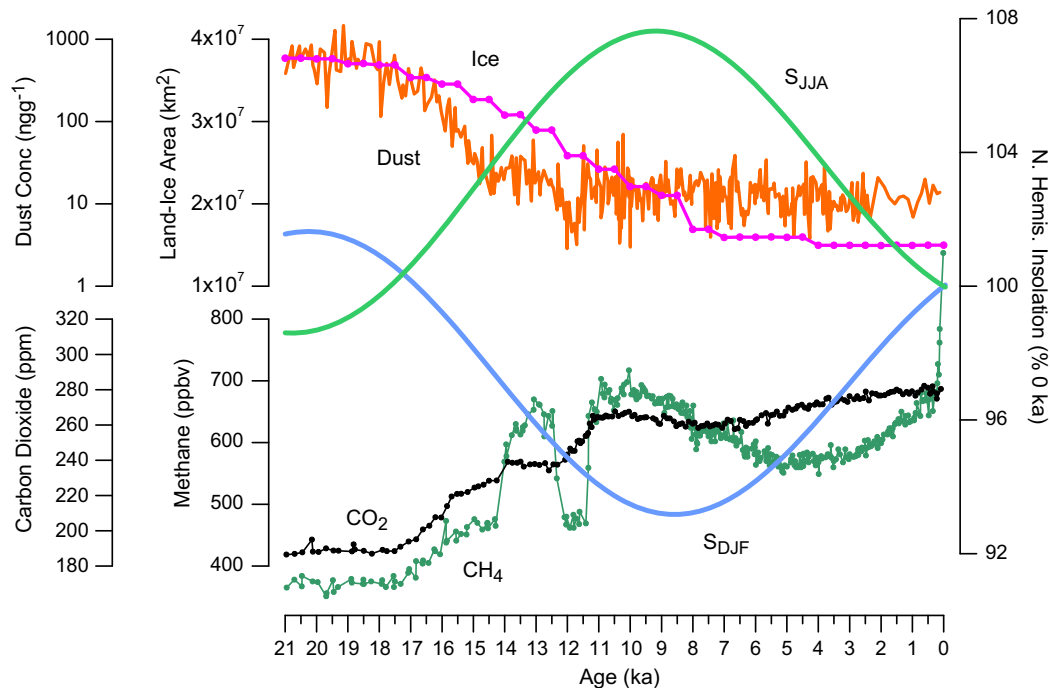
FIGURE 14.6   Changes in boundary conditions over the past 21 kyr. The changes in seasonal insolation (for the Northern Hemisphere) are compared with changes in global ice volume from ICE-5G (Peltier, 2004), and changes in CO_2 (Lüthi et al., 2008), CH_4 (Loulergue et al., 2008), and dust (Lambert et al., 2008) from the EDC ice core. The curves jointly illustrate the natural experiments that provide targets for palaeoclimatic simulations. At 21 ka, the distribution of insolation is close to that at present, but there were large ice sheets, high concentrations of dust, and low concentrations of the greenhouse gases, carbon dioxide and methane, providing an experiment that shows the impact of these 'glacial-age' boundary-condition settings. At 6 ka, most of the boundary conditions were close to their pre-industrial values, except for insolation, providing an experiment involving a perturbation of the Earth−atmosphere energy balance.

of individual drivers on regional climates. At the LGM, and over the first part of deglaciation (i.e., to ~18 ka), insolation levels were near their present ones, but ice sheets were larger than today, greenhouse gas concentrations were lower, and dust loadings higher. In contrast, at 6 ka, the ice sheets were nearly at their present extents, and the atmospheric constituents were close to their 'pre-industrial' (~1750 AD) values.

14.1.5. The Hierarchy of Climatic Variations and the Explanation of Palaeoclimatic Records

Climatic variations occur within a hierarchy of controls and responses, which begin at the top level with the external controls of climate, proceed through global, hemispheric, continental, and regional-scales, and end with the variations of individual climate variables at specific locations at the bottom level (Bartlein, 1997). Responses at any one level of the hierarchy become the controls of variations of the components at lower levels. With the exception of the annual cycle, there is a general tendency for the variations of components at higher levels in the hierarchy to show more long-term variability while those at lower levels experience more short-term variability.

The existence of this hierarchy also has implications for attempts to explain the variations at a particular place, or to interpret the 'signal' encoded in a particular palaeoclimatic record. For example, although climatic variations at a place are ultimately governed by global-scale controls, a specific palaeoclimatic record generally cannot be representative of the general state of the global system. This situation arises because the intermediate controls and responses have the potential of reinforcing, cancelling, or even reversing the longer-term, larger-scale trends. Gradual changes in large-scale controls may sometimes produce abrupt local changes when atmospheric circulation is re-organised. Conversely, abrupt changes in the large-scale circulation may produce warming in some regions and cooling or no change in others, as can be seen in the spatial anomaly patterns of year-to-year variations in climate. Consequently, while it may be difficult or even impossible to ascribe a particular climate variation at a place to a specific configuration of higher-level controls, shorter-term variations at lower levels are strongly conditioned by the particular state of the system at higher levels. Therefore, any discussion of the timescales of climatic variability should explicitly acknowledge the spatial-scale or extent of the system being discussed.

14.1.6. Cycles and Spurious Periodicity: A Warning

Rather than displaying a simple pattern of variability that increases as a function of timespan or record length, as would be typical of a system that obeyed simple 'scaling laws' (Kantz and Schreiber, 2004), the climate system instead has some preferred temporal-scales of variability that reflect the nature of the external forcing of the climate system (e.g., insolation on the orbital timescale), or the internal time constants of the components of the climate system itself − like the slow build-up and decay of ice sheets, or the inter-annual variability associated with the El

Niño−Southern Oscillation (ENSO; Saltzman, 2002; Latif and Park, 2012, this volume). The most common way of describing this apparently organised variability in climatic time series is to refer to the variations as *cycles*.

Several factors can conspire to predispose researchers to see cycles in time series when in fact none exist, and then to invoke some kind of regular cyclical mechanisms, either external (Sun, moon, planets) or internal (oscillatory 'climate-modes') to account for them. Firstly, there *are* cycles in palaeoclimatic time series, in the form of the variations of ice volume and many other variables that occur in response to the orbitally driven variations of insolation or the quasi-periodicities in tropical Pacific ocean−atmosphere interactions (ENSO) that are related to a specific physical mechanism (the propagation of Kelvin waves across the Pacific). Secondly, spectral analysis (Jenkins and Watts, 1968), which was developed for statistical signal processing, has been used successfully to detect the imprint of the orbital variations in many palaeoclimatic time series. Thirdly, there is a tendency for palaeoclimatic time series to vary between general limits; this, coupled with our tendency to seek order in variable data, can lead to the perception of periodic variations when none exist. Fourthly, quasi-periodic variations in time series can arise from simple short-term memory or persistence (as in autoregressive moving-average models; Box and Jenkins, 1976). Fifthly, some common data-analysis tools or procedures can impart spurious periodicity. These last two sources of apparent periodicity are particularly problematic because failure to recognize them can lead to incorrect inferences about causality.

Figure 14.7 shows three examples of time series that feature quasi-periodic variations, each generated by filtering or transforming a series of normally distributed random numbers in an intrinsically aperiodic way. (In each panel, the random numbers are plotted in grey in the background on an arbitrary scale, and the generated series in black.) The top curve shows the output of a second-order auto-regressive or AR(2) model in which the current value of the time series depends on the previous two values, plus the random input (plotted in grey). In this particular example, the parameters of the model are those that apply to the well-known Wölfer sunspot series, which is well-described by an AR(2) model (Box and Jenkins, 1976). The resulting series clearly shows a rough 10 time-step oscillation, and further displays a change in amplitude and regularity of this oscillation midway through the series that would likely provoke additional comment if this were a real palaeoclimatic time series.

The middle series shows a 'difference stationary' time series generated using an integrated autoregressive model (ARI(1,1); Box and Jenkins, 1976), that was linearly detrended. (Long-period trends in time series are of two types: 'difference stationary' series that can be detrended
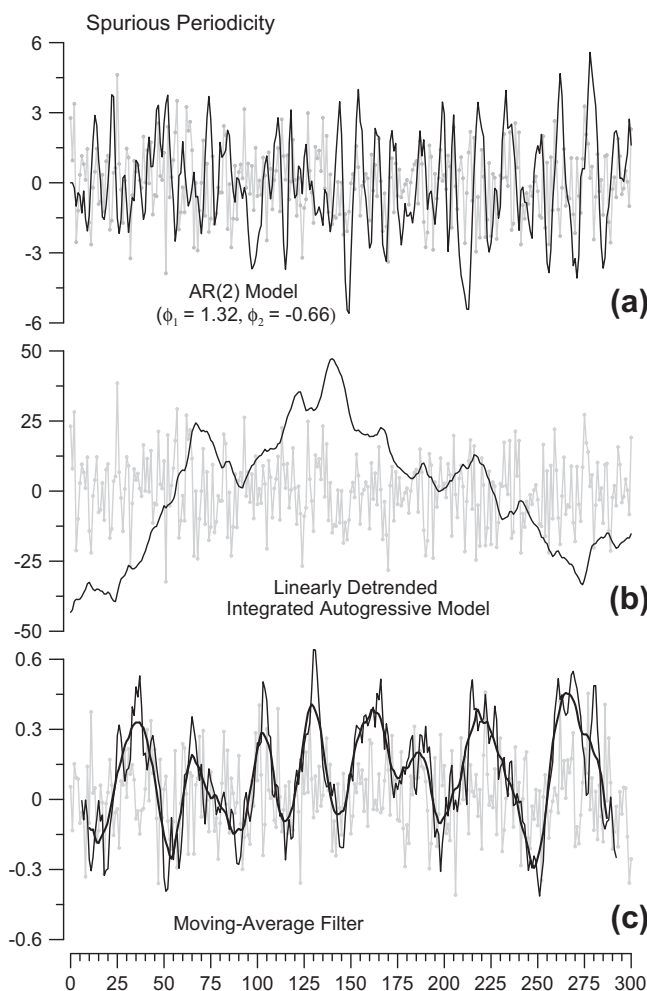

FIGURE 14.7 Illustrations of spurious periodicity. Series plotted in grey are the white-noise time series used to generate the simulations in black; (a) shows a second-order autoregressive process (AR(2)); (b) shows an improperly detrended integrated autoregressive model; (c) shows running mean-filtered white noise (thin black line represents the output from a 15-term running mean, thick black line from a further 10-term running mean of the data represented by the thin line). The curves show how apparent 'cycles' can arise in time series even when no underlying cyclical mechanism exists.

by taking the first differences between observations, and 'trend stationary' series that can be detrended by fitting a straight-line curve to the data: Nelson and Kang, 1981). The example series shows a broad cycle with a wavelength close to the record length and, in this particular realization, happens to also show lower-amplitude, higher-frequency variations, with a period around 20 time-steps. Again, although generated by an aperiodic process, the resulting series would likely be viewed as cyclic. Palaeoclimatic time series are frequently detrended as part of preliminary steps in data analysis.

Probably the most frequently applied method for generating apparently periodic variations in a time series when none really exist is illustrated by the bottom panel of Figure 14.7, which demonstrates the Slutsky−Yule effect (von Storch and Zwiers, 2001). The thin black line in Figure 14.7c is the result of applying a 15-term running mean to a white-noise time series, while the smoother solid line is simply the first series further smoothed by a 10-term running mean. The resulting series are clearly periodic, and it would be hard not to apply the term 'cycle' in describing or explaining these data if they were real. Slutsky's theorem (Jenkins and Watts, 1968, p. 297) shows that by repeated application of summing (as in the running mean) or differencing filters, white noise can be reduced to a sine wave. In practice, the smoothing produced by the running mean can occur naturally in palaeoclimatic records that integrate environmental conditions over time, but most often the smoothing occurs during data analysis.

All three series appear superficially periodic yet were generated by relatively simple processes, without invoking any kind of mechanism that could genuinely be called cyclical or periodic. Because there are multiple ways of generating series with apparent periodicity, some of which are related directly to commonly applied data-analysis procedures, a relatively high standard should exist for declaring a particular series cyclical and therefore explicable using the class of oscillatory or cyclical physical mechanisms. The premature declaration of a series as being cyclical may limit the search for other, possibly better, mechanistic explanations.

14.2. REGIONAL RESPONSES TO MILLENNIAL-SCALE FORCING

Faced with the richness and complexity of the palaeo-record, one strategy adopted by palaeoclimatologists to analyse key aspects of the record has been to study 'snapshots' of the state of the world corresponding to iconic periods with well-defined boundary conditions. An alternative strategy, the analysis of time-dependent changes, has always been the primary focus for the analysis of palaeo-environmental observations, but modelling

of the transient behaviour of the climate system has only recently become feasible with the advent of fast climate models (see e.g., Timm and Timmermann, 2007; Liu et al., 2009). Here we discuss the two most heavily studied intervals of the recent geological record (the LGM and the mid-Holocene) before considering some generalizations that have emerged from two decades of focusing on these intervals.

14.2.1. The Last Glacial Maximum

The LGM (~21,000 years ago; 26.5 ka−20 ka according to Clark et al., 2009) has been a focus for modelling experiments since the early days of palaeoclimate modelling (Williams et al., 1974; Gates, 1976; COHMAP, 1988; Kutzbach et al., 1993; Braconnot et al., 2007a, 2007b, and references therein; Otto-Bleisner et al., 2009). This is, in part, because it represents a time when most of the climate drivers (or boundary conditions) were radically different from today and, in part, because of the wealth of palaeo-environmental data that has been assembled to document regional climate conditions during this period (Figure 14.8).

At the LGM, palaeo-environmental data show colder (Figures 14.8a and 14.8b) and drier conditions in most of the northern extra-tropics. Vegetation records (Figure 14.8c) from Europe, Eurasia, and Alaska indicate a landscape dominated by treeless vegetation, with a significant expansion of graminoid and forb grassland and xerophytic shrubland in northern and central Eurasia (Prentice et al., 2011). Plant macrofossil data, however, indicate that trees persisted in local refugial situations (Willis and Whittaker, 2000; Willis et al., 2000; McLachlan et al., 2005). Forests were present south of the ice sheet in North America. Sedimentary charcoal records indicate a reduction in the amount of biomass burning (Figure 14.8d), partly as a result of a temperature-dependent reduction of fuel loads and partly because colder, drier climates give rise to a reduction in convection and hence lightning ignition (Power et al., 2008). The absence of forest cover, and the generally drier-than-present conditions, gave rise to increased deflation of surface material by winds and hence atmospheric dust loadings were between 2 and 5 times higher than today in the northern extra-tropics (Figure 14.8e; Harrison et al., 2001; Kohfeld and Harrison, 2001). Sea surface temperatures (SSTs) in the Northern Hemisphere were considerably lower than today (Figure 14.8b). The strongest annual mean cooling (up to −10°C) occurred in the mid-latitude North Atlantic, with more pronounced cooling in the eastern than in the western Atlantic (MARGO Project Members, 2009).

In contrast, both vegetation (Figure 14.8c) and lake data (Figure 14.8e) indicate wetter-than-present conditions in the American southwest and in western China, and the
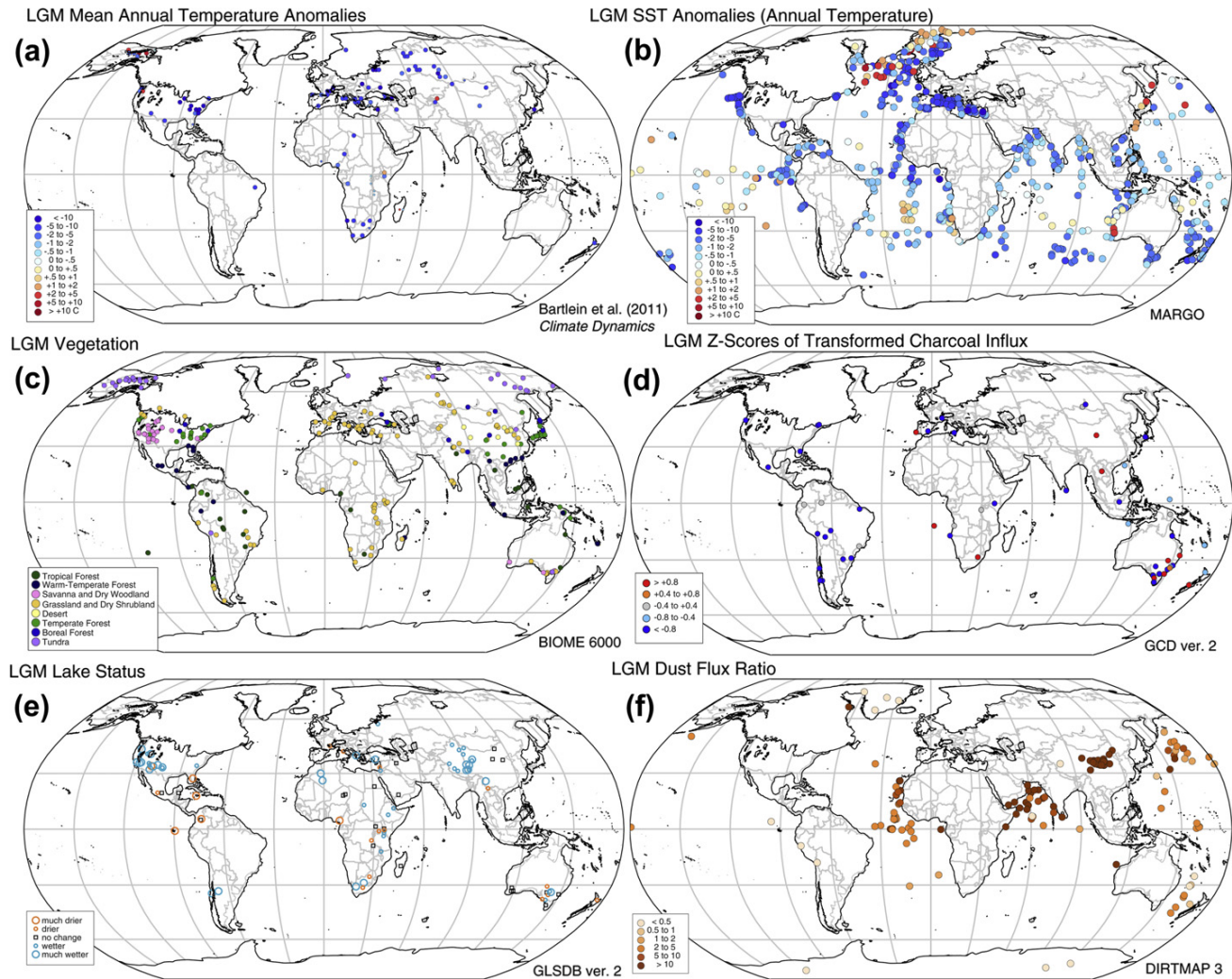
FIGURE 14.8 The world at the LGM (21 ka) as shown by palaeo-environmental data: (a) changes in mean annual temperature (MAT) compared to present-day reconstructed from pollen and plant macrofossil data (Bartlein et al., 2011); (b) changes in mean annual sea surface temperature (SST) compared to present day reconstructed from biological and geochemical climate proxies (MARGO Project Members, 2009); (c) vegetation reconstructions from the BIOME 6000 project (Prentice et al., 2000; Bigelow et al., 2003; Pickett et al., 2004; Marchant et al., 2009; and unpublished data), reclassified using the megabiome scheme described by Harrison and Prentice (2003); (d) changes in biomass burning compared to the long-term average between 21 and 0.25 ka, expressed as, from the Global Palaeofire Working Group Database (Version 2, Daniau et al., submitted); (e) changes in lake status compared to present from the Global Lake Status Database (Kohfeld and Harrison, 2000); (f) changes in dust deposition compared to present from the DIRTMAP database (v2: Kohfeld and Harrison, 2001).

lake data (though not vegetation records) suggest that the region around the Mediterranean Sea was also wetter. Charcoal records from China indicate increased fire (Figure 14.8d).

During the LGM, the tropics were colder and drier than today. Terrestrial records (Figure 14.8a) indicate an average cooling at sea level across the tropics of 2.5−3°C. This average hides considerable regional differentiation, with circum-Pacific regions experiencing relatively little cooling (1−2°C) and stronger cooling (5−6°C) in Central and tropical South America (Farrera et al., 1999; Bartlein et al., 2010). Marine records (MARGO Project Members, 2009)

show an average cooling in the tropics of 3−4°C, but again considerable regional differentiation in the strength of the change (Figure 14.8b). Cooling at high elevations, as shown by the lowering of snowline equilibrium lines, was larger than the cooling registered at sea level (Mark et al., 2005). Thus, tropical lapse rates must have been steeper than today. There was regional differentiation in the degree of high-elevation cooling, with sites in the northern Andes, Central America, and Papua New Guinea showing larger snowline depressions than sites in the Himalayas, the southern Andes, and eastern Africa. The charcoal records (Power et al., 2008) show less fire over most regions of the
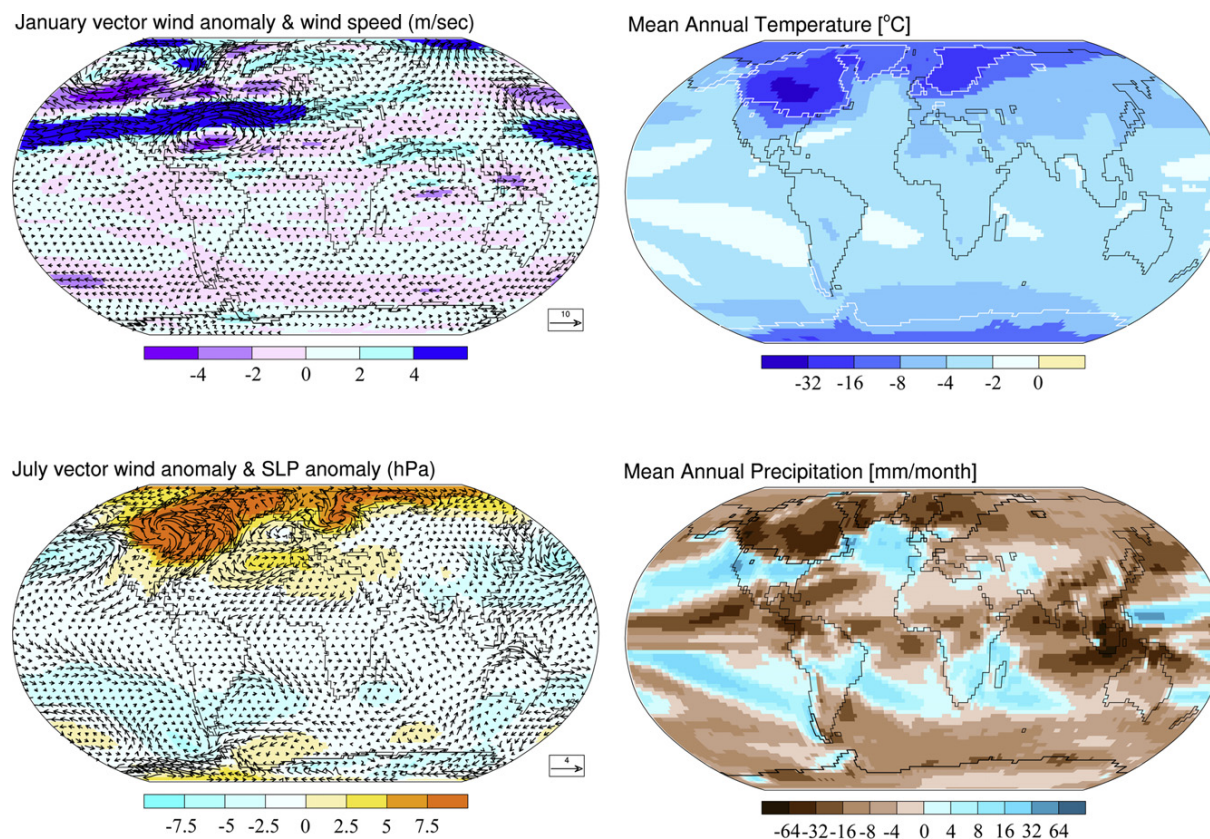
FIGURE 14.9   The world at the LGM (21 ka) as shown by ensemble-averaged differences between 21 ka and a pre-industrial control from coupled ocean−atmosphere climate model simulations from the Palaeoclimate Modelling Intercomparison Project (PMIP2, *http://pmip2.lsce.ipsl.fr*): January 500 hPa wind vector and wind speed (m s^{-1}) anomalies, mean annual temperature anomalies (°C), July sea-level pressure (SLP, hPa), surface-wind vector anomalies, and mean annual precipitation anomalies (mm per month). Comparison of this figure with Figure 14.8 illustrates one of the challenges of comparing palaeoclimatic simulations with observations: the climate model output must be expressed in the same terms as the palaeoclimatic data using 'forward' models, or the palaeoclimatic data must be interpreted in terms of specific climate variables using 'inverse' modelling procedures.

tropics, although some sites in South East Asia and Papua New Guinea (where the regional cooling appears to have been small) show more fire than today (Figure 14.8d).

Regional climate changes in the southern extra-tropics (Figures 14.8a, 14.8b) were less pronounced than those registered in the northern extra-tropics, close to the ice sheets. Nevertheless, both vegetation (Figure 14.8c) and lake (Figure 14.8e) data show colder and drier climates than today, while charcoal records indicate less fire (Figure 14.8d). Dust deposition records indicate that the decrease in vegetation cover and the increased aridity led to an increase in dust erosion and transport in the southern extra-tropics (Figure 14.8f), although this appears to have been less marked than the increase in the Northern Hemisphere. Marine data from the Southern Ocean show a northward shift of the polar front to about 45°S during the LGM, and sea surface temperatures during austral summer up to 2−6°C cooler than today (Figure 14.8b).

The changes in regional climates shown by these various palaeo-environmental sensors can be explained in terms of the glacial-age boundary conditions. Climate model experiments (Figure 14.9) show that the presence of large ice sheets, increased sea-ice cover, and low greenhouse gases led to globally colder and drier conditions (see Braconnot et al., 2007a). The wet conditions in American southwest, in the region around the Mediterranean Sea, and in western China are a specifically predicted consequence of the southern displacement of the Northern Hemisphere Westerlies as a consequence of the presence of the large, mountain-like mass of the Laurentide Ice Sheet (Kutzbach et al., 1993). Model simulations also show that changes in the tropics are more muted than those in the extra-tropics (see Braconnot et al., 2007a). The depression of tropical snowline is a consequence of the lowering of tropical sea surface temperatures, which is responsible for a drier atmosphere and, therefore higher lapse rates (Kageyama et al., 2005). This first-order effect is amplified by a weakening of the Asian monsoon, which led to a further increase in lapse rates in the northern tropics and around the western Pacific.

Although the observed vegetation changes at the LGM (relative to the Holocene) can be partially explained by the differential response of plant functional types to the change in climate at the LGM, vegetation distribution was also influenced by the physiological effects of low atmospheric CO_2 concentration on plant growth (Figure 14.10), and especially the impact of low CO_2 on plants using the C_3 photosynthetic pathway (including nearly all trees: Prentice and Harrison, 2009). Under low CO_2 concentrations, transpiration per unit leaf area is increased as a result of increased stomatal conductance. In plants using the C_3 photosynthetic pathway, photosynthesis is also reduced due to reduced substrate concentration and reduced competition by O_2 for carboxylation sites of the photosynthetic enzyme Rubisco. As a result, plants using the C_4 photosynthesis pathway can compete with C_3 plants more effectively under low CO_2 concentrations (Bond and Midgley, 2000). Atmospheric CO_2 concentration is a limiting factor for C_3

photosynthesis even at modern values (>380 ppmv) and was much more strongly limiting at glacial values (Polley et al., 1993; Guiot et al., 2001; Harrison and Sanchez Goñi, 2010). Modelling experiments have shown that the restricted forest cover during the LGM can only be reproduced accurately when physiologically mediated CO_2 effects on plant competition are taken into account (Harrison and Prentice, 2003). Since the nature of the vegetation cover influences the partitioning of precipitation into evapotranspiration and runoff, the influence of low CO_2 values could also impact on surface hydrology, including the amount of water feeding lakes and rivers at the LGM.

14.2.2. The Mid-Holocene

The mid-Holocene (~6000 years ago, 6 ka) was selected for detailed study because of its capacity to illustrate nearly pure effects of the insolation anomaly centred on 10,000 years ago. Although some high northern latitude records show a temperature maximum close to the peak of the insolation anomaly (Kaufman et al., 2004), most northern mid-latitude regions experienced a delayed temperature maximum due to the persistent regional cooling effect of the Laurentide ice sheet. Ice sheets were nearly at their present extents and atmospheric constituents were close to their pre-industrial values by the mid-Holocene, while the seasonal and latitudinal distribution of insolation was still substantially different from today, with increased summer insolation and enhanced seasonal contrast in the Northern Hemisphere and reduced summer insolation and decreased seasonal contrast in the Southern Hemisphere.

There is considerable asymmetry in the regional climate changes at high northern latitudes (Figures 14.11a, 14.11b), implying modulation of the direct insolation forcing through atmospheric circulation. Vegetation records (Figure 14.11c) show a northward extension of the Arctic tree line in Europe and Eurasia, as a consequence of increased warmth during the growing season (Prentice et al., 2000; Bigelow et al., 2003). Northern temperate forest zones were also shifted northwards, with displacements of even greater magnitude than that shown by the Arctic tree line. Warmer-than-present winters as well as summers are required to explain all of the observed northward shifts in the temperate forest zones. However, vegetation records from much of northern Canada and Alaska show no discernible northward shift (Edwards et al., 2000; Williams et al., 2000) and the tree line in eastern Canada was shifted southward compared to today (Richard, 1995; Williams et al., 2000). The southward expansion of shrub tundra and boreal woodlands was accompanied by an increase in fire in eastern Canada and the limited amount of data from northern Europe suggests that northward expansion of forests led to a reduction in fire (Figure 14.11d; Power et al., 2008).
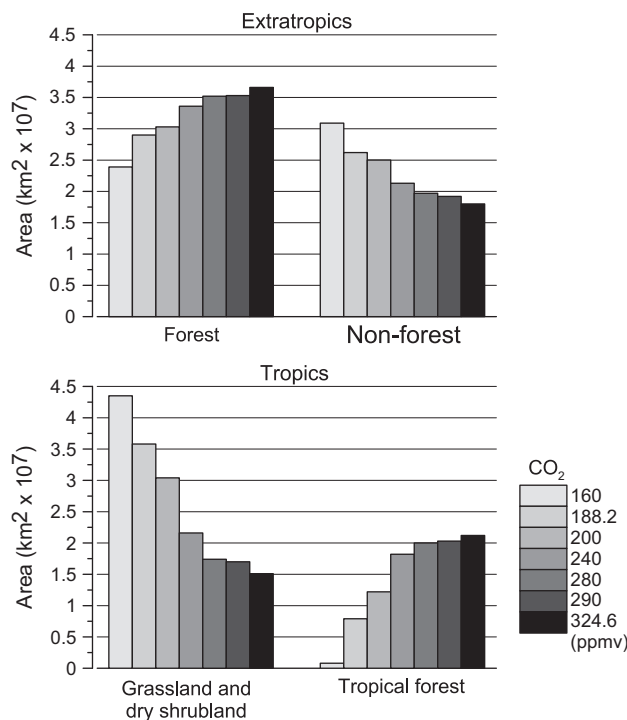

FIGURE 14.10 Simulated changes in biome area as a result of changes in CO_2 on the competition between C_3 and C_4 plants under modern climatic conditions. Changes in extra-tropical regions are summarized by changes in total forest versus total non-forest biomes; changes in the tropics by changes in the area of tropical forest compared to grassland/dry shrubland. In these simulations with the BIOME4 equilibrium biogeography−biochemistry model (Kaplan et al., 2003), atmospheric CO_2 levels have been systematically varied between 180 and 'modern' levels of 324.6 ppmv but climate was kept constant. The simulations show that the direct physiological impact of CO_2 can have major impacts on vegetation distribution *(Source: redrawn from Harrison and Prentice, 2003; Harrison and Sanchez Goñi, 2010).*
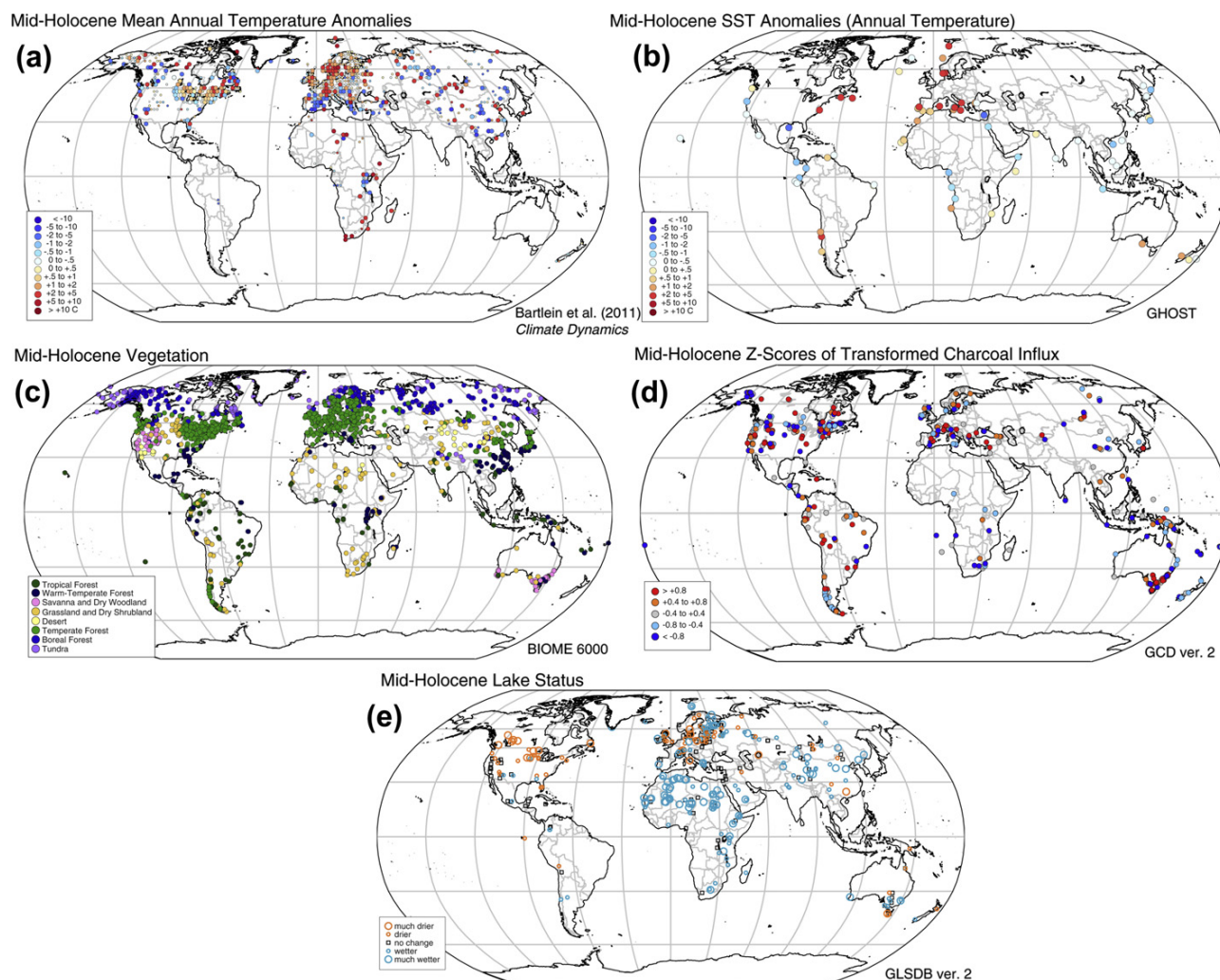
FIGURE 14.11   The world during the mid-Holocene (6 ka) as shown by palaeo-environmental data: (a) changes in mean annual temperature (MAT) compared to present-day, reconstructed from pollen and plant macrofossil data (Bartlein et al., 2010); (b) changes in mean annual SST compared to present-day, reconstructed from biological and geochemical climate proxies (Leduc et al., 2010); (c) vegetation reconstructions from the BIOME 6000 project (Prentice et al., 2000; Bigelow et al., 2003; Pickett et al., 2004; Marchant et al., 2009; and unpublished data, reclassified using the megabiome scheme described by Harrison and Prentice, 2003); (d) changes in biomass burning compared to the long-term average between 21−0.25 ka, expressed as z-cores, from the Global Palaeofire Working Group Database (Version 2, Daniau et al., submitted); (e) changes in lake status compared to present-day from the Global Lake Status Database (Kohfeld and Harrison, 2000). For most of the palaeoclimatic data types, the mid-Holocene is richer than that for the LGM, but the record of SSTs is sparser and confined mainly to oceanic regions with high sedimentation rates.

Temperate deciduous forests extended southward into the Mediterranean zone in Europe at 6 ka (Figure 14.11c), indicating summers wetter than today. Lake data (Figure 14.11e) also show wetter conditions at that time, and a progressive increase in aridity thereafter (Yu and Harrison, 1995). Charcoal records indicate a reduction of fire in lowland parts of the Mediterranean region, although sites at higher elevations tend to show increased biomass burning (Power et al., 2008).

The most pronounced changes in regional climate were registered in the region dominated by the Afro−Asian monsoon. Enhanced monsoons extended forest biomes inland in China, and Sahelian vegetation northward into the Sahara (Figure 14.11c). Lake data (Figure 14.11e) and aeolian data (Kohfeld and Harrison, 2003) also show an expansion of the region influenced by monsoon precipitation in both Africa and Asia. The African tropical rainforest was also reduced in extent (Figure 14.11c), consistent with a northward shift of the inter-tropical convergence zone (ITCZ) and a more seasonal climate in the equatorial zone. Vegetation and lake data show wetter conditions in the American southwest and Central America, consequent on the expansion of the North American monsoon, accompanied by expansion of steppe vegetation and aeolian activity in interior North America; this observed duality is explicitly predicted by climate modelling and attributed to

enhanced subsidence around the monsoon core region (Harrison et al., 2003). The charcoal record shows that changes in fire regimes were highly heterogeneous. This finding is consistent with our understanding that increased precipitation can lead to increased fuel loads and hence more fire in fuel-limited systems while, at sites where fuel is not limiting, increased precipitation suppresses fire (Van der Werf et al., 2008; Daniau et al., submitted).

The monsoon systems of the Southern Hemisphere were generally weaker during the mid-Holocene than today. Vegetation, lake, and charcoal data from South America suggest drier-than-present conditions (Markgraf, 1989; Mayle and Power, 2008; Marchant et al., 2009). Charcoal data indicate reduced fire in the southern tropics of Africa and northern Australia (Power et al., 2008; Mooney et al., 2010), consistent with reduced monsoons. However, some geomorphic evidence from northwestern Australia and the continental interior suggests that the Australian monsoon may have been stronger than at present (Shulmeister, 1999; Wyrwoll and Miller, 2001; Lynch et al., 2007).

Vegetation data from the southern extra-tropics (Figure 14.11c) show comparatively little change from present (Jolly et al., 1998; Marchant et al., 2009). Vegetation data from southern Australia show changes in plant-available moisture during the mid-Holocene, but adjacent regions show opposite signals in the direction of the inferred changes with the southernmost part of the region and Tasmania somewhat wetter than today and sites lying further north and along the east coast showing somewhat drier conditions (Pickett et al., 2004). Mooney et al. (2010) have identified a similar opposition in the regional changes in fire and suggest that this is consistent with shifts in atmospheric circulation. In contrast, lake data (Figure 14.11e) show wetter conditions uniformly across the southern extra-tropics, although this may reflect the comparative paucity of records from these regions.

The mid-Holocene has not been a major focus for the synthesis of marine records, in part because low sedimentation rates make it difficult to identify changes through the Holocene. In general, and in contrast to the marked changes in regional climates shown over the continents, ocean surface temperatures were similar to today over much of the world (Figure 14.11b). Records from the North Atlantic suggest that the mean annual surface ocean temperature was slightly higher than today, although late summer and autumn temperatures at high northern latitudes may have been slightly cooler (Kim et al., 2004; Leduc et al., 2010). Data from the tropical Pacific and Indian Oceans suggest that ocean temperatures there were slightly lower than today (Rimbu et al., 2004; Stott et al., 2004; Lorenz et al., 2006), possibly as a result of reduced ENSO variability (Tudhope et al., 2001). While these regional signals are consistent with changes in adjacent land areas, there is a lack of information from critical oceanic regions.

The first-order features of regional climate shown by these reconstructions can be explained as a consequence of known changes in forcing during the mid-Holocene. Orbitally-induced enhancement of Northern Hemisphere summer insolation at 6 ka resulted in increased heating over the Northern Hemisphere continents (Figure 14.12), deepening the thermal lows over the land and thus intensifying the flux of moisture from the tropical ocean to the continents (Kutzbach and Street-Perrott, 1985; COHMAP, 1988; Joussaume et al., 1999; Braconnot et al., 2007a). Increased heating over the northern subtropics resulted in the northward displacement of the ITCZ, and hence of the monsoon front, leading to drier conditions in the equatorial zone. Monsoon expansion is most pronounced in Africa and Asia because of their large continental area; the expansion of the North American monsoon is correspondingly more muted. Mid-Holocene aridity in the mid-continent of North America is caused by enhanced subsidence over the continental interior that is dynamically linked to the orbitally-induced enhancement of the summer monsoon in the American southwest (Harrison et al., 2003).

Warmer-than-present summers at high northern latitudes, as indicated by the northward shift of the Arctic treeline, are also a consequence of increased Northern Hemisphere summer insolation and the prolongation of warm conditions into the autumn caused by warmer oceans and less extensive sea-ice (Wohlfahrt et al., 2004). The pronounced longitudinal asymmetry in this warming appears to reflect the nature of ocean circulation in the Arctic, which results in sea-ice transport away from the northern coast of Siberia and towards Canada and which therefore amplifies the impact of orbitally-induced sea-ice reduction on the high latitudes of Eurasia while minimizing its impact on the high latitudes of Canada. The observed shifts in Northern Hemisphere temperate forests attest to warmer-than-present winters during the mid-Holocene, a signal opposite to the direct consequence of orbital forcing which would tend in the direction of colder winters (Kutzbach and Guetter, 1986). The paradox of warm mid-Holocene winters has been extensively discussed for Europe (see e.g., Prentice et al., 1998 and references therein), where it is generally attributed to stronger westerly flow around a strengthened Icelandic Low allowing warm air to penetrate further into the continental interior than is the case today.

In general, model simulations show a reduction in the Southern Hemisphere monsoons and comparatively little change in the southern extra-tropics (Braconnot et al., 2007a). However, some simulations have shown an enhancement of the Australasian monsoon during the mid-Holocene (see e.g., Liu et al., 2004; Marshall and Lynch, 2006). Reduction of the Southern Hemisphere monsoons is a direct response to changes in orbital forcing during the mid-Holocene. However, analyses of a large ensemble of mid-Holocene climate simulations (Zhao and Harrison,
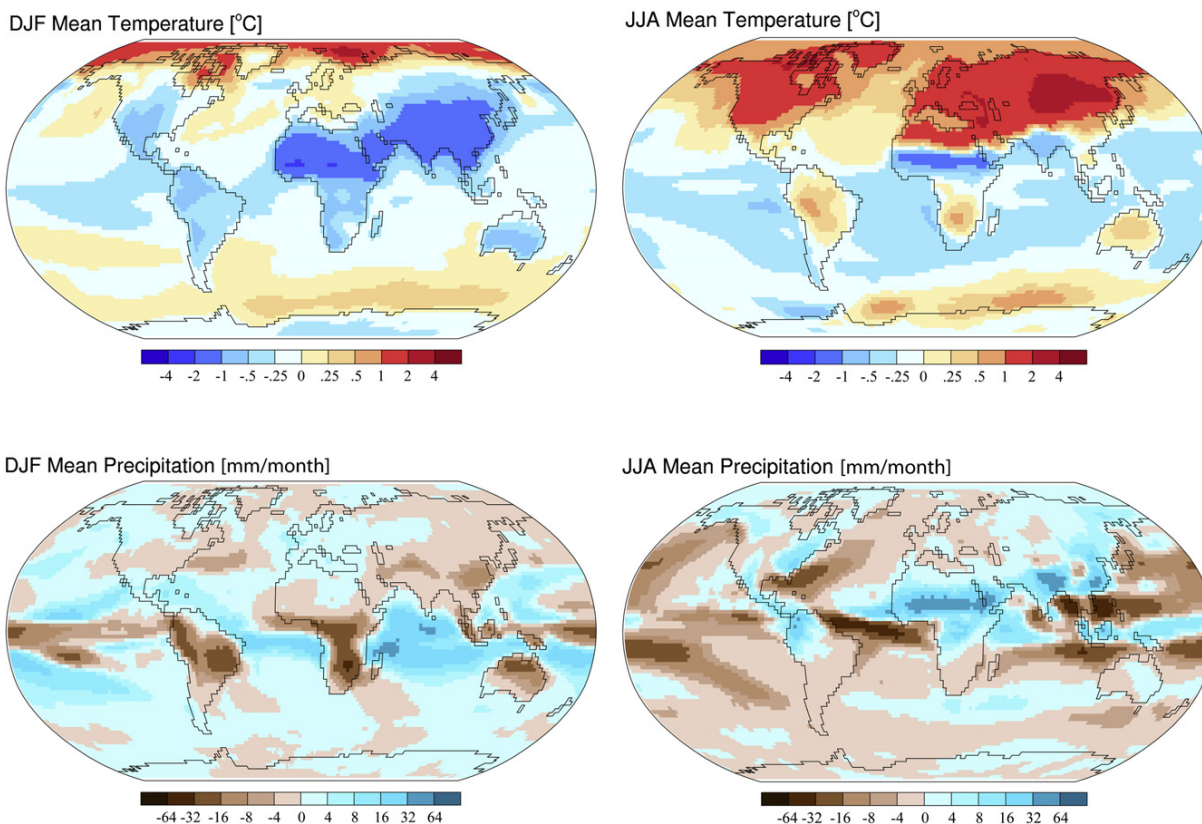
FIGURE 14.12 The world during the mid-Holocene (6 ka) as shown by ensemble averaged differences between 6 ka and a pre-industrial control from coupled ocean–atmosphere climate model simulations from the Palaeoclimate Modelling Intercomparison Project (PMIP2, *http://pmip2.lsce.ipsl.fr*): boreal winter (December, January, February, DJF) and boreal summer (June, July, August, JJA) mean temperature (°C) and precipitation (mm per month) anomalies.

in press) suggest that ocean feedbacks weaken the impact of orbital forcing in the Southern Hemisphere leading to a smaller decrease in monsoon rainfall than might otherwise be expected. In the case of the Australian monsoon, local changes in SSTs that generate a low-pressure cell over the Indian Ocean can create increased precipitation (compared to present) in northern and central Australia depending on the exact location of the low-pressure cell (Zhao and Harrison, in press). Observed differences in the timing of maximum monsoon expansion during the Holocene between different parts of the Afro–Asian monsoon region can be explained parsimoniously by two facts: (i) that the seasonal timing of the summer monsoon onset differs among subregions; and (ii) that the Holocene timing of the peak insolation anomaly is different for different months of the year (Marzin and Braconnot, 2009).

14.2.3. Consistency of Spatial Responses in Warm and Cold Climates

The palaeorecord shows that there are common features of the response to climate forcing in both cold and warm

climates, and that these features can be explained relatively simply. Most prominent among these is the comparatively muted response of the tropics to changes in forcing. At the LGM, for example, ice core (Stenni et al., 2001; Jouzel et al., 2003; Masson-Delmotte et al., 2005), sea-ice (Gersonde et al., 2005), permafrost (Renssen and Vandenberghe, 2003), and vegetation data (Prentice et al., 2000; Bigelow et al., 2003; Bartlein et al., 2010) all show major changes in temperature in the higher latitudes (>10°C) while both terrestrial (Farrera et al., 1999) and marine (Ballantyne et al., 2005; MARGO Project Members, 2009) data show comparatively small changes in temperature (<4°C) in the tropics. Climate changes during the glacial, associated with D–O cycles, are also stronger in the extra-tropics than in the tropics (Hessler et al., 2010; Harrison and Sanchez Goñi, 2010). Polar amplification (Masson-Delmotte et al., 2006) of temperature changes is also a feature of warm climates, including the mid-Holocene, the Last Interglacial, and the mid-Pliocene (CAPE-Last Interglacial Project Members, 2006; Jansen et al., 2007; Miller et al., 2010), and of projected future climates (Holland and Bitz, 2003; Masson-Delmotte et al., 2006; Meehl et al., 2007). Polar

amplification of temperature changes is, at least in part, a predictable consequence of feedbacks associated with changes in sea-ice, snow cover, and vegetation, and is reproduced in climate models.

Palaeo-environmental data show larger changes of land than of ocean temperatures in both cold and warm climate intervals, and this difference is observed in both tropical (e.g., Figure 14.13) and extra-tropical regions. Climate model projections of the response to greenhouse gas forcing consistently show that temperatures over land increase more rapidly than over sea, with a ratio in the range 1.36−1.84 independent of the simulated global mean temperature change (Sutton et al., 2007; Crook et al., 2011). The difference between land and ocean warming appears to be associated with land-surface feedbacks (Joshi et al., 2008). Analyses of palaeoclimate simulations (Lainé et al., 2009) suggest that this 'land/sea warming ratio' appears to be remarkably consistent through time.

Although glacial−interglacial temperature changes in the tropics are comparatively muted, there are large changes in precipitation associated with the waxing and waning of the monsoons (e.g., Dupont et al., 2000; Weldeab et al., 2007; Cai et al., 2010; Revel et al., 2010). The palaeorecord emphasizes the fact that climate changes in mid- to high latitudes are dominated by shifts in temperature, whereas changes in precipitation are the dominant

influence in tropical latitudes. The debate about polar amplification has, to some extent, obscured the importance of the large variations in tropical precipitation.

14.2.4. Different Spatial Scales of Response

The broad-scale patterns shown by palaeo-environmental data at the LGM and mid-Holocene can be explained as a consequence of changes in surface energy balance and atmospheric circulation due to large-scale changes in climate forcing. However, mapped patterns of environmental variables always show some heterogeneity: either individual sites that show a signal different from that registered at nearby sites, or small-scale regional patterns that run counter to the more zonal pattern of climate change. This heterogeneity is frequently thought of as noise or attributed to errors in the interpretation of the palaeo-records or to uncertainties in dating. However, this is not necessarily the case.

The characteristics of the sensor itself influence its sensitivity to climate change. For example, the response of the level of a lake to increased precipitation is determined by the relative size and shape of the lake and of its catchment (Harrison et al., 2002). The same change in precipitation is expected to produce different changes in lake level and area in nearby lakes that are otherwise

FIGURE 14.13 Comparison of simulated and observed changes in tropical temperatures at the LGM (21 ka) relative to present. The inferred temperature changes from pollen are from Ferrara et al. (1999), the inferred changes in SST are from the MARGO data set (MARGO Project Members, 2009). Zonally-averaged temperatures from the models are shown in grey for atmosphere-only simulations from PMIP1 and in colour for coupled ocean−atmosphere simulations from PMIP2 (Pinot et al., 1999; Kohfeld and Harrison, 2000). The data clearly illustrate the greater temperature anomaly over land relative to that over the ocean.
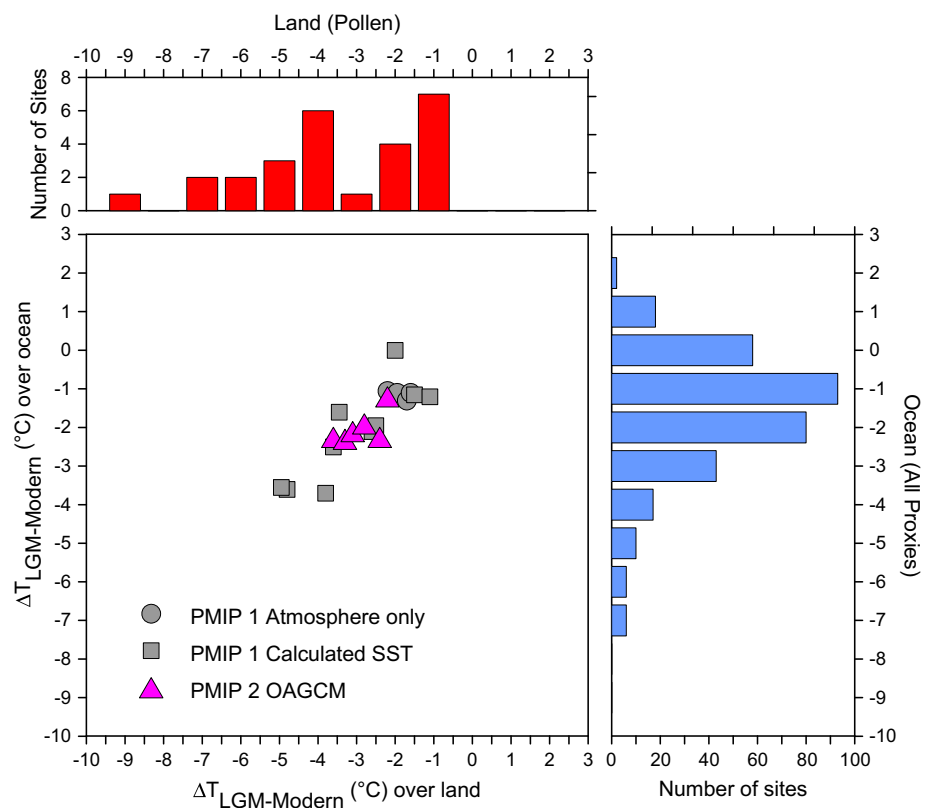
identical, for example, if the size of the catchment differs. Similarly, plants growing close to the limit of their range are expected to be more sensitive to a climate change of a given magnitude than the same plants growing in the middle of their range (Bartlein et al., 2010). A decrease in precipitation could lead to either an increase or a decrease in fire depending on whether the change leads to a decrease in the amount of fuel available or an increase in the dryness of the fuel (Van der Werf et al., 2008; Daniau et al., submitted.). Changes in the oxygen isotopic composition of ice reflect local temperatures but can also be influenced by changes in the seasonal timing of the precipitation that produced the ice (Werner et al., 2000; see also Lee et al., 2008). Changes in the composition of foraminiferal assemblages reflect the growth temperature of the assemblage, but may not directly reflect SST if changes in the structure of the mixed layer have caused changes in the depth at which the organisms live (Morey et al., 2005) or if other environmental factors influence productivity change (Siccha et al., 2009).

Spatial heterogeneity can also reflect the fact that contiguous areas of climate space are not necessarily contiguous in geographical space. This is most obvious in areas of complex terrain, where large spatial variations of climate occur in a limited geographical area. Physiography exerts an additional influence on climate through its modulation of the large-scale atmospheric circulation and results in the occurrence of distinctly different climate regimes in close proximity. The modern climate of the Yellowstone area in the western USA, for example, is characterized by a mosaic of summer- and winter-dominated rainfall areas (Figure 14.14). During the mid-Holocene, the vegetation record shows that sites that lie today in summer-dominated rainfall areas showed conditions wetter than present while sites from winter-dominated rainfall areas showed conditions drier than present. The apparently contradictory patterns of climate change in closely adjacent sites shown by the palaeorecords from this region (Figure 14.14) are nevertheless a predictable consequence of orbitally-induced changes in the North American monsoon. Sites fed by summer rains today received more rainfall with the amplified monsoon, while sites that are now summer-dry were drier still because of increased evaporation (Shafer et al., 2005).
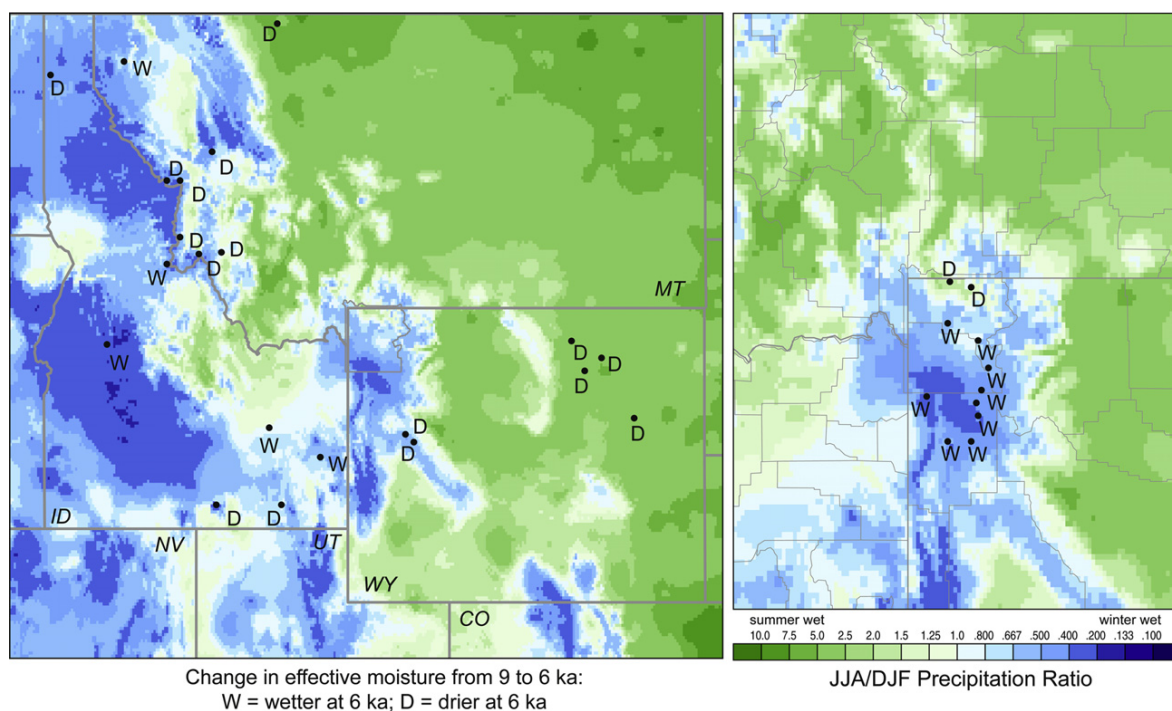

FIGURE 14.14 Relationship between modern climate patterns, as mediated by topography, and mid-Holocene climate changes in the northern Rocky Mountains, USA. The left panel shows modern precipitation seasonality (ratio of total precipitation in June−July−August, JJA, to December−January−February, DFJ), where green indicates a summer maximum and blue a winter maximum. The overlain letters indicate the change in moisture, as reconstructed from pollen data, between the early (~9 ka) and mid-Holocene (MH, ~6 ka) where W equals sites that have become wetter since the early Holocene and D equals sites that have become drier. The right panel is a blow-up of the region around Yellowstone National Park. The direction of the change in moisture between the MH and today is predicted by the modern seasonality. Sites that today are in the summer-dry/winter-wet region (blue) were drier in the early Holocene, while those in the summer-wet/winter-dry region (green) were wetter, paralleling the climate changes that made the summer-dry regions drier in the early Holocene and the summer-wet regions wetter *(Source: see Harrison et al., 2003. Redrawn from Shafer et al., 2005.)*

Physiography also has an impact at larger regional-scales. For example, lake records from the peri-Baltic region show drier conditions during the mid-Holocene (Figure 14.11e), and vegetation records show a more northerly penetration of warmth-demanding forests along the coast than in the interior of Sweden (Figure 14.11c). The Baltic was larger than today during the mid-Holocene, and the presence of this water body would have led to warmer winters (thus favouring northward penetration of temperate forest) and somewhat cooler summers with a circulation regime that would have favoured blocking of the Westerlies and hence increased aridity (Yu and Harrison, 1995). Vegetation records from northeastern North America (Figure 14.11c) show that Hudson Bay also had a localized impact on seasonal climates (Prentice et al., 2000; Bartlein et al., 2010). However, just as climate varies on multiple temporal-scales, so there is variability on multiple spatial-scales, reflecting the modulation of large-scale controls by a hierarchy of regional and local influences. The strength of the overall climate changes may determine the coherency of the spatial response: larger climate changes (e.g., LGM climates) may be sufficient to override topographic and physiographic influences.

14.2.5. Changes in Teleconnections/ Short-Term Variability

Interpretation of inter-annual/inter-decadal variability from palaeo-environmental records is complicated by the complexity of the climatic and environmental controls on these sensors. One interpretative approach that has been used is to link the observed variability in the recent past to variations in modes of atmospheric circulation (e.g., the North Atlantic Oscillation; ENSO; the Southern Annular Mode) and then to interpret longer-term variability shown in an individual palaeorecord as evidence for the changing strength of these modes (see e.g., Bradbury et al., 1993; Hammarlund et al., 2002; Donders et al., 2005; Björck et al., 2006; Quigley et al., 2010). This approach assumes that observed teleconnections are stable through time. However, analyses of meteorological records have shown that the strength of correlations between specific modes and local climate variables have changed even through the twentieth century (e.g., Figure 14.15) and certainly over the historical period (Cole and Cook, 1998; McCabe and Dettinger, 1998). Cole and Cook (1998; see also Cook et al., 2000) have shown that the modern correlation between ENSO and droughts in the southwestern USA was not present in the early part of the nineteenth century. Climate model simulations of the mid-Holocene response to orbital forcing are characterized by changes in the spatial patterns of teleconnections associated with the Arctic Oscillation (Otto-Bliesner et al., 2003; Figure 14.16) and

somewhat weaker ENSO teleconnections than seen in simulations of the present day (Otto-Bliesner et al., 2003; Figure 14.16), reinforcing the idea that such linkages are time-varying. Thus, while short-term variability in the region directly influenced by a specific mode may reflect changes in that mode, the use of this approach to interpret variability in more distant regions, teleconnected today, will lead to spurious conclusions. Furthermore, it obscures the work that is required: namely the use of networks of palaeo-environmental records to reconstruct modes of climate variability through time, paralleling the approach used with, for example, documentary evidence to reconstruct circulation patterns during the historical period (e.g., Luterbacher et al., 2002; Brázdil et al., 2005; Luterbacher et al., 2010).

14.3. RAPID CLIMATE CHANGES

A common feature of palaeoclimatic time series that appears on many different timescales (Figure 14.1) is the frequent occurrence of rapid or abrupt changes in the level or variability of the time series. These are also features of great importance for future climates (e.g., Lenton, 2012, this volume). The definition of what constitutes 'rapid' or 'abrupt' is somewhat arbitrary (Alley et al., 2002; Clark et al., 2008), but in general includes the idea of a change that occurs over several decades (or longer, on longer timescales), and that persists for an interval several times longer than the time taken for the change. The National Research Council (US) Committee on Abrupt Climate Change (Alley et al., 2002), in a definition adopted by the IPCC (Meehl et al., 2007), define *abrupt climate change* as one that takes place more rapidly than the underlying forcing, pointing out that this kind of behaviour can only occur when the climate system crosses a critical threshold defining the limit between two different climate states. This definition provides a theoretical basis for understanding abrupt climate changes (see e.g., Kageyama et al., 2010) but the rapidity of the climate change is a function of the temporal-scale of the specific forcing involved and the definition is thus difficult to apply in the case of palaeo-records where the nature of the forcing is *a priori* unknown. For practical reasons, many authors therefore identify abrupt climate changes in geological records in terms of some combination of magnitude of the change and the rapidity with which it is accomplished (see e.g., Martrat et al., 2004; Clark et al., 2008; Belcher and Mander, 2012, this volume). Although rapid transitions are inevitable in any time series that show the kind of short- or long-memory behaviour that climate time series do, there is a particular combination of mechanism and spatial pattern of response that involves the Atlantic Meridional Overturning Circulation (AMOC; also referred to as the thermohaline
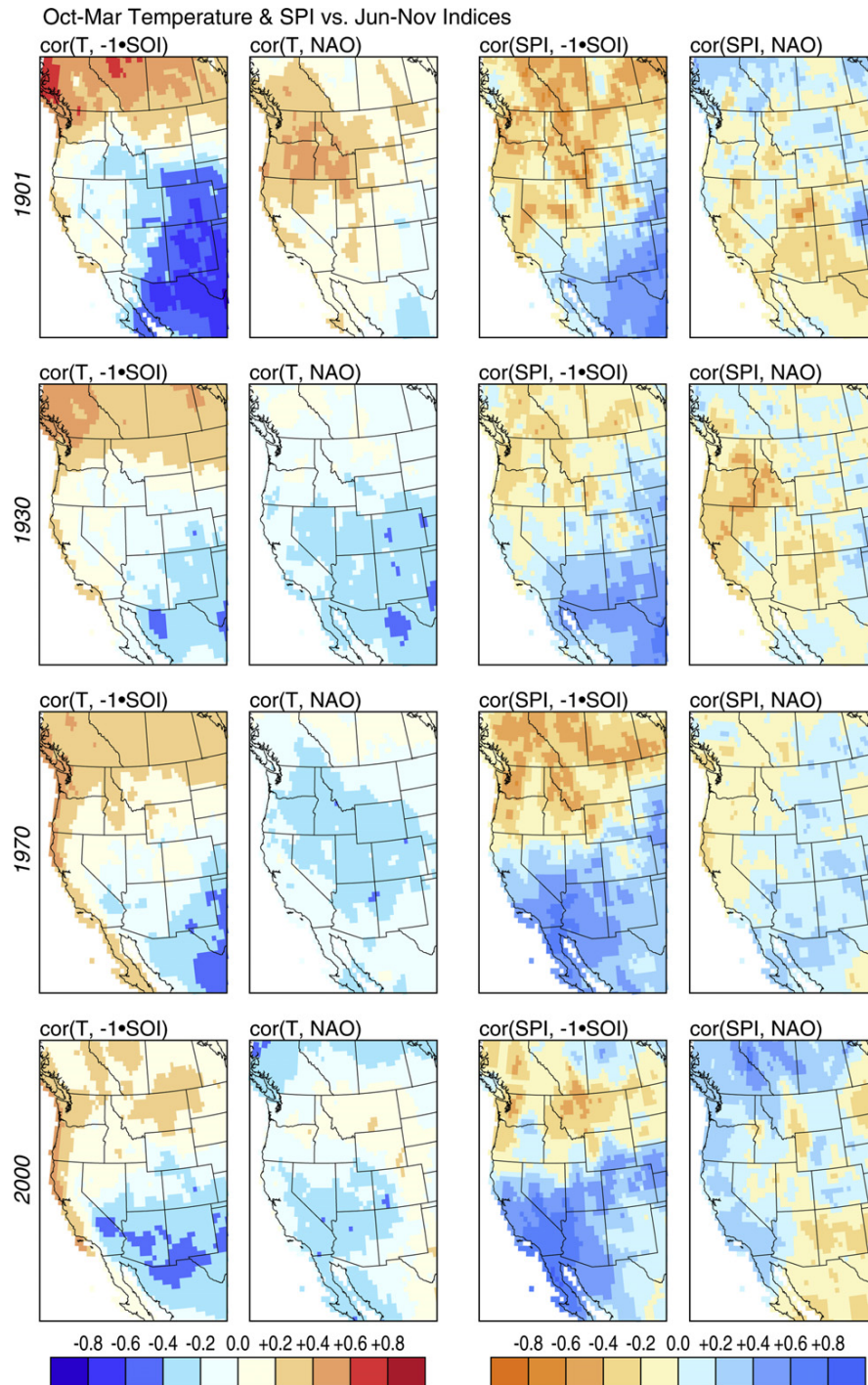
FIGURE 14.15   Maps of the correlations between temperature (left two columns) and the standardized precipitation index (SPI, right two columns) with two climate-mode indices, the Southern Oscillation Index (SOI) and the North Atlantic Oscillation (NAO) over western North America. The maps show correlations for four periods during the twentieth century (from top to bottom: 1901−1915, 1915−1945, 1955−1985, 1985−2000). The climate data are from the CRU TS 2.0 data set (Mitchell and Jones, 2005), the SOI was obtained at *http://www.cpc.noaa.gov/data/indices/* and the NAO index was obtained at *http://www.esrl.noaa.gov/psd/data/climateindices/list/*. Although the sign of the teleconnections (correlations) remain constant in the 'core' regions of the teleconnections (i.e., western Canada and the southwestern United States) the magnitudes and spatial patterns of the correlations vary, and in many regions correlations change sign over the twentieth century.
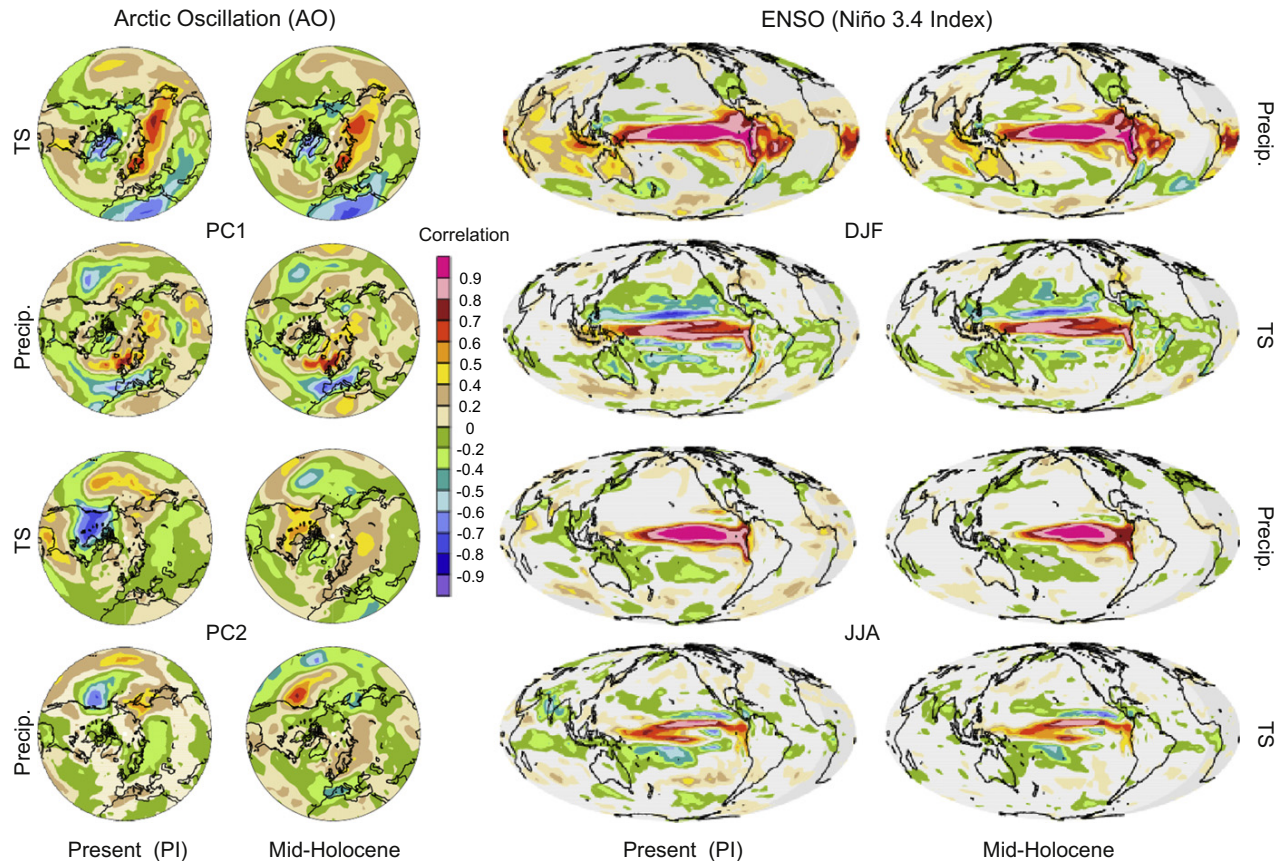
FIGURE 14.16   Correlations between two climate-mode indices, the Arctic Oscillation (left panels) and the El Niño−Southern Oscillation (ENSO), as represented by the Niño 3.4 index, and temperature (TS) and precipitation (Precip.) in pre-industrial (PI) and mid-Holocene simulations with the NCAR CCSM coupled ocean−atmosphere climate model (Otto-Bliesner et al., 2003). The PI is conventionally used for the modern baseline (control) simulation to avoid the impact of twentieth century climate change. As was the case for the regional teleconnection patterns shown in Figure 14.15, global teleconnection patterns vary between the mid-Holocene and pre-industrial (PI).

circulation, THC) that recurs frequently enough to warrant discussion as a distinct class of climate variability.

14.3.1. Examples of Rapid/Abrupt Climate Changes

On the longest of timescales (Figures 14.1a and 14.1b), climatic time series can be seen to experience changes in level (such as that around 34 Ma, accompanying the glaciations of Antarctica) or variability (such as that at 2.6 Ma, when the oxygen isotopic variations on the 41-kyr obliquity timescale became amplified and the repeated Northern Hemisphere glaciations began, or about 1 Ma, when 100-kyr variations became prominent). These transitions, which are rapid from the perspective of the particular timescale at which they appear, tend not to recur.

In contrast, on the millennial timescale over the past glacial interval (~80,000 to 11,700 years ago), there is a series of 20 instances of abrupt warming (Figure 14.1c), followed by more gradual cooling, referred to as D−O

'cycles' or Greenland Interstadials/Stadials (GI/GS) (Steffensen et al., 2008; Sanchez-Goñi and Harrison, 2010; Wolff et al., 2010). Although spaced roughly 1500 years apart, the specific length and form of the variations vary too much for the series to be regarded as periodic. Embedded in these variations are series of six occurrences of extreme cooling, known as Heinrich events or stadials. The individual warming events involved temperature increases on the order of 10°C in Greenland, and were accompanied by changes in climate, and in terrestrial and marine ecosystems, on a global scale.

During the last deglaciation (Figure 14.1d), there was an abrupt warming in the Northern Hemisphere ~14.7 ka, known as the Bølling−Allerød (BA) interstadial, that was followed by gradual cooling into the Younger Dryas chronozone (YDC). In the Southern Hemisphere, which had been warming gradually since the LGM (not evident in Figure 14.1), the Antarctic Cold Reversal − an episode of cooler temperatures − began around the time of the BA, and lasted through the YDC. The apparent opposition in deglacial temperature trends in the two

hemispheres is apparent in polar ice-core records throughout the last glacial, and has been referred to as the 'bipolar see-saw'. However, as will be discussed further below, the majority of the variability in temperature throughout the last glacial and into the deglaciation has been coherent between the hemispheres (Shakun and Carlson, 2010).

The abrupt changes apparent during the last glacial period (between 80,000 and 11,700 years ago) are also apparent in higher resolution marine and terrestrial records that span the past four glacial—interglacial cycles (Martrat et al., 2007), and so are a pervasive feature of past climatic variability. The particular abrupt changes of the last deglaciation are also present in some previous glacial terminations (i.e., Termination III, ~250,000 years ago), and so these abrupt changes are also not unique to the last glacial—interglacial cycle (Cheng et al., 2009).

During the Holocene (i.e., since 11,700 years ago), there are also examples of abrupt changes, some of these related to deglaciation (such as the '8.2 ka event' visible in Figure 14.1d), but others related to the effects of insolation on mid-continental aridity and the strength of the monsoon (reviewed in Cook et al., 2008; see also Williams et al., 2010). In general, these tend to be regional in extent, rather than global. On the centennial and decadal timescales over the past 1000 years, abrupt changes in the form of multi-centennial droughts are also evident in palaeoclimatic records (Cook et al., 2008, 2010), related to ocean—atmosphere interactions.

14.3.2. Characteristics of Dansgaard—Oeschger (D—O) Cycles

The nature of the D—O events can be explored using time series of terrestrial and marine records, and mapped syntheses of data similar to those reviewed above (Vogelsang et al., 2001; Voelker, 2002; Harrison and Sanchez Goñi, 2010). A typical terrestrial (pollen) record that spans the past glacial interval and is of high enough resolution to reveal the structure of the D—O cycles is that from Lago Grande di Monticchio, Italy (Allen et al., 2000; Fletcher et al., 2010; Figure 14.17). The record shows alternations between grassland and steppe vegetation during the cold (GS) part of one D—O cycle, and forest, with temperate elements during the warm (GI) part, reflecting variation in climate between cool/dry and warm/moist conditions (Allen et al., 2000; Fletcher et al., 2010). This pattern is superimposed on longer-term climatic variations related to orbital timescale variations in global ice volume, with more steppic vegetation during cool stages (i.e., Marine Isotopic Stages 4, MIS 4, ~74,000 to 59,000 years ago, and MIS 2, ~27,500 to 15,000 years ago), and more forested vegetation during warm stages

(i.e., MIS 3, ~59,000 to 27,500 years ago) (see also Berger and Yin, 2012, this volume).

These variations, which involve biome-level variations in vegetation (as opposed to more modest changes in species abundance), are registered in terrestrial records globally (Figure 14.17). In the northern extra-tropics, in particular, the difference in vegetation between a GI and GS consists of one or more 'steps' along a vegetation continuum between forest and steppe, or between tropical, warm, temperate, or boreal forest — changes in vegetation that encompass much of the total range of vegetation change between full glacial and interglacial conditions. Furthermore, the rapidity of the change in vegetation seen in these records attests to the rapid response of vegetation to the underlying change in climate.

The different components of the climate system adjust to, or participate in, these rapid climate changes with very little delay. The characteristic response of different variables can be seen by superimposing segments of (appropriately detrended) individual time series, aligning them relative to key times (such as the times of the GIs and GSs), a procedure known as superposed epoch analysis. If there is a consistent response, then this emerges as a distinct pattern in the average of the superimposed series; if not, the individual events cancel one another out, and no pattern appears. Confidence limits for the average series can be calculated using a Monte Carlo approach.

The NGRIP Greenland oxygen isotope record (Figure 14.18a), an index of regional temperature (North Greenland Ice Core Project Members, 2004; Svensson et al., 2008), shows the characteristic saw-tooth pattern of an individual D—O cycle, and all of the other records show distinctive responses associated with the occurrence of abrupt warming or cooling. The responses of all time series to the events are non-linear (linear responses would appear as inverted mirror images). The individual responses to abrupt warming can be categorized as *rapid* with no appreciable lag, such as those for methane (Loulergue et al., 2008; Figure 14.18b), dust (Lambert et al., 2008; Figure 14.18e), and biomass burning (Daniau et al., 2010; Figure 14.18f), all influenced by the hydrological status of the land surface, the nature of the vegetation cover and vegetation productivity, and *progressive* such as those for CO_2 (Ahn and Brook, 2008; Figure 14.18c) and N_2O (Figure 14.18d), which apply to atmospheric constituents with longer lifetimes. The responses to rapid cooling are similarly mixed, with those for CH_4 and dust again abrupt and rapid with no lag, and those for CO_2 and N_2O more gradual. There is an initial decrease of biomass burning in response to cooling, followed by a gradual recovery.

The superposed epoch analysis curves show that all parts of the climate system examined here co-vary with the
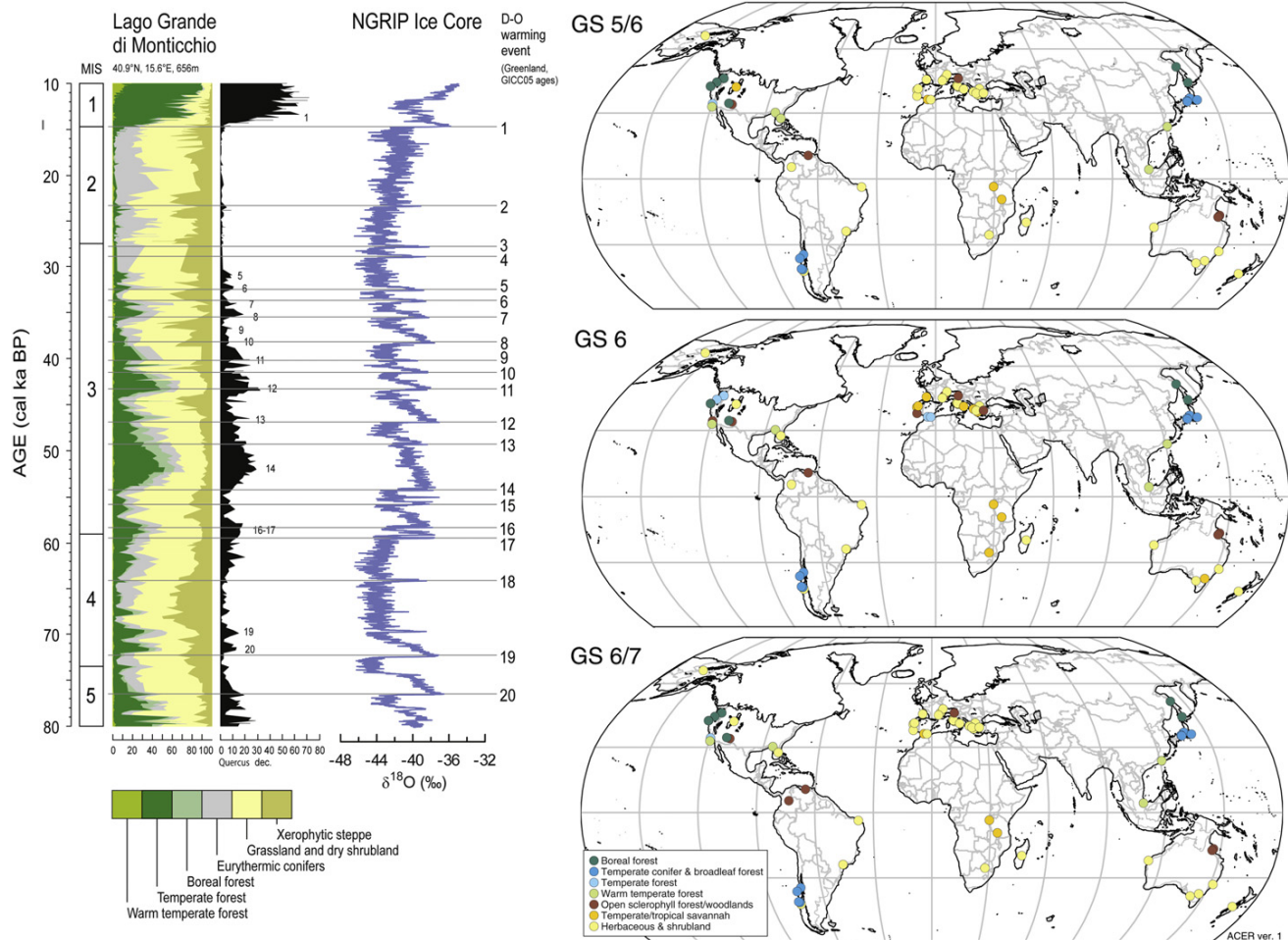
FIGURE 14.17 Vegetation changes associated with Dansgaard–Oeschger (D–O) cycles during the last glacial. The record from the Lago Grande di Monticchio, Italy *(Source: redrawn from Fletcher et al., 2010)* shows oscillations between grassland or steppe during colder intervals and forest during warm intervals. These changes can be related to the D–O cycles as registered by changes in $\delta^{18}O$ in the NGRIP ice core *(Source: redrawn from Wolff et al., 2010)*. The individually numbered D–O warming events are also shown. The maps show the biome registered at individual sites during a single D–O cycle (D–O 6): Greenland Stadial (GS) 6/7 through Greenland Interstadial (GI) 6 and into GS 5/6 *(Source: redrawn from Harrison and Sanchez-Goñi, 2010)*.

D–O events. Furthermore, the feedbacks from these co-variations are all positive, reinforcing either the warming or cooling recorded by the ice-core records. A general observation could be made that the response to the D–O changes is rapid, especially for those processes where changes in hydrology, productivity, or biophysics are involved, and are somewhat longer for carbon- and nitrogen-cycle related responses.

14.3.3. Mechanisms for D–O Cycles

The mechanism most often invoked for the generation of D–O variability involves variations in the strength of the AMOC, and the changes in ocean heat transport associated with that circulation (Rial et al., 2004; Delworth et al., 2008). The AMOC is the vertical component of the circulation of the North Atlantic that is driven by

increases in the density (through decreases in temperature and increases in salinity) of surface water in the North Atlantic and its consequent sinking (Kuhlbrodt et al., 2007; Latif and Park, 2012, this volume). Heat transported by both the AMOC, and by atmospheric circulation, into the North Atlantic ultimately warms the whole of the Northern Hemisphere and adjacent southern tropics (Stouffer et al., 2006; Pitman and Stouffer, 2006). Because the AMOC is driven in part by increasing salinity of the North Atlantic (as water evaporates from the warm, northward-flowing Gulf Stream), the intensity of the circulation can be diminished by increasing the flow of freshwater into the North Atlantic from increases in precipitation relative to evaporation, melting sea and land ice, and from river flow into the Arctic basin and North Atlantic. Both modelling studies and palaeoclimatic observations suggest that the changes in
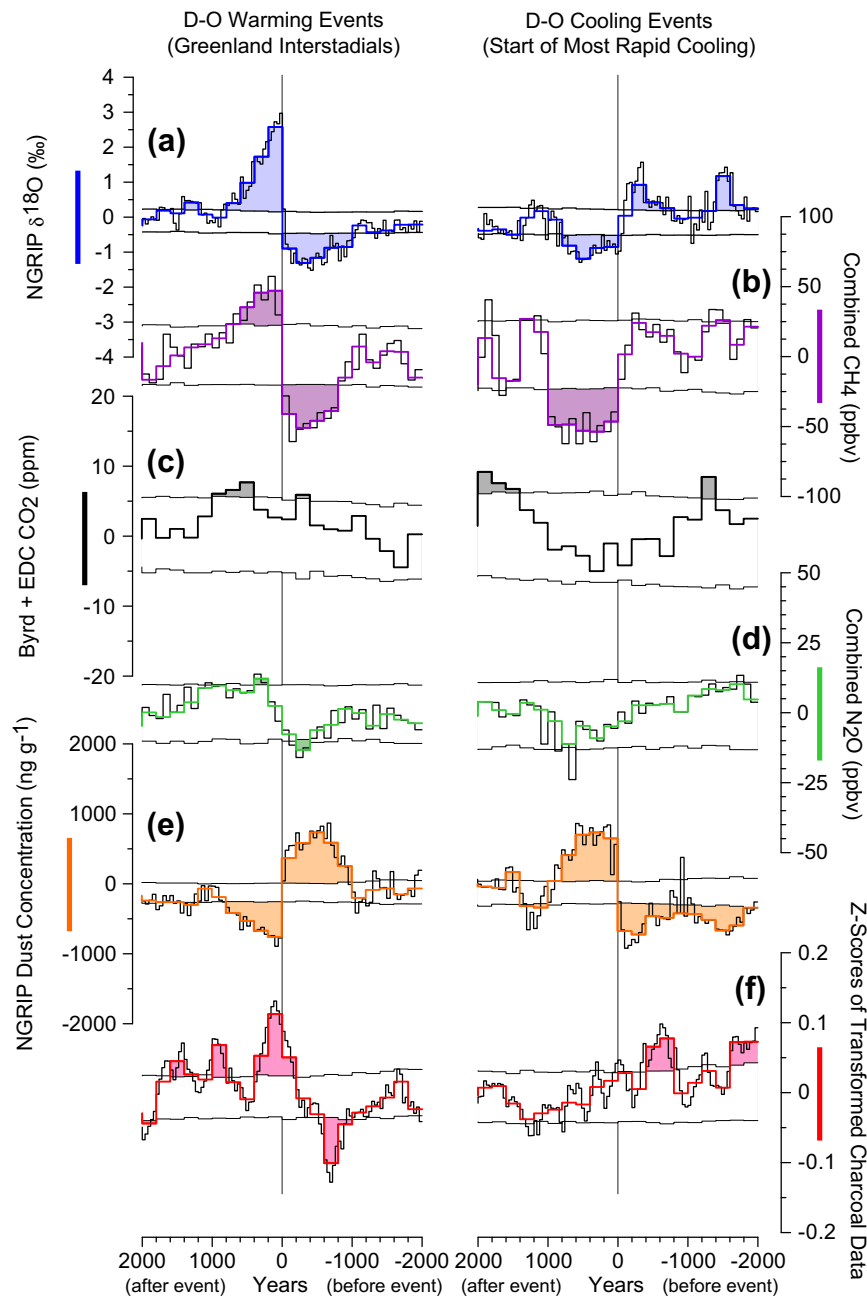
FIGURE 14.18 Superposed epoch analysis (SEA) of ice-core and biomass-burning records over the interval 80 ka to 10 ka. This analysis shows the consistent response of a time series to the repeated occurrence of the abrupt warming and cooling events that define the D−O cycles during the last glacial (MIS 4, 3, and 2). Shading indicates significant patterns in the response of the time series to the events of abrupt warming and rapid cooling. (a) The Greenland oxygen isotope record, an index of regional temperature, shows the characteristic saw-tooth pattern of an individual D−O cycle; (b−f) Distinctive responses of greenhouse gases (CO_2, CH_4, N_2O), dust, and fire associated with the occurrence of abrupt warming or cooling. BYRD: Byrd station, Antarctica; EDC: EPICA Dome C; NGRIP: North Greenland Ice Core Project. Redrawn from Arneth et al. (2010), see text for data sources. The curves show that all of the components of the climate system represented by these variables respond or co-vary with the abrupt changes recorded in the Greenland oxygen isotope record, with variables that describe terrestrial ecosystems or surface hydrology (dust, CH_4, biomass burning) responding relatively rapidly.

intensity can be abrupt, involving both threshold exceedance and hysteresis (Ganopolski and Rahmstorf, 2001; Rind et al., 2001; Roche et al., 2004; Braun et al., 2005; Rahmstorf et al., 2005; Clement and Peterson, 2008). In a typical progression through a GS and GI pair, the AMOC gradually slows or collapses producing the cold stadial (or Heinrich event) and then abruptly resumes, producing the rapid warming. However, the magnitude of the variations in greenhouse gases and dust accompanying the abrupt warming or cooling (Figures 14.18a−14.18e), indicates that the radiative

forcing by these controls of the energy balance, when further amplified by, for example, water vapour, cloud, and land-cover changes, must contribute significantly to the amplitude of the D−O variations.

14.3.4. Spatial Patterns of D−O Cycles

As might be expected, the D−O variations are strongly expressed in the circum-North Atlantic region, but Figure 14.17b suggests that the variations are expressed globally to one extent or another. There are three potential

mechanisms for 'transmission' of the North Atlantic-focused climatic variations: (i) transmission by the AMOC itself, (ii) transmission via atmospheric circulation changes, and (iii) transmission via changes in atmospheric composition and its influence on radiative forcing; or some combination of these mechanisms. Transmission by changes in the AMOC circulation is consistent with the idea of a 'bipolar see-saw' in which the high-latitude climates of both hemispheres vary in opposition with one another. When the AMOC circulation shuts down, or diminishes in intensity, the heat formerly transported to the high northern latitudes would remain in the tropics (and presumably also in the Southern Hemisphere). This mechanism has been invoked to explain the apparent inverse correlation between millennial-scale variations in the Arctic and Antarctic ice cores (EPICA Community Members, 2006). Transmission by atmospheric circulation changes has been proposed, motivated by the large impact that the North American ice sheet and North Atlantic sea-ice have on atmospheric circulation of the Northern Hemisphere, including that of the monsoon regions (Clark et al., 2002). Although plausible changes in the Laurentide Ice Sheet that accompany Heinrich events evoke a large-scale response in an atmospheric model, it is not clear whether the same responses would occur for smaller variations in the ice sheets or in a coupled atmosphere−ocean model. The potential of the third mechanism, changes in atmospheric composition, can be seen in the superposed epoch analysis (SEA) (Figure 14.18), where the effects of the changes in greenhouse gases and dust accompanying both the warming and cooling events would be almost instantaneous (on this timescale) around the globe.

Although the polar ice core records support the idea of opposition (and the AMOC circulation mechanism), the latitudinal extents of the opposition cannot be ascertained from those records alone. Analyses of networks of palaeoclimatic time series suggest, however, that the latitudinal extent of the opposition is indeed restricted. Shakun and Carlson (2010) analysed 104 high-resolution records (primarily marine, but including some terrestrial records) spanning the last deglaciation and found that over 60% of the total variability among the records had a coherent global pattern that was similar in sign, while a hemispherically contrasting pattern explained only 11% of the total variability. The time series describing the expression of the first pattern could be related to the general trend of both CO_2 concentration and sea level over the interval, while that for the second pattern resembled an indicator of AMOC strength. Clark et al. (2007) examined 39 records spanning MIS 3 and found a similar ordering of modes, with the 'northern' (i.e., general global) mode again more important than a hemispherically contrasting one. These results support the transmission of the D−O variations by the atmospheric circulation or atmospheric composition

mechanisms, but do not preclude a role for AMOC changes in their origin.

14.4. BIOSPHERE FEEDBACKS

Palaeo-environmental records document large-scale changes in vegetation, surface hydrology, and other land-surface properties in response to changes in external forcing. These changes tracked changes in climate with no discernible lag, even in response to rapid climate changes (Arneth et al., 2010; Harrison and Sanchez Goñi, 2010). Such readjustments necessarily affected the surface-water and surface-energy balances, leading to feedbacks to climate at a regional scale. Biophysical feedbacks have been identified as playing an important role in, for example, maintaining differences in the ratio of land/sea responses to climate forcing (Lainé et al., 2009), amplification of high latitude climate changes (Foley et al., 1994; Ganopolski et al., 1998; Jahn et al., 2005), and monsoon enhancement (Kutzbach et al., 1996; Schurgers et al., 2007; Dallmeyer et al., 2010; Dekker et al., 2010).

High latitude climate warming causes expansion of forest at the expense of tundra vegetation. In addition to being darker, trees shelter the surface, thus reducing the contribution of snow cover to surface albedo and leading to increased surface warming. The immediate effect of these changes in albedo (and associated changes in surface roughness and evapotranspiration rates) is large, potentially doubling the orbitally induced warming; but perhaps a more important consequence of such biosphere feedbacks is on the persistence of the influence of the climate forcing. Model-based studies have shown that vegetation feedback leads to year-round warming (de Noblet et al., 1996; Ganopolski et al., 1998; Wohlfahrt et al., 2004), effectively reversing the impact of direct orbital forcing on winter temperatures. Model-based studies of the Northern Hemisphere monsoons have also shown that land-surface feedbacks affect precipitation seasonality, prolonging the monsoon season into the autumn when the direct effect on insolation forcing is waning (Broström et al., 1998; Braconnot et al., 1999; Irizarry-Ortiz et al., 2003; Dallmeyer et al., 2010). Thus, biospheric feedback provides a mechanism for producing counterintuitive responses to orbital forcing.

Biophysical feedbacks have also been implicated in the generation of abrupt responses to gradual changes in insolation. Studies with simplified climate models, for example, have suggested a role for vegetation−climate feedback in hastening the apparent collapse of the northern African monsoon around 5.4 ka (e.g., Claussen et al., 1999, Renssen et al., 2003), although this mechanism is not supported by more recent simulations with coupled atmosphere−ocean−vegetation models (Liu et al., 2006, 2007; Braconnot et al., 2007b).

Vegetation-controlled changes in atmospheric dust concentrations have also been implicated in rapid climate change, through both biophysical and biogeochemical mechanisms. During Heinrich Stadials and the last deglaciation, for example, atmospheric dust concentration decreased rapidly (deMenocal et al., 2000; Peck et al., 2004; Mulitza et al., 2008), implying a rapid decay of both its net radiative cooling effect (Claquin et al., 2003) and the aeolian supply of iron to the Southern Ocean, which may have increased marine export production and thus contributed to keeping CO_2 low during cold climate phases (Bopp et al., 2003). Analyses of records of marine export production records during the last interglacial and glacial periods show that iron fertilization cannot explain the initial glacial drawdown in CO_2 but could be responsible for the further 15−20 ppmv lowering that occurred during the glacial maximum (Kohfeld et al., 2005).

Carbon cycle feedbacks involving the terrestrial biosphere are potentially important on various timescales. A pervasive *negative* feedback results from the CO_2 fertilization effect on terrestrial primary production. This effect is needed to explain the 300−700 PgC increase of terrestrial carbon storage from the LGM to the Holocene, as indicated by $\delta^{13}C$ in marine benthic foraminiferal tests (Bird et al., 1996; Prentice and Harrison, 2009). This storage increase opposed the CO_2 rise, by taking additional carbon out of the atmosphere. Rapid terrestrial biosphere growth has also been invoked to account for the observed (transient) dip in atmospheric CO_2 concentration that culminated around 8000 years ago, after the initial deglacial rise (Joos et al., 2004). On the other hand, warming alone is expected to reduce terrestrial carbon storage (a positive feedback: Denman et al., 2007; Dickinson, 2012,

this volume). This mechanism has been invoked to explain the observed dip in CO_2 concentration during the Little Ice Age (Figure 14.19: Joos and Prentice, 2004; Friedlingstein and Prentice, 2010). Furthermore, the oceanic $CaCO_3$ compensation mechanism may partially explain the steady (about 20 ppmv) rise in atmospheric CO_2 that took place during the Holocene, after 8 ka (Joos et al., 2004). This mechanism involves the slow (multimillennial-scale) response of marine $CaCO_3$ sedimentation to the extraction of CO_2 from the ocean−atmosphere system as the deglaciation progressed.

Modelling of carbon cycle changes over these timescales has generally neglected the role of peatlands, yet these are a significant and dynamic carbon store (Figure 14.19). Northern peatlands cover around 4 million km^2, contain an estimated 545 PgC (Yu et al., 2010), and also contribute as much as 5−20% of total contemporary CH_4 emissions (Zhuang et al., 2004; Denman et al., 2007; Harvey, 2012, this volume). Peatland growth has been estimated to produce a long-term carbon sink of 0.07−0.1 PgC per year (Dean and Gorham, 1998; Yu et al., 2010). There was little or no peatland in the high northern latitudes during the LGM (Figure 14.19). New peatland growth over large areas began during the deglaciation; almost half of the modern area of peatlands accumulated before 8 ka (Figure 14.19; MacDonald et al., 2006; Gorham et al., 2007; Yu et al., 2010). It has been estimated that peatland growth prior to 8 ka sequestered about 100 PgC, potentially contributing to the observed dip in CO_2 and also to the peak in atmospheric CH_4 in the early Holocene (Yu et al., 2010). Peatland productivity and decomposition are highly sensitive to temperature changes; hence, carbon sequestration in peatlands can vary on decadal to millennial timescales
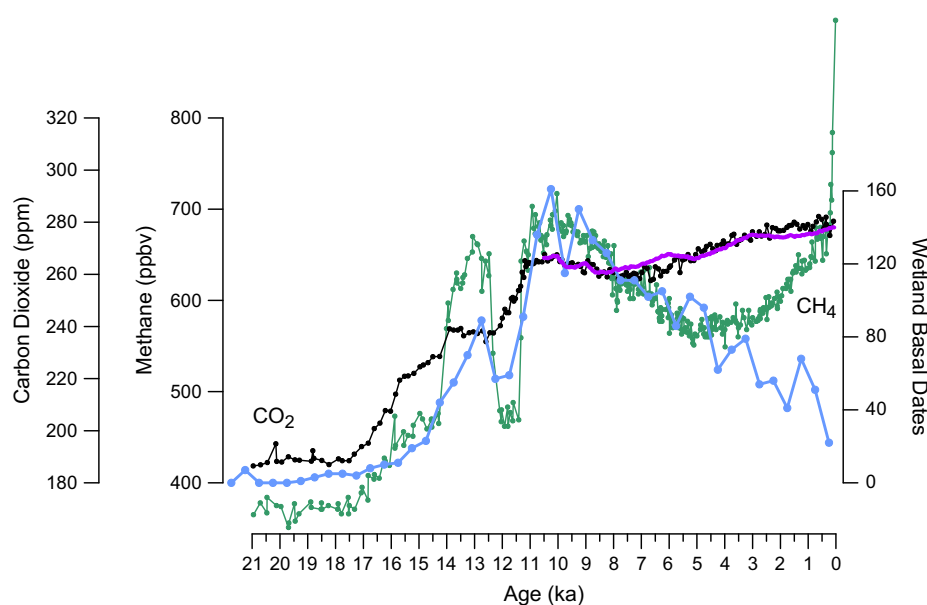

FIGURE 14.19 Relationship between peatland growth and carbon cycle indicators since the LGM (~21 ka). Basal radiocarbon dates on northern peatlands (blue dots, Harrison, unpublished data) provide an index for the timing of peatland initiation and spread. The CO_2 (black: Lüthi et al., 2008) and CH_4 (green: Loulergue et al., 2008) records are from Antarctic ice cores. Simulated changes in CO_2 during the Holocene (purple) from Joos et al. (2004).

(Singarayer et al., 2011). Increased accumulation rates are registered during the early to mid-Holocene thermal maximum (e.g., Kaufman et al., 2004), for example, and substantially reduced accumulation occurred during the cold intervals of the Younger Dryas and the Little Ice Age (e.g., Mauquoy et al., 2002; Charman et al., in review). The impact of changes in peatland accumulation on climate is uncertain because of the competing influences of changes in C sequestration and CH_4 emission and the timescales over which these operate. Frolking et al. (2006) have suggested that the initial impact of northern peatland growth is net warming that peaks after about 50 years after peatland initiation but remains positive for the next several hundred to several thousand years, depending on the rate of carbon sequestration, although in the longer term this would change and peatlands would have an increasing net cooling impact. However, these calculations were made without taking into account the impact of climate variability on peatland growth, carbon uptake, and CH_4 emissions.

Analyses of inter-hemispheric gradients in ice core CH_4 concentrations and carbon isotope composition ($\delta^{13}C\text{-}CH_4$) have been interpreted as suggesting that changes in wetland emissions drove glacial−interglacial changes in CH_4 concentration (Chappellaz et al., 1993, 1997; Schaefer et al., 2006; Harvey, 2012, this volume). However, published simulations to date using simple formulations of wetland extent and emissions have been unable to reduce wetland sources sufficiently to effect the observed changes in atmospheric CH_4 concentration (Kaplan, 2002; Valdes et al., 2005). It has been speculated that rapid shifts in atmospheric CH_4 during the last glacial (associated with D−O events) and after the deglaciation were caused by changes in Northern Hemisphere wetland emissions (Brook et al., 2000; Dallenbach et al., 2000; Korhola et al., 2010), although this finding is not consistent with recent modelling experiments (Singarayer et al., 2011).

The large-scale changes in vegetation distribution and productivity, and in fire regimes, shown on both glacial−interglacial and millennial timescales could potentially have had significant impacts on other biogeochemical cycles, and most particularly on the release of atmospheric trace gases and aerosol precursors. Model simulations show a substantial reduction (about 40%) in non-methane biogenic volatile organic compound emissions at the LGM, resulting in an increased atmospheric sink for CH_4 and, thus, potentially helping to explain the reduction of methane during glacial intervals (Valdes et al., 2005). However, this result could be negated by the finding that isoprene emission is enhanced at low CO_2 concentration (Arneth et al., 2010). N_2O variations during warm periods have also been tentatively attributed to changes in vegetation (e.g., Flückiger et al., 2002; Spahni et al., 2005). Thonicke et al. (2005) suggested that biomass burning was reduced by only 25% globally but with a marked increase

in fire in the equatorial zone. The overall reduction in pyrogenic emissions was insufficient to explain observed changes in atmospheric composition. However, Thonicke et al. (2005) argued that enhanced NO_x emissions as a result of increased burning in the tropics could have increased the oxidizing capacity of the atmosphere and helped to explain the observed low atmospheric CH_4 concentrations during the glacial. This hypothesis has not been examined quantitatively. There remain large uncertainties regarding the control of atmospheric CH_4 and N_2O.

Models used to project the emissions of greenhouse gases consistent with stabilization of climate at different levels usually assume a quasi-linear behaviour of the climate system that does not produce abrupt changes, even if feedbacks are considered (House et al., 2008). However, this modelling approach would not fully account for the observational record of the past (Alley et al., 2003; Jansen et al., 2007), which shows that periods of stability or gradual change (e.g., due to orbital forcing) have been interrupted by rapid state transitions, with large-scale warming and cooling events linked to atmospheric circulation shifts that in some cases took less than a decade to complete (Steffensen et al., 2008). Abrupt transitions and events have occurred during periods when changes in external drivers were much more gradual. Furthermore, rapid changes have commonly been associated with changes in atmospheric composition, including changes in atmospheric concentrations of greenhouse gases (CO_2, CH_4, N_2O) and aerosols (e.g., black carbon, mineral dust) that indicate changes in the land biosphere and/or the circulation and biogeochemistry of the oceans, with the potential to reinforce the climate change. For example, concentrations of these three greenhouse gases closely tracked polar temperatures during the global warming intervals that initiated the Holocene and last interglacial periods (EPICA Community Members, 2004). The change in CO_2, especially, was large enough to contribute substantially to the subsequent maintenance of warm conditions, implying a positive feedback that presumably contributed to the rapidity of the warming (Jansen et al., 2007). Ice core records show that atmospheric composition has tracked changes in climate at least over the past 800,000 years (EPICA Community Members, 2004; Spahni et al., 2005; Lambert et al., 2008; Loulergue et al., 2008; Lüthi et al., 2008), with the phasing of changes in individual greenhouse gases modulated by differences in the temporal and spatial patterning of biospheric feedbacks (see e.g., Flückiger et al., 2002).

14.5. LESSONS FROM THE PAST FOR THE STUDY OF CLIMATE CHANGES

The palaeorecord is rich in information, providing opportunities for exploring the mechanisms of climate changes

and cautioning against simplistic or single-factor explanations for such changes.

Climate changes impact on all aspects of the environment, which provides a wealth of different possible indicators or sensors. However, each of these sensors responds to a different set of climate controls and on different timescales. The hierarchical nature of the climate system means that changes in these climate controls can be brought about in many different ways. Thus, individual sensors may apparently display congruent or non-congruent responses depending on how the overarching controls impact on the direct controls of the individual sensors. The inherent complexity of the climate system makes it important to develop a mechanistic understanding of the direct controls on individual sensors in order to be able to interpret the records in terms of climate change.

The hierarchical nature of the climate system also makes it clear that simple, single-factor climate explanations for changes in palaeorecords are inherently likely to be wrong. This point applies equally to geochemical and biological sensors. By exploiting the fact that individual sensors have different controls, and that no one sensor is more closely tied to climate than any other, we should be able to exploit multiple sensors to reconstruct a more complete picture of the nature of climate change at any time. As a corollary, forcing multiple sensors to reconstruct the same climate variable (e.g., July temperature) involves both a loss of explanatory power and an incomplete understanding of how the climate system works.

The hierarchical nature of climate is also apparent in terms of spatial patterns. Large-scale controls can be registered quasi-globally, but regional atmospheric circulation patterns and local factors (e.g., the presence of water bodies, complex topography) modulate the global signal. Processes affecting the sensor, and that themselves are influenced by climate, may further modulate the global signal. As a consequence of the mediation of large-scale controls by local features and processes, climate changes display spatial patterns at multiple scales. Furthermore, simple patterns in climate space may not map into simple patterns in geographical space. The ice-core records of well-mixed greenhouse gases are an important exception, but most records (including ice-core records of temperature) can only represent local or regional climate signals. Consequently, iconic or 'golden spike' records do not provide an adequate description of past climate changes. Such records should not be extrapolated to continental, hemispheric, or global-scales. Large-scale data syntheses frequently disprove simplistic interpretations based on one or a few sites. Large-scale, large magnitude climate changes may produce a homogeneous response, but spatial heterogeneity is much more common.

A further consequence of the non-stationarity and hierarchical nature of climate is that teleconnection patterns must vary through time. This can be verified both in historical observations and palaeoclimate simulations. The interpretation of palaeorecords in terms of an apparent modern linkage to some distant phenomenon, in the absence of a mechanistic relationship, is therefore not justified.

Many authors have identified multiple cycles or periodicities in palaeoclimate time series. However, this does not make them real. Apparent cyclicity can be generated by simple time series models or by data-analytic techniques. While this does not preclude the existence of real cyclicity in palaeorecords, the only periodicities that can be explained mechanistically are those tied to orbital forcing and the seasonal cycle. Identification of periodicities does not provide insights into the mechanisms of climate change, although understanding of the mechanisms helps to distinguish between real and spurious climate cycles.

We have shown that orbital forcing, and concomitant re-organisation of the atmospheric and oceanic circulations, explains many aspects of the temporal and spatial variability of climate during the late Quaternary. Nevertheless, much remains unclear about the detailed mechanisms by which these initial forcings are translated into the observed patterns of spatial and temporal variability. While it is clear that orbital variations drive climate variability on glacial—interglacial timescales, for example, the precise cause of glacial initiation and the explanation of the strength of the 100 kyr cycle remain obscure. Similarly, D—O cycles are linked to changes in the AMOC but such changes fail to explain why this signal is quasi-global or the differences among D—O cycles and between D—O cycles and Heinrich events. Biosphere feedbacks are likely to play a role here, both in amplifying the impact of relatively small changes in forcing and, through their control of greenhouse gas concentrations, in translating a localized forcing into a global response. Biophysical feedbacks associated with the terrestrial biosphere, and carbon cycle feedbacks associated with both the marine and terrestrial biosphere, are now being taken into account in modelling. However, the exploration of how changes in biogeochemical cycles interact with one another, and how these changes impact on atmospheric chemistry, offers many more possibilities for explaining observed climate patterns. The development of Earth system models that allow the complexity of biogeochemical cycles to be taken into consideration is a research priority and will likely shed considerable light on the mechanisms of past climate changes.
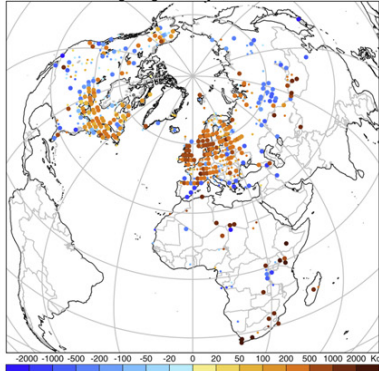
The complexity of the climate system, the multiple inter-linkages between different components, the existence of feedbacks, and the high degree of spatial and temporal variability, all militate against explaining past climate changes from observations alone. The use of a hierarchy of mechanistic models in conjunction with appropriate
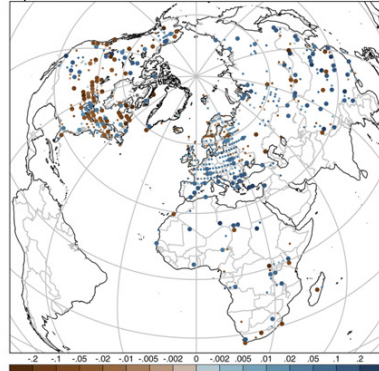
Mid-Holocene
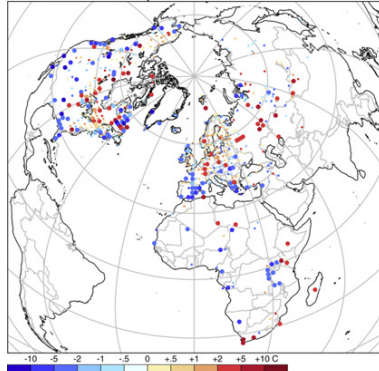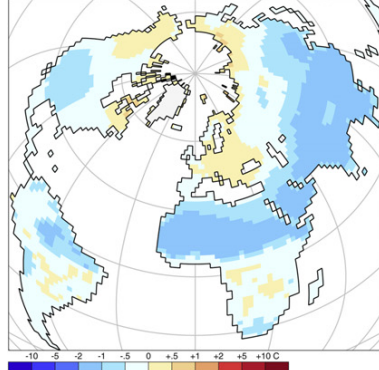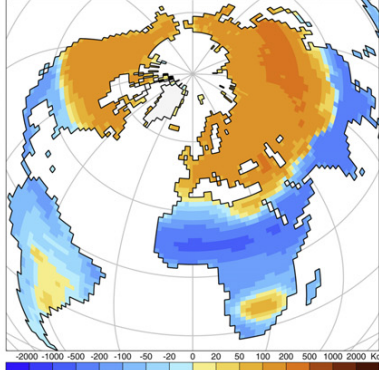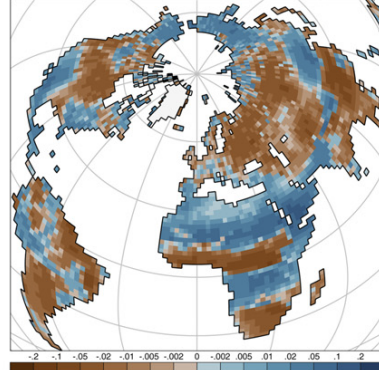
Last Glacial Maximum
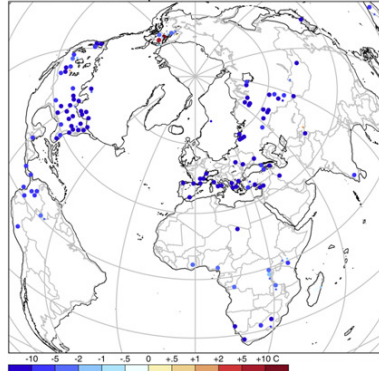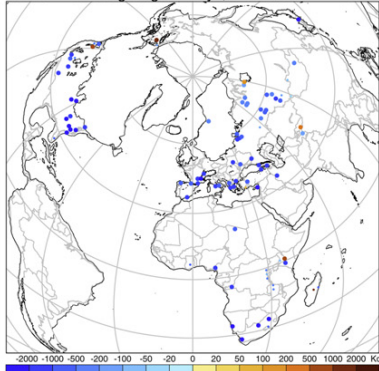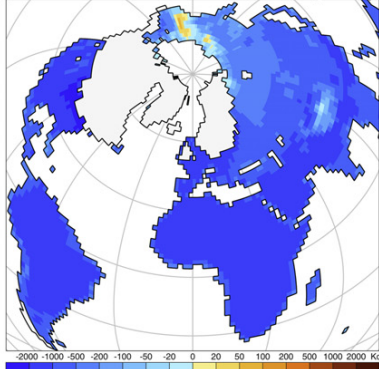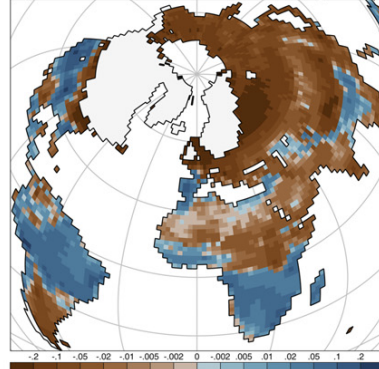
large-scale syntheses of data is the best way forward. Although this approach is often advocated, it has rarely been practised.

14.6. LESSONS FROM THE PAST FOR FUTURE CLIMATES

The palaeoclimate record shows climate variability well outside the range seen during the twentieth century, or indeed during the last two millennia. This means that the recent period does not provide an adequate sampling of how climate behaves. Changes in the controls of climate in recent decades, and those expected during the twenty-first century, exceed those of the last two millennia but are comparable in magnitude to changes seen on longer palaeoclimate timescales. Thus, on the one hand, past climate provides insights into mechanisms that cannot be studied in the historical past and, on the other hand, includes changes that are comparable in magnitude (though not cause) to future climate changes.

Changes in forcing that drive natural climate variability, and give rise to natural climate cycles, will not offset the impacts of anthropogenically induced climate changes. Ongoing changes in orbital parameters, for example, would not be expected to trigger the next ice age for 50 kyr (Berger and Loutre, 2002). Cyclicity on non-orbital timescales is not supported by the palaeoclimate record, and thus cannot be invoked as a potential mechanism to offset anthropogenically induced changes.

Nevertheless, the palaeoclimate record does show instances of short-term and rapid climate changes, both during cold-climate and warm-climate states. Evidence suggests that the MOC is weakening and will continue to do so, but it is unlikely that the MOC will collapse during the twenty-first century. Thus, the D–O cycles do not provide a guide to what might happen in the future. However, the palaeoclimate record shows that rapid re-organisations of the climate system trigger adjustments in biogeochemical cycles on timescales of decades to centuries. Thus, any mechanisms that generate rapid climate changes in the future will evoke a range of feedbacks that could substantially amplify the initial climate change, as they have in the past. Furthermore, these feedbacks have the potential to translate regional forcings into quasi-global responses.

Feedbacks play an important role in generating some of the large-scale patterns seen in simulations of future climate, most noticeably the fact that the high latitudes warm considerably more than other regions. The palaeoclimate record shows that the amplitude of climate variations at high latitudes was greater than that at low latitudes during both the mid-Holocene and the LGM. This suggests that polar amplification is a pervasive feature of the climate system. In both future and palaeoclimate simulations, this high-latitude warming is triggered by feedbacks associated with changes in the extent of sea-ice and biophysical changes in land-surface properties. However, the palaeorecord indicates that further amplification of the signal is likely through changes in the carbon cycle, in particular through changes in methane emissions from peatlands.

The ice-core record shows that atmospheric CO_2 has varied over a narrowly defined range (~180−280 ppmv) on glacial−interglacial timescales. The terrestrial biosphere takes up CO_2 during warming intervals, and thus opposes the observed trend, so the mechanism must lie in changes in the ocean carbon cycle. Although the details remain enigmatic, the asynchronous responses of the terrestrial biosphere and $CaCO_3$ compensation in the ocean broadly explain Holocene changes in CO_2. Furthermore, palaeo-observations in conjunction with biogeochemical modelling experiments place limits on the possible impact of ocean fertilization on glacial−interglacial timescales. While our incomplete understanding of the carbon cycle on palaeotimescales suggest a need to exercise caution when interpreting projections of future changes, the palaeorecord supports model results that indicate that afforestation/reforestation on land and iron fertilization of the ocean have a strictly limited role to play in mitigating future changes in CO_2 (House et al., 2008). Furthermore, $CaCO_3$ compensation operates on multimillennial timescales and so will not mitigate anthropogenic changes in CO_2 on centennial timescales.

The palaeorecord provides insights into the mechanisms of climate change that have direct relevance of our understanding of likely future climate changes. Palaeoclimate data, however, also have an additional role to play through the evaluation of state-of-the-art climate and Earth system models. This is best done through confronting model simulations with well-documented global-scale reconstructions of climate or environmental data (see e.g., Figure 14.20); such comparisons can provide a quantitative assessment of individual model performance, discrimination between models, and

FIGURE 14.20 Comparison of reconstructed and simulated mean temperature of the coldest month (MTCO), accumulated temperature above 5°C during the growing season (GDD5), and plant-available moisture as measured by the ratio between actual and potential evapotranspiration (alpha) at 6 ka and 21 ka. The reconstructions are from Bartlein et al. (2011) and the simulations are an ensemble average of the coupled ocean−atmosphere simulations runs in PMIP2 (Braconnot et al., 2007a). The ensemble-average simulations show anomaly patterns that are much smoother than the reconstructions. The reconstructions include spatial variations of climate that are not realizable in the simulations because of the coarse resolution of the models and the averaging across models.

diagnosis of the sources of model error. The Palaeo-climate Modelling Intercomparison Project (PMIP) is coordinating the systematic use of the palaeorecord for climate model evaluation at an international level. This evaluation should inform model development or improvement by individual modelling groups and identify high-impact priorities for data gathering and synthesis.

References

Ahn, J., and E. J. Brook (2008), Atmospheric CO_2 and climate on millennial time ccales during the Last Glacial Period, *Science*, *322*(5898), 83-85, DOI:10.1126/science.1160832.

Allen, J. R. M., W. A. Watts, and B. Huntley (2000), Weichselian palynostratigraphy, palaeovegetation and palaeoenvironment; The record from Lago Grande di Monticchio, southern Italy, *Quatern. Int.*, *73–74*(1), 91–110, doi:10.1016/S1040-6182(00)00067-7.

Alley, R. B., J. Marotzke, W. D. Nordhaus, J. T. Overpeck, D. M. Peteet, R. A. Pielke Jr., R. T. Pierrehumbert, P. B. Rhines, T. F. Stocker, L. D. Talley, and J. M. Wallace (2002), Abrupt climate change: Inevitable surprises, US National Research Council Report, Washington, DC.

Alley, R. B., J. Marotzke, W. D. Nordhaus, J. T. Overpeck, D. M. Peteet, R. A. Pielke, R. T. Pierrehumbert, P. B. Rhines, T. F. Stocker, L. D. Talley, and J. M. Wallace (2003), Abrupt climate change, *Science*, *299*(5615), 2005–2010, doi:10.1126/science.1081056.

Arneth, A., S. P. Harrison, S. Zaehle, K. Tsigaridis, S. Menon, P. J. Bartlein, J. Feichter, A. Korhola, M. Kulmala, D. O'Donnell, G. Schurgers, S. Sorvari, and T. Vesala (2010), Terrestrial biogeochemical feedbacks in the climate system, *Nat. Geosci.*, *3*(8), 525–532, doi:10.1038/ngeo905.

Ballantyne, A. P., M. Lavine, T. J. Crowley, J. Liu, and P. B. Baker (2005), Meta-analysis of tropical surface temperatures during the Last Glacial Maximum, *Geophys. Res. Lett.*, *32*(5), doi:10.1029/2004GL021217.

Barbante, C., H. Fischer, V. Masson-Delmotte, C. Waelbroeck, and E. W. Wolff (2010), Climate of the last million years: New insights from EPICA and other records, *Quaternary Sci. Rev.*, *29*(1–2), 1–7, doi:10.1016/j.quascirev.2009.11.025.

Bartlein, P. J. (1997), Past environmental changes: Characteristic features of Quaternary climate variations, in *Past and Future Rapid Environmental Changes: The Spatial and Evolutionary Responses of Terrestrial Biota*, edited by B. Huntley et al., Springer-Verlag, Berlin, pp. 11-29.

Bartlein, P. J., and I. C. Prentice (1989), Orbital variations, climate and paleoecology, *Trends Ecol. Evol.*, *4*(7), 195–199, doi:10.1016/0169-5347(89)90072-4.

Bartlein, P. J., and S. W. Hostetler (2004), Modeling paleoclimates, in *The Quaternary Period in the United States*, edited by A. Gillespie et al., pp. 563–582, Elsevier, Amsterdam.

Bartlein, P. J., S. P. Harrison, S. Brewer, S. Connor, B. Davis, K. Gajewski, J. Guiot, T. Harrison-Prentice, A. Henderson, O. Peyron, I. Prentice, M. Scholze, H. Seppä, B. Shuman, S. Sugita, R. Thompson, A. Viau, J. Williams, and H. Wu (2011), Pollen-based continental climate reconstructions at 6 and 21 ka: A global synthesis, *Clim. Dynam.*, *37*(3-4), 775-802, doi:10.1007/s00382-010-0904-1.

Behling, H. (1995), A high-resolution Holocene pollen record from Lago Do Pires, Se Brazil – Vegetation, climate and fire history, *J. Paleolimnol.*, *14*(3), 253–268, doi:10.1007/BF00682427.

Belcher, C. M., and L. Mander (2011), Catastrophe: Extraterrestrial impacts, massive volcanism, and the biosphere, in *The Future of the World's Climate*, edited by A. Henderson-Sellers and K. McGuffie, Elsevier, Amsterdam.

Bennett, K. D. (2004), Continuing the debate on the role of Quaternary environmental change for macroevolution, *Philos. T. Roy. Soc. B*, *359*(1442), 295–303, doi:10.1098/rstb.2003.1395.

Berger, A. (1978), Long-term variations of daily insolation and Quaternary climatic changes, *J. Atmos. Sci.*, *35*(12), 2361–2367, doi:10.1016/0033-5894(78)90064-9.

Berger, A. (Ed.) (1981), *Climatic Variations and Variability: Facts and Theories*, D. Riedel Publishing Company, Dordrecht, Holland.

Berger, A. (1988), Milankovitch theory and climate, *Rev. Geophys.*, *26*(4), 624–657, doi:10.1029/RG026i004p00624.

Berger, A., and M. F. Loutre (2002), An exceptionally long interglacial ahead?, *Science*, *297*(5585), 1287–1288, doi:10.1126/science.1076120.

Berger, A., and Q. Z. Yin (2011), Modelling the past and future interglacials in response to astronomical and greenhouse gas forcing, in *The Future of the World's Climate*, edited by A. Henderson-Sellers and K. McGuffie, Elsevier, Amsterdam.

Berger, A., J. L. Melice, and L. Hinnov (1991), A strategy for frequency spectra of Quaternary climate records, *Clim. Dynam.*, *5*(4), 227–240, doi:10.1016/0277-3791(93)90013-C.

Berger, A., M.-F. Loutre, and Q. Z. Yin (2010), Total irradiation during any time interval of the year using elliptic integrals, *Quaternary Sci. Rev.*, 29(17-18), 1968–1982, doi:10.1016/j.quascirev.2010.05.007.

Berrio, J. C., H. Hooghiemstra, H. Behling, P. Botero, and K. Van der Borg (2002), Late-Quaternary savanna history of the Colombian Llanos Orientales from Lagunas Chenevo and Mozambique: A transect synthesis, *Holocene*, *12*(1), 35–48, doi:10.1191/0959683602hl518rp.

Bigelow, N. H., L. B. Brubaker, M. E. Edwards, S. P. Harrison, I. C. Prentice, P. M. Anderson, A. A. Andreev, P. J. Bartlein, T. R. Christensen, W. Cramer, J. O. Kaplan, A. V. Lozhkin, N. V. Matveyeva, D. F. Murray, A. D. McGuire, V. Y. Razzhivin, J. C. Ritchie, B. Smith, D. A. Walker, K. Gajewski, V. Wolf, B. H. Holmqvist, Y. Igarashi, K. Kremenetskii, A. Paus, M. F. J. Pisaric, and V. S. Volkova (2003), Climate change and Arctic ecosystems: 1. Vegetation changes north of 55 degrees N between the Last Glacial Maximum, mid-Holocene, and present, *J. Geophys. Res.-Atmos.*, *108*(D19), doi:10.1029/2002JD002558.

Bird, M. I., J. Lloyd, and G. D. Farquhar (1996), Terrestrial carbon-storage from the Last Glacial Maximum to the present, *Chemosphere*, *33*(9), 1675–1685, doi:10.1016/0045-6535(96)00187-7.

Björck, S., T. Rittenour, P. Rosén, Z. França, P. Möller, I. Snowball, S. Wastegård, O. Bennike, and B. Kromer (2006), A Holocene lacustrine record in the central North Atlantic: Proxies for volcanic activity, short-term NAO mode variability, and long-term precipitation changes, *Quaternary Sci. Rev.*, *25*(1–2), 9–32, doi:10.1016/j.quascirev.2005.08.008.

Bond, G., W. Broecker, S. Johnsen, J. McManus, L. Labeyrie, J. Jouzel, and G. Bonani (1993), Correlations between climate records from North Atlantic sediments and Greenland ice, *Nature*, *365*(6442), 143–147.

Bond, W. J., and G. F. Midgley (2000), A proposed CO_2-controlled mechanism of woody plant invasion in grasslands and savannas, *Glob. Change Biol.*, *6*(8), 865–869.

Booth, R. K., S. T. Jackson, S. L. Forman, J. E. Kutzbach, E. A. Bettis, J. Kreig, and D. K. Wright (2005), A severe centennial-scale drought in mid-continental North America 4200 years ago and apparent global linkages, *Holocene*, *15*(3), 321–328.

Bopp, L., K. E. Kohfeld, C. Le Quéré, and O. Aumont (2003), Dust impact on marine biota and atmospheric CO_2 during glacial periods, *Paleoceanography*, *18*(2), 1046. doi:10.1029/2002PA000810.

Bowman, D. M. J. S., J. K. Balch, P. Artaxo, W. J. Bond, J. M. Carlson, M. A. Cochrane, C. M. D'Antonio, R. S. DeFries, J. C. Doyle, S. P. Harrison, F. H. Johnston, J. E. Keeley, M. A. Krawchuk, C. A. Kull, J. B. Marston, M. A. Moritz, I. C. Prentice, C. I. Roos, A. C. Scott, T. W. Swetnam, G. R. van der Werf, and S. J. Pyne (2009), Fire in the Earth system, *Science*, *324*(5926), 481–484.

Box, G. E. P., and G. Jenkins (1976), *Time Series Analysis: Forecasting and Control*, Holden-Day, San Francisco, CA.

Braconnot, P., S. Joussaume, O. Marti, and N. de Noblet (1999), Synergistic feedbacks from ocean and vegetation on the African monsoon response to mid-Holocene insolation, *Geophys. Res. Lett.*, *26*(16), 2481–2484, doi:10.1029/1999GL006047.

Braconnot, P., B. Otto-Bliesner, S. P. Harrison, S. Joussaume, J. Y. Peterchmitt, A. Abe-Ouchi, M. Crucifix, E. Driesschaert, T. Fichefet, C. D. Hewitt, M. Kageyama, A. Kitoh, A. Lainé, M. F. Loutre, O. Marti, U. Merkel, G. Ramstein, P. Valdes, S. L. Weber, Y. Yu, and Y. Zhao (2007a), Results of PMIP2 coupled simulations of the mid-Holocene and Last Glacial Maximum: 1. Experiments and large-scale features, *Clim. Past*, *3*(2), 261–277, doi:10.5194/cp-3-261-2007.

Braconnot, P., B. Otto-Bliesner, S. P. Harrison, S. Joussaume, J. Y. Peterchmitt, A. Abe-Ouchi, M. Crucifix, E. Driesschaert, T. Fichefet, C. D. Hewitt, M. Kageyama, A. Kitoh, M. F. Loutre, O. Marti, U. Merkel, G. Ramstein, P. Valdes, L. Weber, Y. Yu, and Y. Zhao (2007b), Results of PMIP2 coupled simulations of the mid-Holocene and Last Glacial Maximum: 2. Feedbacks with emphasis on the location of the ITCZ and mid- and high latitudes heat budget, *Clim. Past*, *3*(2), 279–296, doi:10.5194/cp-3-279-2007.

Braconnot, P., C. Marzin, L. Grégoire, E. Mosquet, and O. Marti (2008), Monsoon response to changes in Earth's orbital parameters: Comparisons between simulations of the Eemian and of the Holocene, *Clim. Past*, *4*(2), 281–294, doi:10.5194/cp-4-281-2008.

Bradbury, J. P., W. E. Dean, and R. Y. Anderson (1993), Holocene climatic and limnologic history of the North-Central United States as recorded in the varved sediments of Elk Lake, Minnesota: A synthesis, *Geol. S. Am. S.*, (276), 309.

Bradley, R. S. (1999), *Paleoclimatology: Reconstructing Climates of the Quaternary*, Academic Press, San Diego, California; London.

Braun, H., M. Christl, S. Rahmstorf, A. Ganopolski, A. Mangini, C. Kubatzki, K. Roth, and B. Kromer (2005), Possible solar origin of the 1470-year glacial climate cycle demonstrated in a coupled model, *Nature*, *438*(7065), 208–211, doi:10.1038/nature04121.

Brázdil, R., C. Pfister, H. Wanner, H. V. Storch, and J. Luterbacher (2005), Historical climatology in Europe – The state of the art, *Climatic Change*, *70*(3), 363–430, doi:10.1007/s10584-005-5924-1.

Brook, E. J., S. Harder, J. Severinghaus, E. J. Steig, and C. M. Sucher (2000), On the origin and timing of rapid changes in atmospheric methane during the Last Glacial Period, *Glob. Biogeochem. Cy.*, *14*(2), 559–572, doi:10.1029/1999GB001182.

Broström, A., M. Coe, S. P. Harrison, R. Gallimore, J. E. Kutzbach, J. Foley, I. C. Prentice, and P. Behling (1998), Land surface feedbacks and palaeomonsoons in northern Africa, *Geophys. Res. Lett.*, *25*(19), 3615–3618.

Cai, Y. J., H. Cheng, Z. S. An, R. L. Edwards, X. F. Wang, L. C. Tan, and J. Wang (2010), Large variations of oxygen isotopes in precipitation over South-Central Tibet during Marine Isotope Stage 5, *Geology*, *38*(3), 243–246, doi:10.1126/science.1177840.

CAPE Last Interglacial Project Members (2006), Last Interglacial Arctic warmth confirms polar amplification of climate change, *Quaternary Sci. Rev.*, *25*(13-14), 1383–1400, doi:10.1016/j.quascirev.2006.01.033.

Chappellaz, J. A., I. Y. Fung, and A. M. Thompson (1993), The atmospheric CH_4 increase since the Last Glacial Maximum: 1. Source estimates, *Tellus B*, *45*(3), 228, doi:10.1034/j.1600-0889.1993.t01-2-00002.x.

Chappellaz, J., T. Blunier, S. Kints, A. Dallenbach, J. M. Barnola, J. Schwander, D. Raynaud, and B. Stauffer (1997), Changes in the atmospheric CH_4 gradient between Greenland and Antarctica during the Holocene, *J. Geophys. Res.-Atmos.*, *102*(D13), 15987–15997, doi:10.1029/97JD01017.

Charman, D. J., D. W. Beilman, M. Blaauw, R. K. Booth, S. Brewer, F. M. Chambers, J. A. Christen, A. Gallego-Sala, S. P. Harrison, P. D. M. Hughes, S. T. Jackson, A. Korhola, D. Mauquoy, F. J. G. Mitchell, I. C. Prentice, M. van der Linden, F. de Vleeschouwer, Z. C. Yu, J. Alm, I. E. Bauer, Y. M. C. Corish, M. Garneau, V. Hohl, Y. Huang, E. Karofeld, G. Le Roux, R. Moschen, J. E. Nichols, T. Nieminen, G. M. McDonald, N. R. Phadtare, N. Rausch, W. Shotyk, U. Sillasoo, G. T. Swindles, E. S. Tuittila, L. Ukonmaanaho, M. Väliranta, S. van Bellen, B. van Geel, D. H. Vitt, Y. Zhao (2011), Climate-driven changes in peatland carbon accumulation during the last millennium, (in review).

Cheng, H., R. L. Edwards, W. S. Broecker, G. H. Denton, X. Kong, Y. Wang, R. Zhang, and X. Wang (2009), Ice Age terminations, *Science*, *326*(5950), 248–252, doi:10.1126/science.1177840.

Claquin, T., C. Roelandt, K. E. Kohfeld, S. P. Harrison, I. Tegen, I. C. Prentice, Y. Balkanski, G. Bergametti, M. Hansson, N. Mahowald, H. Rodhe, and M. Schulz (2003), Radiative forcing of climate by Ice-Age atmospheric dust, *Clim. Dynam.*, *20*(2–3), 193–202, doi:10.1007/s00382-002-0269-1.

Clark, P. U., N. G. Pisias, T. F. Stocker, and A. J. Weaver (2002), The role of the thermohaline circulation in abrupt climate change, *Nature*, *415*(6874), 863–869, doi:10.1038/415863a.

Clark, P. U., S. W. Hostetler, N. G. Pisias, A. Schmittner, and K. J. Meissner (2007), Mechanisms for a ca.7-kyr climate and sea-level oscillation during Marine Isotope Stage 3, *AGU Geophys. Monogr.*, *173,* 209–246.

Clark, P. U., A. J. Weaver, E. Brook, E. R. Cook, T. L. Delworth, and K. Steffen (2008), Abrupt climate change, a report by the U.S. Climate Change Science Program and the Subcommittee on Global Change Research, U.S. Geological Survey, Reston, VA.

Clark, P. U., A. S. Dyke, J. D. Shakun, A. E. Carlson, J. Clark, B. Wohlfarth, J. X. Mitrovica, S. W. Hostetler, and A. M. McCabe (2009), The Last Glacial Maximum, *Science*, *325*(5941), 710–714, doi:10.1126/science.1172873.

Claussen, M., C. Kubatzki, V. Brovkin, A. Ganopolski, P. Hoelzmann, and H. J. Pachur (1999), Simulation of an abrupt change in Saharan vegetation in the mid-Holocene, *Geophys. Res. Lett.*, *26*(14), 2037, doi:10.1029/1999GL900494.

Clement, A. C., and L. C. Peterson (2008), Mechanisms of abrupt climate change of the last glacial period, *Rev. Geophys.*, 46, RG4002, doi:10.1029/2006RG000204.

COHMAP Members (1988), Climatic changes of the last 18,000 years: Observations and model simulations, *Science*, *241*(4869), 1043–1052, doi:10.1126/science.241.4869.1043.

Cole, J. E., and E. R. Cook (1998), The changing relationship between ENSO variability and moisture balance in the Continental United States, *Geophys. Res. Lett.*, *25*(24), 4529–4532, doi:10.1029/1998GL900145.

Cook, E. R., B. M. Buckley, R. D. D'Arrigo, and M. J. Peterson (2000), Warm-season temperatures since 1600 BC reconstructed from Tasmanian tree rings and their relationship to large-scale sea surface temperature anomalies, *Clim. Dynam.*, *16*(2), 79–91, doi:10.1007/s003820050006.

Cook, E. R., P. J. Bartlein, N. S. Diffenbaugh, R. Seager, B. N. Shuman, R. S. Webb, and J. W. Williams (2008), Hydrological variability and change, in Abrupt climate change, a report by the US Climate Change Science Program and the Subcommittee on Global Change Research, edited by P. U. Clark et al., *Synthesis and Assessment Product 3.4.*, US Climate Change Research Program.

Cook, E. R., K. J. Anchukaitis, B. M. Buckley, R. D. D'Arrigo, G. C. Jacoby, and W. E. Wright (2010), Asian monsoon failure and megadrought during the last millennium, *Science*, *328*(5977), 486–489.

Crook, J. A., P. M. Forster, and N. Stuber (2011), Spatial patterns of modeled climate feedback and contributions to temperature response and polar amplification, *J. Climate, 24,* 3575-3592. doi:10.1175/2011JCLI3863.1.

Crucifix, M., M. Claussen, G. Ganssen, J. Guiot, Z. Guo, T. Kiefer, M.-F. Loutre, D.-D. Rousseau, and E. Wolff (2009) Climate change: From the geological past to the uncertain future – A symposium honouring André Berger, *Clim. Past*, *5*(4), 707–711.

Dällenbach, A., T. Blunier, J. Flückiger, B. Stauffer, J. Chappellaz, and D. Raynaud (2000), Changes in the atmospheric CH_4 gradient between Greenland and Antarctica during the Last Glacial and the transition to the Holocene, *Geophys. Res. Lett.*, *27*(7), 1005–1008, doi:10.1029/1999GL010873.

Dallmeyer, A., M. Claussen, and J. Otto (2010), Contribution of oceanic and vegetation feedbacks to Holocene climate change in monsoonal Asia, *Clim. Past*, *6*(2), 195–218.

Daniau, A. L., S. P. Harrison, and P. J. Bartlein (2010), Fire regimes during the Last Glacial, *Quaternary Sci. Rev.*, *29*(21–22), 2918–2930.

Daniau, A. L., P. J. Bartlein, S. P. Harrison, I. C. Prentice, S. Brewer, P. Friedlingstein, T. I. Harrison-Prentice, J. Inoue, J. R. Marlon, S. D. Mooney, M. J. Power, J. Stevenson, W. Tinner, and M. J. A. Andrič, H. Behling, M. Black, O. Blarquez, K. J. Brown, C. Carcaillet, E. Colhoun, D. Colombaroli, B. A. S. Davis, D. D'Costa, J. Dodson, L. Dupont, Z. Eshetu, D. G. Gavin, A. Genries, S. Gebru, S. Haberle, D. J. Hallett, S. Horn, G. Hope, F. Katamura, L. Kennedy, P. Kershaw, S. Krivonogov, C. Long, D. Magri, E. Marinova, G. M. McKenzie, P. I. Moreno, P. Moss, F. H. Neumann, E. Norström, C. Paitre, D. Rius, N. Roberts, G. Robinson, N. Sasaki, L. Scott, H. Takahara, V. Terwilliger, F. Thevenon, R. B. Turner, V. G. Valsecchi, B. Vannière, M. Walsh, N. Williams, and Y. Zhang (2011), Predictability of biomass burning in response to climate changes, (submitted).

Dansgaard, W., S. J. Johnsen, H. B. Clausen, D. Dahl-Jensen, N. Gundestrup, C. U. Hammer, and H. Oeschger (1984), North Atlantic climatic oscillations revealed by deep Greenland ice cores, in *Climatic Processes and Climate Sensitivity – Geophysical Monograph*, edited by J. E. Hansen, et al., pp. 288–298, Maurice Ewing Series 29.

Davis, M. B., R. G. Shaw, and J. R. Etterson (2005) Evolutionary responses to changing climate, *Ecology*, *286*(7), 1704–1714.

Dean, W.E., and E. Gorham (19980, Magnitude and significance of carbon burial in lakes, reservoirs, and peatlands. *Geology*, *26*(6), 535-538, doi: 10.1130/0091-7613(1998)026<0535:MASOCB>2.3.CO;2.

Dekker, S. C., H. J. de Boer, V. Brovkin, K. Fraedrich, M. J. Wassen, and M. Rietkerk (2010) Biogeophysical feedbacks trigger shifts in the modelled vegetation-atmosphere system at multiple scales, *Biogeosciences*, *7*(4), 1237–1245.

Delworth, T. L., P. U. Clark, M. Holland, W. E. Johns, T. Kuhlbrodt, J. Lynch-Stieglitz, C. Morrill, R. Seager, A. J. Weaver, and R. Zhang (2008) The potential for abrupt change in the Atlantic Meridional Overturning Circulation, in Abrupt climate change, a report by the US Climate Change Science Program and the Subcommittee on Global Change Research, edited by P.U. Clark et al., pp. 258–359,

Synthesis and Assessment Product 3.4, US Climate Change Research Program.

deMenocal, P., J. Ortiz, T. Guilderson, J. Adkins, M. Sarnthein, L. Baker, and M. Yarusinsky (2000), Abrupt onset and termination of the African Humid Period: Rapid climate responses to gradual insolation forcing, *Quaternary Sci. Rev*, *19*(1–5), 347–361, doi:10.1006/qres.2001.2261.

de Noblet, N., I.C. Prentice, S. Joussaume, D. Texier, A. Botta and A. Haxeltine (1996), Possible role of atmosphere-biosphere interactions in triggering the last glaciation. *Geophys. Res. Lett.*, *23*(22), 3191-3194.

Denman, K. L., A. Chidthaisong, P. Ciais, P. M. Cox, R. E. Dickinson, D. Hauglustaine, C. Heinze, E. Holland, D. Jacob, U. Lohmann, S. Ramachandran, P. Leite da Silva Dias, S. C. Wofsy, and X. Zhang (2007), Couplings between changes in the climate system and biogeochemistry, in *Climate Change 2007: The Physical Science Basis*, edited by D. Q. Solomon et al., pp. 499–587, Cambridge University Press, Cambridge, UK.

Dickinson, R. E. (2011), Interaction between future climate and terrestrial carbon and nitrogen, in *The Future of the World's Climate*, edited by A. Henderson-Sellers and K. McGuffie, Elsevier, Amsterdam.

Donders, T. H., F. Wagner, D. L. Dilcher, and H. Visscher (2005), Mid-to-late-Holocene El Niño–Southern Oscillation dynamics reflected in the subtropical terrestrial realm, *Proc. Natl. Acad. Sci. USA*, *102*(31), 10904–10908.

Dupont, L. M., S. Jahns, F. Marret, and S. Ning (2000), Vegetation change in equatorial West Africa: Time-slices for the last 150 ka, *Palaeogeogr. Palaeoclimatol. Palaeoecol.*, *155*(1–2), 95–122, doi:10.1016/S0031-0182(99)00095-4.

Dwyer, E., S. Pinnock, J. M. Gregoire, and J. M. C. Pereira (2000), Global spatial and temporal distribution of vegetation fire as determined from satellite observations, *Int. J. Remote Sens.*, *21*(6–7), 1289–1302.

Edwards, M. E., P. M. Anderson, L. B. Brubaker, T. A. Ager, A. A. Andreev, N. H. Bigelow, L. C. Cwynar, W. R. Eisner, S. P. Harrison, F. S. Hu, D. Jolly, A. V. Lozhkin, G. M. MacDonald, C. J. Mock, J. C. Ritchie, A. V. Sher, R. W. Spear, J. W. Williams, and G. Yu (2000), Pollen-based biomes for Beringia 18,000, 6000 and 0 C-14 yr B.P, *J. Biogeogr.*, *27*(3), 521–554, doi:10.1046/j.1365–2699.2000.00426.x.

EPICA (2004), Eight glacial cycles from an Antarctic ice core, *Nature*, *429*(6992), 623–628, doi:10.1038/nature02599.

EPICA Community Members, C. Barbante, J. M. Barnola, S. Becagli, J. Beer, M. Bigler, C. Boutron, T. Blunier, E. Castellano, and O. Cattani (2006), One-to-one coupling of glacial climate variability in Greenland and Antarctica, *Nature*, *444*(7116), 195–198, doi:10.1038/nature05301.

Farrera, I., S. P. Harrison, I. C. Prentice, G. Ramstein, J. Guiot, P. J. Bartlein, R. Bonnefille, M. Bush, W. Cramer, U. von Grafenstein, K. Holmgren, H. Hooghiemstra, G. Hope, D. Jolly, S. E. Lauritzen, Y. Ono, S. Pinot, M. Stute, and G. Yu (1999), Tropical climates at the Last Glacial Maximum: A new synthesis of terrestrial palaeoclimate data: 1. Vegetation, lake levels and geochemistry, *Clim. Dynam.*, *15*(11), 823–856, doi:10.1007/s003820050317.

Fletcher, S. E. M., N. Gruber, A. R. Jacobson, M. Gloor, S. C. Doney, S. Dutkiewicz, M. Gerber, M. Follows, F. Joos, and K. Lindsay (2007), Inverse estimates of the oceanic sources and sinks of natural CO_2 and the implied oceanic carbon transport *Glob. Biogeochem. Cy.*, *21*, GB1010, doi:10.1029/2006GB002751.

Fletcher, W. J., M. F. Sánchez Goñi, J. R. M. Allen, R. Cheddadi, N. Combourieu-Nebout, B. Huntley, I. Lawson, L. Londeix, D. Magri, V. Margari, U. C. Müller, F. Naughton, E. Novenko, K. Roucoux, and P. C. Tzedakis (2010), Millennial-scale variability during the last glacial in vegetation records from Europe, *Quaternary Sci. Rev.*, *29*(21–22), 2839–2864, doi:10.1016/j.quascirev.2010.06.031.

Flückiger, J., E. Monnin, B. Stauffer, J. Schwander, T. F. Stocker, J. Chappellaz, D. Raynaud, and J.-M. Barnola (2002), High-resolution Holocene N_2O ice core record and its relationship with CH_4 and CO_2, *Glob. Biogeochem. Cy.*, *16*(1), 1010, doi:10.1029/2001GB001417.

Foley, J. A., J. E. Kutzbach, M. T. Coe, and S. Levis (1994), Feedbacks between climate and boreal forests during the Holocene Epoch, *Nature*, *371*(6492), 52–54, doi:10.1038/371052a0.

Forster, P., V. Ramaswamy, P. Artaxo, T. Berntsen, R. Betts, D. W. Fahey, J. Haywood, J. Lean, D. C. Lowe, G. Myhre, J. Nganga, R. Prinn, G. Raga, M. Schulz and R. Van Dorland (2007), Changes in atmospheric constituents and in radiative forcing, in *Climate Change 2007: The Physical Science Basis, contribution of Working Group I to the Fourth Assessment Report (FAR) of the Intergovernmental Panel on Climate Change (IPCC)*.

Friedlingstein, P., and I. C. Prentice (2010), Carbon-climate feedbacks: A review of model and observation based estimates, *Curr. Opin. Environ. Sustain.*, *2*(4), 251–257, doi:10.1016/j.cosust.2010.06.002.

Frolking, S., N. Roulet, and J. Fuglestvedt (2006), How northern peatlands influence the Earth's radiative budget: Sustained methane emission versus sustained carbon sequestration, *J. Geophys. Res.*, *111*, G01008, doi:10.1029/2005JD006588.

Ganopolski, A., and S. Rahmstorf (2001), Rapid changes of glacial climate simulated in a coupled climate model, *Nature*, *409*(6817), 153–158, doi:10.1038/35051500.

Ganopolski, A., C. Kubatzki, M. Claussen, V. Brovkin, and V. Petoukhov (1998), The influence of vegetation-atmosphere-ocean interaction on climate during the mid-Holocene, *Science*, *280*(5371), 1916–1919, doi:10.1126/science.280.5371.1916.

Gates, W. L. (1976), The numerical simulation of Ice-Age climate with a global general circulation model, *J. Atmos. Sci.*, *33*(10), 1844–1873.

Gersonde, R., X. Crosta, A. Abelmann, and L. Armand (2005), Sea-surface temperature and sea ice distribution of the southern ocean at the EPILOG Last Glacial Maximum – A circum-Antarctic view based on siliceous microfossil records, *Quaternary Sci. Rev.*, *24*(7-9), 869–896, doi:10.1016/j.quascirev.2004.07.015.

Giglio, L., J. T. Randerson, G. R. Van Der Werf, P. S. Kasibhatla, G. J. Collatz, D. C. Morton, and R. S. Defries (2010), Assessing variability and long-term trends in burned area by merging multiple satellite fire products, *Biogeosciences*, *7*(3), 1171–1186.

Gorham, E., C. Lehman, A. Dyke, J. Janssens, and L. Dyke (2007), Temporal and spatial aspects of peatland initiation following deglaciation in North America, *Quaternary Sci. Rev.*, *26*(3–4), 300–311, doi:10.1016/j.quascirev.2006.08.008.

Guiot, J., I. C. Prentice, C. Peng, D. Jolly, F. Laarif, and B. Smith (2001), Reconstructing and modelling past changes in terrestrial primary production, in *Terrestrial Global Productivity*, edited by J. Roy et al., Academic Press, London.

Hammarlund, D., L. Barnekow, H. J. B. Birks, B. R. Buchardt, and T. W. D. Edwards (2002), Holocene changes in atmospheric circulation recorded in the oxygen-isotope stratigraphy of lacustrine carbonates from northern Sweden, *Holocene*, *12*(3), 339–351, doi:10.1191/0959683602hl548rp.

Hansen, J., A. Lacis, D. Rind, G. Russell, P. Stone, I. Fung, R. Ruedy, and J. Lerner (1984), Climate sensitivity: Analysis of feedback mechanisms – Geophysical monograph, in *Climatic Processes and Climate Sensitivity*, edited by J. E. Hansen and T. Takahash, pp. 130–163, Maurice Ewing Series 29.

Harrison, S. P., and A. I. Prentice (2003), Climate and CO_2 controls on global vegetation distribution at the Last Glacial Maximum: Analysis based on palaeovegetation data, biome modelling and palaeoclimate simulations, *Glob. Change Biol.*, *9*(7), 983–1004, doi:10.1046/j.1365-2486.2003.00640.x.

Harrison, S. P., and M. F. Sánchez Goñi (2010), Global patterns of vegetation response to millennial-scale variability and rapid climate change during the last glacial period, *Quaternary Sci. Rev.*, *29*(21–22), 2957–2980, doi:10.1016/j.quascirev.2010.07.016.

Harrison, S. P., K. E. Kohfeld, C. Roelandt, and T. Claquin (2001), The role of dust in climate changes today, at the Last Glacial Maximum and in the future, *Earth-Sci. Rev.*, *54*(1–3), 43–80, doi:10.1016/S0012-8252(01)00041-1.

Harrison, S. P., G. Yu, and J. Vassiljev (2002), Climate changes during the Holocene recorded by lakes from Europe, in *Climate Development and History of the North Atlantic Realm*, edited by G. Wefer et al., pp. 191–204, Springer-Verlag, Berlin/Heidelberg.

Harrison, S. P., J. E. Kutzbach, Z. Liu, P. J. Bartlein, B. Otto-Bliesner, D. Muhs, I. C. Prentice, and R. S. Thompson (2003), Mid-Holocene climates of the Americas: A dynamical response to changed seasonality, *Clim. Dynam.*, *20*(7–8), 663–688, doi:10.1007/s00382-002-0300-6.

Harrison, S. P., J. R. Marlon, and P. J. Bartlein (2010), Fire in the Earth system, in *Changing Climates, Earth Systems and Society*, edited by J. Dodson, pp. 21–48, Springer-Verlag, Dordrecht.

Harvey, L. D. D. (2011), Fast and slow feedbacks in future climates, in *The Future of the World's Climate*, edited by A. Henderson-Sellers and K. McGuffie, Elsevier, Amsterdam.

Hessler, I., L. Dupont, R. Bonnefille, H. Behling, C. Gonzalez, K. F. Helmens, H. Hooghiemstra, J. Lebamba, M. P. Ledru, A. M. Lezine, J. Maley, F. Marret, and A. Vincens (2010), Millennial-scale changes in vegetation records from tropical Africa and South America during

the last glacial, *Quaternary Sci. Rev.*, *29*(21–22), 2882–2899, doi:10.1016/j.quascirev.2009.11.029.

Holland, M. M., and C. M. Bitz (2003), Polar amplification of climate change in coupled models, *Clim. Dynam.*, *21*(3–4), 221–232, doi:10.1007/s00382-003-0332-6.

House, J. I., C. Huntingford, W. Knorr, S. E. Cornell, P. M. Cox, G. R. Harris, C. D. Jones, J. A. Lowe, and I. C. Prentice (2008), What do recent advances in quantifying climate and carbon cycle uncertainties mean for climate policy?, *Env. Res. Lett.*, *3*(4), doi:10.1088/1748–9326/3/4/044002.

Huntley, B., and T. Webb, III (1989), Migration: Species' response to climatic variations caused by changes in the Earth's orbit, *J. Biogeogr.*, *16*(1), 5–19.

Huybers, P., and C. Wunsch (2005), Obliquity pacing of the late-Pleistocene glacial terminations, *Nature*, *434*(7032), 491–494, doi:10.1038/nature03401.

Imbrie, J., J. D. Hays, D. G. Martinson, A. McIntyre, A. C. Mix, J. J. Morley, N. G. Pisias, W. L. Prell, and N. J. Shackleton (1984), The orbital theory of Pleistocene climate: Support from a revised chronology of the marine δ18 O record, in *Milankovitch and Climate*, edited by A. Berger et al., D. Reidel Publishing, Dordrecht.

Imbrie, J., E. A. Boyle, S. C. Clemens, A. Duffy, W. R. Howard, G. Kukla, J. Kutzbach, D. G. Martinson, A. McIntyre, A. C. Mix, B. Molfino, J. J. Morley, L. C. Peterson, N. G. Pisias, W. L. Prell, M. E. Raymo, N. J. Shackleton, and J. R. Toggweiler (1992), On the structure and origin of major glaciation cycles: 1. Linear responses to Milankovitch forcing, *Paleoceanography*, *7*(6), 701–738, doi:10.1029/92PA02855.

Irizarry-Ortiz, M. M., G. Wang, and E. A. B. Eltahir (2003), Role of the biosphere in the mid-Holocene climate of West Africa, *J. Geophys. Res.*, *108*(D2), 4042, doi:10.1029/2001JD000989.

Jahn, A., M. Claussen, A. Ganopolski, and V. Brovkin (2005), Quantifying the effect of vegetation dynamics on the climate of the Last Glacial Maximum, *Clim. Past*, *1*(1), 1–7.

Jansen, E., J. Overpeck, K. R. Briffa, J. C. Duplessy, F. Joos, V. Masson-Delmotte, D. Olago, B. Otto-Bliesner, W. R. Peltier, S. Rahmstorf, R. Ramesh, D. Raynaud, D. Rind, O. Solomina, R. Villalba, and D. Zhang (2007), Palaeoclimate, in *Climate Change 2007: The Physical Science Basis, contribution of Working Group I to the Fourth Assessment Report (FAR) of the Intergovernmental Panel on Climate Change (IPCC)*, edited by S. Solomon et al., pp. 434–497.

Jenkins, G., and D. Watts (1968), *Spectral Analysis and Its Applications*, Holden-Day, San Francisco.

Jolly, D., S. P. Harrison, B. Damnati, and R. Bonnefille (1998), Simulated climate and biomes of Africa during the Late Quaternary: Comparison with pollen and lake status data, *Quaternary Sci. Rev.*, *17*(6–7), 629–657, doi:10.1016/S0277-3791(98)00015-8.

Joos, F. P., and I. C. Prentice, (2004), A paleo-perspective on changes in atmospheric CO_2 and climate, in *The Global Carbon Cycle*, edited by C. B. Field and M. R. Raupach, pp. 165–186, Island Press, Washington.

Joos, F. P., S. Gerber, I. C. Prentice, B. L. Otto-Bliesner, and P. J. Valdes (2004), Transient simulations of Holocene atmospheric carbon dioxide and terrestrial carbon since the Last Glacial Maximum, *Glob. Biogeochem. Cy.*, *18*(2), GB2002, doi:10.1029/2003GB002156.

Joshi, M. M., J. M. Gregory, M. J. Webb, D. M. H. Sexton, and T. C. Johns (2008), Mechanisms for the land/sea warming contrast exhibited by simulations of climate change, *Clim. Dynam.*, *30*(5), 455–465, doi:10.1007/s00382-007-0306-1.

Joussaume, S., and P. Braconnot (1997), Sensitivity of paleoclimate simulation results to season definitions, *J. Geophys. Res.*, *102*(D2), 1943–1956.

Joussaume, S., K. E. Taylor, P. Braconnot, J. F. B. Mitchell, J. E. Kutzbach, S. P. Harrison, I. C. Prentice, A. J. Broccoli, A. Abe-Ouchi, P. J. Bartlein, C. Bonfils, B. Dong, J. Guiot, K. Herterich, C. D. Hewitt, D. Jolly, J. W. Kim, A. Kislov, A. Kitoh, M. F. Loutre, V. Masson, B. McAvaney, N. McFarlane, N. de Noblet, W. R. Peltier, J. Y. Peterschmitt, D. Pollard, D. Rind, J. F. Royer, M. E. Schlesinger, J. Syktus, S. Thompson, P. Valdes, G. Vettoretti, R. S. Webb, and U. Wyputta (1999), Monsoon changes for 6000 years ago: Results of 18 simulations from the Paleoclimate Modeling Intercomparison Project (PMIP), *Geophys. Res. Lett.*, *26*(7), 859–862, doi:10.1029/1999GL900126.

Jouzel, J., F. Vimeux, N. Caillon, G. Delaygue, G. Hoffmann, V. Masson-Delmotte, and F. Parrenin (2003), Magnitude of isotope/temperature scaling for interpretation of central Antarctic ice

cores, *J. Geophys. Res.*, *108*(D12), 4361, doi:10.1029/2002JD002677.

Jouzel, J., V. Masson-Delmotte, O. Cattani, G. Dreyfus, S. Falourd, G. Hoffmann, B. Minster, J. Nouet, J. M. Barnola, J. Chappellaz, H. Fischer, J. C. Gallet, S. Johnsen, M. Leuenberger, L. Loulergue, D. Luethi, H. Oerter, F. Parrenin, G. Raisbeck, D. Raynaud, A. Schilt, J. Schwander, E. Selmo, R. Souchez, R. Spahni, B. Stauffer, J. P. Steffensen, B. Stehni, T. F. Stocker, J. L. Tison, M. Werner, and E. W. Wolff (2007a), Orbital and millennial Antarctic climate variability over the past 800,000 years, *Science*, *317*(5839), 793–796.

Jouzel, J., M. Stievenard, S. J. Johnsen, A. Landais, V. Masson-Delmotte, A. Sveinbjornsdottir, F. Vimeux, U. von Grafenstein, and J. W. White (2007b), The GRIP deuterium-excess record, *Quaternary Sci. Rev.*, *26*(1–2), 1–17, doi:10.1016/j.quascirev.2006.07.015.

Kageyama, M., S. P. Harrison, and A. Abe-Ouchi (2005), The depression of tropical snowlines at the Last Glacial Maximum: What can we learn from climate model experiments?, *Quatern. Int.*, *138–139*(1), 202–219.

Kageyama, M., A. Paul, D. M. Roche, C. J. Van Meerbeeck (2010), Modelling glacial climatic millennial-scale variability related to changes in the Atlantic Meridional Overturning Circulation: A review, *Quaternary Sci. Rev.,* *29*(21-22), 2931–2956, doi:10.1016/j.quascirev.2010.05.029.

Kantz, H., and T. Schreiber (2004), *Nonlinear Time Series Analysis*, 2nd edition, Cambridge University Press, Cambridge, UK.

Kaplan, J. O. (2002), Wetlands at the Last Glacial Maximum: Distribution and methane emissions, *Geophys. Res. Lett.*, *29*(6), 1079.

Kaplan, J. O., N. H. Bigelow, I. C. Prentice, S. P. Harrison, P. J. Bartlein, T. R. Christensen, W. Cramer, N. V. Matveyeva, A. D. McGuire, D. F. Murray, V. Y. Razzhivin, B. Smith, D. A. Walker, P. M. Anderson, A. A. Andreev, L. B. Brubaker, M. E. Edwards, and A. V. Lozhkin (2003), Climate change and Arctic ecosystems: 2. Modeling, paleodata-model comparisons, and future projections, *J. Geophys. Res.-Atmos.*, *108*(D19).

Kaufman, D. S., T. A. Ager, N. J. Anderson, P. M. Anderson, J. T. Andrews, P. J. Bartlein, L. B. Brubaker, L. L. Coats, L. C. Cwynar, M. L. Duvall, A. S. Dyke, M. E. Edwards, W. R. Eisner, K. Gajewski, A. Geirsdottir, F. S. Hu, A. E. Jennings, M. R. Kaplan, M. N. Kerwin, A. V. Lozhkin, G. M. MacDonald, G. H. Miller, C. J. Mock, W. W. Oswald, B. L. Otto-Bliesner, D. F. Porinchu, K. Ruhland, J. P. Smol, E. J. Steig, and B. B. Wolfe (2004), Holocene thermal maximum in the Western Arctic (0–180 degrees W), *Quaternary Sci. Rev.*, *23*(5–6), 529–560, doi:10.1016/j.quascirev.2003.09.007.

Kershaw, A. P., J. S. Clark, A. M. Gill, and D. M. D'Costa (2002), A history of fire in Australia, in *Flammable Australia; The Fire Regimes and Biodiversity of a Continent*, edited by R. Bradstock et al., Cambridge University Press, Cambridge, UK.

Kim, J. H., N. Rimbu, S. J. Lorenz, G. Lohmann, S. I. Nam, S. Schouten, C. Rühlemann, and R. R. Schneider (2004), North Pacific and North Atlantic sea-surface temperature variability during the Holocene, *Quaternary Sci. Rev.*, *23*(20–22), 2141–2154, doi:10.1016/j.quascirev.2004.08.010.

Kohfeld, K. E., and S. P. Harrison (2000), How well can we simulate past climates? Evaluating the models using global palaeoenvironmental datasets, *Quaternary Sci. Rev.*, *19*(1–5), 321–346.

Kohfeld, K. E., and S. P. Harrison (2001), DIRTMAP: The geological record of dust, *Earth-Sci. Rev.*, *54*(1–3), 81–114.

Kohfeld, K. E., and S. P. Harrison (2003), Glacial-interglacial changes in dust deposition on the Chinese Loess Plateau, *Quaternary Sci. Rev.*, *22*(18–19), 1859–1878.

Kohfeld, K. E., C. Le Quéré, S. P. Harrison, and R. F. Anderson (2005), Role of marine biology in glacial-interglacial CO_2 cycles, *Science*, *308*(5718), 74–78, doi:10.1126/science.1105375.

Köhler, P., H. Fischer, and J. Schmitt (2010), Atmospheric $\delta^{13}CO_2$ and its relation to pCO_2 and deep ocean $\delta^{13}C$ during the Late Pleistocene, *Paleoceanography*, 25, PA1213.

Korhola, A., M. Ruppel, H. Sieppa, M. Valiranta, T. Virtanen and J. Weckstrom (2010), The importance of northern peatland expansion to the Late-Holocene rise of atmospheric methane, *Quaternary Sci. Rev.*, *29*(5-6), 611–617, doi:10.1016/j.quascirev.2009.12.010.

Kuhlbrodt, T., A. Griesel, M. Montoya, A. Levermann, M. Hofmann, and S. Rahmstorf (2007), On the driving processes of the Atlantic Meridional Overturning Circulation, *Rev. Geophys.*, *45*(2), RG2001.

Kutzbach, J. E., and F. A. Street-Perrott (1985), Milankovitch forcing of fluctuations in the level of tropical lakes from 18 to 0 kyr B.P, *Nature*, *317*(6033), 130–134, doi:10.1038/317130a0.

Kutzbach, J. E., and P. J. Guetter (1986), Influence of changing orbital parameters and surface boundary conditions on climate simulations for the past 18,000 years, *J. Atmos. Sci.*, *43*(16), 1726–1759.

Kutzbach, J. E., and R. G. Gallimore (1988), Sensitivity of a coupled atmosphere/mixed layer ocean model to changes in orbital forcing at 9000 years B.P, *J. Geophys. Res.*, *93*(D1), 803–821.

Kutzbach, J. E., P. J. Guetter, P. J. Behling, R. Selin (1993), Simulated climatic changes: Results of the COHMAP climate-model experiments, in *Global Climates Since the Last Glacial Maximum*, edited by H. E. Wright, Jr. et al., University of Minnesota Press, Minneapolis.

Kutzbach, J., G. Bonan, J. Foley, and S. P. Harrison (1996), Vegetation and soil feedbacks on the response of the African monsoon to orbital forcing in the Early to Middle Holocene, *Nature*, *384*(6610), 623–626.

Lainé, A., M. Kageyama, P. Braconnot, and R. Alkama (2009), Impact of greenhouse as concentration changes on surface energetics in IPSL-CM4: Regional warming patterns, land-sea warming ratios, and glacial-interglacial differences, *J. Climate*, *22*(17), 4621–4635.

Lambert, F., B. Delmonte, J. R. Petit, M. Bigler, P. R. Kaufmann, M. A. Hutterli, T. F. Stocker, U. Ruth, J. P. Steffensen, and V. Maggi (2008), Dust-climate couplings over the past 800,000 years from the EPICA Dome C ice core, *Nature*, *452*(7187), 616–619, doi:10.1038/nature06763.

Latif, M., and W. Park (2011), Climatic variability on decadal to century timescales, in *The Future of the World's Climate*, edited by A. Henderson-Sellers and K. McGuffie, Elsevier, Amsterdam.

Leduc, G., R. Schneider, J. H. Kim, and G. Lohmann (2010), Holocene and Eemian sea surface temperature trends as revealed by alkenone and Mg/Ca paleothermometry, *Quaternary Sci. Rev.*, *29*(7–8), 989–1004.

Lee, J.-E., I. Fung, D. J. DePaolo, and B. Otto-Bliesner (2008), Water isotopes during the Last Glacial Maximum: New general circulation model calculations, *J. Geophys. Res.*, 113, D19109, doi:10.1029/2008JD009859.

Lenton, T. M. (2011), Future climate surprises, in *The Future of the World's Climate*, edited by A. Henderson-Sellers and K. McGuffie, Elsevier, Amsterdam.

Lisiecki, L. E., and M. E. Raymo (2007), Plio-Pleistocene climate evolution: Trends and transitions in glacial cycle dynamics, *Quaternary Sci. Rev.*, *26*(1–2), 56–69, doi:10.1016/j.quascirev.2006.09.005.

Liu, Z., S. P. Harrison, J. Kutzbach, and B. Otto-Bliesner (2004), Global monsoons in the mid-Holocene and oceanic feedback, *Clim. Dynam.*, *22*(2–3), 157–182, doi:10.1007/s00382-003-0372-y.

Liu, Z., Y. Wang, R. Gallimore, M. Notaro, and I. C. Prentice (2006), On the cause of abrupt vegetation collapse in North Africa during the Holocene: Climate variability vs. vegetation feedback, *Geophys. Res. Lett.*, *33*, L22709, doi:10.1029/2006GL028062.

Liu, Z., B. L. Otto-Bliesner, F. He, E. C. Brady, R. Tomas, P. U. Clark, A. E. Carlson, J. Lynch-Stieglitz, W. Curry, E. Brook, D. Erickson, R. Jacob, J. Kutzbach, and J. Cheng (2009), Transient simulation of last deglaciation with a new mechanism for Bølling-Allerød warming, *Science*, 325 (5938), 310–314, doi:10.1126/science.1171041.

Lorenz, S. J., J.-H. Kim, N. Rimbu, R. R. Schneider, and G. Lohmann (2006), Orbitally driven insolation forcing on Holocene climate trends: Evidence from alkenone data and climate modeling, *Paleoceanography*, *21*(1), PA1002.

Loulergue, L., A. Schilt, R. Spahni, V. Masson-Delmotte, T. Blunier, B. Lemieux, J. M. Barnola, D. Raynaud, T. F. Stocker, and J. Chappellaz (2008), Orbital and millennial-scale features of atmospheric CH_4 over the past 800,000 years, *Nature*, *453*(7193), 383–386, doi:10.1038/nature06950.

Loutre, M.-F. (2009), Eccentricity, in *Encyclopedia of Paleoclimatology and Ancient Environments*, edited by V. Gornitz, pp. 825–826, Springer, Dordrecht.

Luterbacher, J., E. Xoplaki, D. Dietrich, R. Rickli, J. Jacobeit, C. Beck, D. Gyalistras, C. Schmutz, and H. Wanner (2002), Reconstruction of sea level pressure fields over the eastern North Atlantic and Europe back to 1500, *Clim. Dynam.*, *18*(7), 545–561, doi:10.1007/s00382-001-0196-6.

Luterbacher, J., S. Koenig, J. Franke, G. van der Schrier, E. Zorita, A. Moberg, J. Jacobeit, P. Della-Marta, M. Küttel, E. Xoplaki, D. Wheeler, T. Rutishauser, M. Stössel, H. Wanner, R. Brázdil, P. Dobrovolný, D. Camuffo, C. Bertolin, A. van Engelen, F. Gonzalez-Rouco, R. Wilson, C. Pfister, D. Limanówka, Ø. Nordli, L. Leijonhufvud, J. Söderberg, R. Allan, M. Barriendos, R. Glaser, D. Riemann, Z. Hao, and C. Zerefos (2010), Circulation dynamics and its influence on European and Mediterranean January–April climate over the past half millennium: Results and insights from instrumental data, documentary evidence and coupled climate models, *Climatic Change*, *101*(1), 201–234.

Lüthi, D., M. Le Floch, B. Bereiter, T. Blunier, J. M. Barnola, U. Siegenthaler, D. Raynaud, J. Jouzel, H. Fischer, K. Kawamura, and T. F. Stocker (2008), High-resolution carbon dioxide concentration record 650,000–800,000 years before present, *Nature*, *453*(7193), 379–382, doi:10.1038/nature06949.

Lynch, A. H., J. Beringer, P. Kershaw, A. Marshall, S. Mooney, N. Tapper, C. Turney, and S. Van Der Kaars (2007), Using the paleorecord to evaluate climate and fire interactions in Australia, *Annu. Rev. Earth Planet. Sci.*, *35*(1), 215–240.

MacDonald, G. M., D. W. Bielman, K. V. Kremenetski, Y. Sheng, L. C. Smith, and A. A. Velichko (2006), Rapid early development of circumarctic peatlands and atmospheric CH_4 and CO_2 variations, *Science*, *314*(5797), 285–288, doi:10.1126/science.1131722.

Mann, M. E., Z. Zhang, S. Rutherford, R. S. Bradley, M. K. Hughes, D. Shindell, C. Ammann, G. Faluvegi, and F. Ni (2009), Global signatures and dynamical origins of the Little Ice Age and medieval climate anomaly, *Science*, *326*(5957), 1256–1260, doi:10.1126/science.1177303.

Marchant, R., and H. Hooghiemstra (2004), Rapid environmental change in African and South American tropics around 4000 years before present: A review, *Earth-Sci. Rev.*, *66*(1-2), 217–260.

Marchant, R., A. Cleef, S. P. Harrison, H. Hooghiemstra, V. Markgraf, J. van Boxel, T. Ager, L. Almeida, R. Anderson, C. Baied, H. Behling, J. C. Berrio, R. Burbridge, S. Bjorck, R. Byrne, M. Bush, J. Duivenvoorden, J. Flenley, P. De Oliveira, B. van Geel, K. Graf, W. D. Gosling, S. Harbele, T. van der Hammen, B. Hansen, S. Horn, P. Kuhry, M. P. Ledru, F. Mayle, B. Leyden, S. Lozano-Garcia, A. M. Melief, P. Moreno, N. T. Moar, A. Prieto, G. van Reenen, M. Salgado-Labouriau, F. Schabitz, E. J. Schreve-Brinkman, and M. Wille (2009), Pollen-based biome reconstructions for Latin America at 0, 6000 and 18 000 radiocarbon years ago, *Clim. Past*, *5*(4), 725–767, doi:10.5194/cp-5-725-2009.

MARGO Project Members (2009), Constraints on the magnitude and patterns of ocean cooling at the Last Glacial Maximum, *Nat. Geosci.*, *2*(2), 127–132, doi:10.1038/ngeo411.

Mark, B. G., S. P. Harrison, A. Spessa, M. New, D. J. A. Evans, and K. F. Helmens (2005), Tropical snowline changes at the Last Glacial Maximum: A global assessment, *Quatern. Int.*, *138*(1), 168–201.

Markgraf, V. (1989), Palaeoclimates in Central and South America since 18,000 B.P based on pollen and lake-level records, *Quaternary Sci. Rev.*, *8*(1), 1–24.

Marlon, J. R., P. J. Bartlein, C. Carcaillet, D. G. Gavin, S. P. Harrison, P. E. Higuera, F. Joos, M. J. Power, and I. C. Prentice (2008), Climate and human influences on global biomass burning over the past two millennia, *Nat. Geosci.*, *1*(10), 697–702.

Marshall, A. G., and A. H. Lynch (2006), Time-slice analysis of the Australian summer monsoon during the Late Quaternary using the Fast Ocean Atmosphere Model, *J. Quatern. Sci.*, *21*(7), 789–801.

Martinson, D. G., N. G. Pisias, J. D. Hays, J. Imbrie, T. C. Moore, Jr., and N. J. Shackleton (1987), Age dating and the orbital theory of the ice ages: Development of a high-resolution 0 to 300,000-year chronostratigraphy, *Quatern. Res.*, *27*(1), 1–29.

Martrat, B., J. O. Grimalt, C. Lopez-Martinez, I. Cacho, F. J. Sierro, J. A. Flores, R. Zahn, M. Canals, J. H. Curtis, and D. A. Hodell (2004), Abrupt temperature changes in the western Mediterranean over the past 250,000 years, *Science*, *306*(5702), 1762–1765, doi:10.1126/science.1101706.

Martrat, B., J. O. Grimalt, N. J. Shackleton, L. De Abreu, M. A. Hutterli, and T. F. Stocker (2007), Four climate cycles of recurring deep and surface water destabilizations on the Iberian margin, *Science*, *317*(5837), 502–507, doi:10.1126/science.1139994.

Marzin, C., and P. Braconnot (2009), Variations of Indian and African monsoons induced by insolation changes at 6 and 9.5 kyr B.P, *Clim. Dynam.*, *33*(2), 215–231, doi:10.1007/s00382-009-0538-3.

Masson-Delmotte, V., J. Jouzel, A. Landais, M. Stievenard, S. J. Johnsen, J. W. C. White, M. Werner, A. Sveinbjornsdottir, and K. Fuhrer (2005), Atmospheric science: GRIP deuterium excess reveals rapid and orbital-scale changes in Greenland moisture origin, *Science*, *309*(5731), 118–121, doi:10.1126/science.1108575.

Masson-Delmotte, V., M. Kageyama, P. Braconnot, S. Charbit, G. Krinner, C. Ritz, E. Guilyardi, J. Jouzel, A. Abe-Ouche, M. Crucifix, R. M. Gladstone, C. D. Hewitt, A. Kitoh, A. N. LeGrande, O. Marti, U. Merkel, T. Motoi, R. Ohgaito, B. Otto-Bliesner, W. R. Peltier, I. Ross, P. J. Valdes, G. Vettoretti, S. L. Weber, F. Wolk, and Y. Yu (2006), Past and future polar amplification of climate change: Climate model intercomparisons and ice-core constraints, *Clim. Dynam.*, *26*(5), 513–529, doi:10.1007/s00382-005-0081-9.

Mauquoy, D., T. Engelkes, M. H. M. Groot, F. Markesteijn, M. G. Oudejans, J. van der Plicht, and B. van Geel (2002), High-resolution records of Late-Holocene climate change and carbon accumulation in two North-West European ombrotrophic peat bogs, *Palaeogeogr. Palaeoclimatol. Palaeoecol.*, *186*(3–4), 275–310, doi:10.1016/S0031-0182(02)00513-8.

Mayle, F. E., and M. J. Power (2008), Impact of a drier early-mid-Holocene climate upon Amazonian forests, *Philos. T. Roy. Soc. B*, *363*(1498), 1829–1838, doi:10.1098/rstb.2007.0019.

McCabe, G. J., and M. D. Dettinger (1999), Decadal variations in the strength of ENSO teleconnections with precipitation in the western United States, *Int. J. Climatol.*, *19*(13), 1399–1410.

McLachlan, J. S., J. S. Clark, and P. S. Manos (2005), Molecular indicators of tree migration capacity under rapid climate change, *Ecology*, *86*(8), 2088–2098.

Meehl, G. A., T. F. Stocker, W. D. Collins, P. Friedlingstein, A. T. Gaye, J. M. Gregory, A. Kitoh, R. Knutti, J. M. Murphy, A. Noda, S. C. B. Raper, I. G. Watterson, A. J. Weaver, and Z.-C. Zhao (2007), Global climate projections, *Climate Change 2007: The Physical Science Basis, contribution of Working Group I to the Fourth Assessment Report (FAR) of the Intergovernmental Panel on Climate Change (IPCC)*, edited by S. Solomon et al.

Menviel, L., A. Timmermann, O. E. Timm, and A. Mouchet (2011), Deconstructing the Last Glacial termination: The role of millennial and orbital-scale forcings, *Quaternary Sci. Rev.*, *30*(9-10), 1155–1172, doi:10.1016/j.quascirev.2011.02.005.

Metz, B., O. R. Davidson, P. R. Bosch, R. Dave, and L. A. Meyer (Eds.) (2007), *Contribution of Working Group III to the Fourth Assessment Report (FAR) of the Intergovernmental Panel on Climate Change (IPCC)*, Cambridge University Press, Cambridge, UK, and New York, NY.

Miller, G. H., R. B. Alley, J. Brigham-Grette, J. J. Fitzpatrick, L. Polyak, M. C. Serreze, and J. W. C. White (2010), Arctic amplification: Can the past constrain the future?, *Quaternary Sci. Rev.*, *29*(15–16), 1779–1790, doi:10.1016/j.quascirev.2010.02.008.

Mitchell, T. D., and P. D. Jones (2005), An improved method of constructing a database of monthly climate observations and associated high-resolution grids, *Int. J. Climatol.*, *25*(6), 693–712.

Mooney, S. D., S. P. Harrison, P. J. Bartlein, A. L. Daniau, J. Stevenson, K. C. Brownlie, S. Buckman, M. Cupper, J. Luly, M. Black, E. Colhoun, D. D'Costa, J. Dodson, S. Haberle, G. S. Hope, P. Kershaw, C. Kenyon, M. McKenzie, and N. Williams (2010), Late-Quaternary fire regimes of Australasia, *Quaternary Sci. Rev.*, *30*(1–2), 28–46, doi:10.1016/j.quascirev.2010.10.010.

Morey, A. E., A. C. Mix, and N. G. Pisias (2005), Planktonic foraminiferal assemblages preserved in surface sediments correspond to multiple environment variables, *Quaternary Sci. Rev.*, *24*(7-9), 925–950, doi:10.1016/j.quascirev.2003.09.011.

Moss, T., M. Babiker, S. Brinkman, E. Calvo, T. Carter, J. Edmonds, I. Elgizouli, S. Emori, L. Erda, K. Hibbard, R. Jones, M. Kainuma, J. Kelleher, J.-F. Lamarque, M. Manning, B. Matthews, G. Meehl, L. Meyer, J. Mitchell, N. Nakicenovic, B. O'Neill, T. Pichs, K. Riahi, S. Rose, P. Runci, R. Stouffer, D. van Vuuren, J. Weyant, T. Wilbanks, J. P. van Ypersele, and M. Zurek (2008), Towards new scenarios for analysis of emissions, climate change, impacts, and response strategies, Intergovernmental Panel on Climate Change (IPCC), Geneva.

Mouillot, F., and C. B. Field (2005), Fire history and the global carbon budget: a $1° \times 1°$ fire history reconstruction for the 20th century, *Glob. Change Biol.*, *11*(3), 398–420.

Mulitza, S., M. Prange, J.-B. Stuut, M. Zabel, T. von Dobeneck, A. C. Itambi, J. Nizou, M. Schulz, and G. Wefer (2008), Sahel megadroughts triggered by glacial slowdowns of Atlantic Meridional Overturning, *Paleoceanography*, *23*(4), PA4206.

Nelson, C. R., and H. Kang (1981), Spurious periodicity in inappropriately detrended time series, *Econometrica*, *49*(3), 741–751.

North Greenland Ice Core Project Members (2004), High-resolution record of Northern Hemisphere climate extending into the last interglacial period, *Nature*, *431*(7005), 147–151, doi:10.1038/nature02805.

Otto-Bliesner, B. L., E. C. Brady, S. I. Shin, Z. Liu, and C. Shields (2003), Modeling El-Niño and its tropical teleconnections during the last glacial-interglacial cycle, *Geophys. Res. Lett.*, *30*(23), 2198.

Otto-Bliesner, B., R. Schneider, E. Brady, M. Kucera, A. Abe-Ouchi, E. Bard, P. Braconnot, M. Crucifix, C. Hewitt, M. Kageyama, O. Marti, A. Paul, A. Rosell-Melé, C. Waelbroeck, S. Weber, M. Weinelt, and Y. Yu (2009), A comparison of PMIP2 model simulations and the MARGO proxy reconstruction for tropical sea surface temperatures at Last Glacial Maximum, *Clim. Dynam.*, *32*(6), 799–815, doi:10.1007/s00382-008-0509-0.

Peck, J. A., R. R. Green, T. Shanahan, J. W. King, J. T. Overpeck, and C. A. Scholz (2004), A magnetic mineral record of Late-Quaternary tropical climate variability from Lake Bosumtwi, Ghana, *Palaeogeogr. Palaeoclimatol. Palaeoecol.*, *215*(1-2), 37–57, doi:10.1016/j.palaeo.2004.08.003.

Peltier, W. R. (2004), Global glacial isostasy and the surface of the Ice-Age Earth: The ICE-5G (VM2) model and GRACE, *Annu. Rev. Earth & Planet. Sci.*, *32*(1), 111–149.

Pickett, E. J., S. P. Harrison, G. Hope, K. Harle, J. R. Dodson, A. P. Kershaw, I. C. Prentice, J. Backhouse, E. A. Colhoun, D. D'Costa, J. Flenley, J. Grindrod, S. Haberle, C. Hassell, C. Kenyon, M. Macphail, H. Martin, A. H. Martin, M. McKenzie, J. C. Newsome, D. Penny, J. Powell, J. I. Raine, W. Southern, J. Stevenson, J. P. Sutra, I. Thomas, S. van der Kaars, and J. Ward (2004), Pollen-based reconstructions of biome distributions for Australia, Southeast Asia and the Pacific (SEAPAC region) at 0, 6000 and 18,000 C-14 yr B.P, *J. Biogeogr.*, *31*(9), 1381–1444.

Pinot, S., G., Ramstein, S. P. Harrison, I. C. Prentice, J. Guiot, S. Joussaume, M. Stute, and PMIP participating groups (1999), Tropical palaeoclimates at the Last Glacial Maximum: comparison of Paleoclimate Modeling Intercomparison Project (PMIP) simulations and paleodata. *Climate Dynamics 15*(11), 857-874.

Pitman, A. J., and N. de Noblet-Ducoudré (2011), Human effects on climate through land-use-induced land-cover change, in *The Future of the World's Climate*, edited by A. Henderson-Sellers and K. McGuffie, Elsevier, Amsterdam.

Pitman, A. J., and R. J. Stouffer (2006), Abrupt change in climate and climate models, *Hydrol. Earth Syst. Sc.*, *10*(6), 903–912.

Polley, H. W., H. B. Johnson, B. D. Marinot, and H. S. Mayeux (1993), Increase in C_3 plant water-use efficiency and biomass over glacial to present CO_2 concentrations, *Nature*, *361*(6407), 61–64, doi:10.1038/361061a0.

Power, M. J., J. Marlon, N. Ortiz, P. J. Bartlein, S. P. Harrison, F. E. Mayle, A. Ballouche, R. H. W. Bradshaw, C. Carcaillet, C. Cordova, S. Mooney, P. I. Moreno, I. C. Prentice, K. Thonicke, W. Tinner, C. Whitlock, Y. Zhang, Y. Zhao, A. A. Ali, R. S. Anderson, R. Beer, H. Behling, C. Briles, K. J. Brown, A. Brunelle, M. Bush, P. Camill, G. Q. Chu, J. Clark, D. Colombaroli, S. Connor, A. L. Daniau, M. Daniels, J. Dodson, E. Doughty, M. E. Edwards, W. Finsinger, D. Foster, J. Frechette, M. J. Gaillard, D. G. Gavin, E. Gobet, S. Haberle, D. J. Hallett, P. Higuera, G. Hope, S. Horn, J. Inoue, P. Kaltenrieder, L. Kennedy, Z. C. Kong, C. Larsen, C. J. Long, J. Lynch, E. A. Lynch, M. McGlone, S. Meeks, S. Mensing, G. Meyer, T. Minckley, J. Mohr, D. M. Nelson, J. New, R. Newnham, R. Noti, W. Oswald, J. Pierce, P. J. H. Richard, C. Rowe, M. F. S. Goni, B. N. Shuman, H. Takahara, J. Toney, C. Turney, D. H. Urrego-Sanchez, C. Umbanhowar, B. Vanniere, E. Vescovi, M. Walsh, X. Wang, N. Williams, J. Wilmshurst, and J. H. Zhang (2008), Changes in fire regimes since the Last Glacial Maximum: An assessment based on a global synthesis and analysis of charcoal data, *Clim. Dynam.*, *30*(7–8), 887–907, doi:10.1007/s00382-007-0334-x.

Prentice, I. C., and S. P. Harrison (2009), Ecosystem effects of CO_2 concentration: Evidence from past climates, *Clim. Past*, *5*(3), 297–307.

Prentice, I. C., S. P. Harrison, D. Jolly, and J. Guiot (1998), The climate and biomes of Europe at 6000 yr B.P: Comparison of model simulations and pollen-based reconstructions, *Quaternary Sci. Rev.*, *17*(6–7), 659–668, doi:10.1016/S0277-3791(98)00016-X.

Prentice, I. C., D. Jolly, and Biome 6000 Participants (2000), Mid-Holocene and glacial-maximum vegetation geography of the northern continents and Africa, *J. Biogeogr.*, *27*(3), 507–519.

Prentice, I. C., S. P. Harrison, and P. J. Bartlein (2011), Tropical forests, ice ages and the carbon cycle, *New Phytol.*, *189*(4), 988–998.

Quigley, M. C., T. Horton, J. C. Hellstrom, M. L. Cupper, and M. Sandiford (2010), Holocene climate change in arid Australia from

speleothem and alluvial records, *Holocene*, *20*(7), 1093–1104, doi:10.1177/0959683610369508.

Rahmstorf, S., M. Crucifix, A. Ganopolski, H. Goosse, I. V. Kamenkovich, R. Knutti, G. Lohmann, R. Marsh, L. A. Mysak, Z. Wang, and A. J. Weaver (2005), Thermohaline circulation hysteresis: A model intercomparison, *Geophys. Res. Lett.*, *32*, L23605, doi:10.1029/2005GL023655.

Raymo, M. E., and K. Nisancioglu (2003), The 41 kyr world: Milankovitch's other unsolved mystery, *Paleoceanography*, *18*(1), 1011.

Renssen, H., and J. Vandenberghe (2003), Investigation of the relationship between permafrost distribution in NW Europe and extensive winter sea-ice cover in the North Atlantic Ocean during the cold phases of the Last Glaciation, *Quaternary Sci. Rev.*, *22*(2–4), 209–223, doi:10.1016/S0277-3791(02)00190-7.

Renssen, H., V. Brovkin, T. Fichefet, and H. Goosse (2003), Holocene climate instability during the termination of the African Humid Period, *Geophys. Res. Lett.*, *30*(4), 1184.

Revel, M., E. Ducassou, F. E. Grousset, S. M. Bernasconi, S. Migeon, S. Revillon, J. Mascle, A. Murat, S. Zaragosi, and D. Bosch (2010), 100,000 years of African monsoon variability recorded in sediments of the Nile margin, *Quaternary Sci. Rev.*, *29*(11–12), 1342–1362, doi:10.1016/S0277-3791(02)00190-7.

Rial, J. A., R. A. Pielke, Sr., M. Benniston, M. Claussen, J. Canadell, P. Cox, J. Held, N. de Noblet-Ducoudré, R. Prinn, J. F. Reynolds, and J. D. Salas (2004), Nonlinearities, feedbacks and critical thresholds within the Earth's climate system, *Climatic Change*, *65*(1-2), 11–38.

Rice, M., and A. Henderson-Sellers (2011), Future climate: One vital component of trans-disciplinary Earth system science, in *The Future of the World's Climate*, edited by A. Henderson-Sellers and K. McGuffie, Elsevier, Amsterdam.

Richard, P. J. H. (1995), Le couvert végétal du Québec-Labrador il y a 6000 ans B.P: Essai, *Geogr. Phys. Quatern.*, *49*(1), 117–140.

Rimbu, N., G. Lohmann, S. J. Lorenz, J. H. Kim, and R. R. Schneider (2004), Holocene climate variability as derived from alkenone sea surface temperature and coupled ocean-atmosphere model experiments, *Clim. Dynam.*, *23*(2), 215–227, doi:10.1007/s00382-004-0435-8.

Rind, D., P. DeMenocal, G. Russell, S. Sheth, D. Collins, G. Schmidt, and J. Teller (2001), Effects of glacial meltwater in the GISS coupled atmosphere-ocean model: 1. North Atlantic deep water response, *J. Geophys. Res. D*, *106*(D21), 27335–27353, doi:10.1029/2000JD000070.

Roche, D., D. Paillard, A. Ganopolski, G. Hoffmann (2004), Oceanic oxygen-18 at the present day and LGM: Equilibrium simulations with a coupled climate model of intermediate complexity, *Earth Planet Sci Lett.*, *218*(3-4), 317–330.

Rodó, X., E. Baert, and F. A. Comín (1997), Variations in seasonal rainfall in southern Europe during the present century: Relationships with the North Atlantic Oscillation and the El Niño–Southern Oscillation, *Clim. Dynam.*, *13*(4), 275–284, doi: 10.1007/s003820050165.

Rohling, E. J., and H. Palike (2005), Centennial-scale climate cooling with a sudden cold event around 8200 years ago, *Nature*, *434*(7036), 975–979.

Ruddiman, W. F. (2006), What is the timing of orbital-scale monsoon changes?, *Quaternary Sci. Rev.*, *25*(7–8), 657–658, doi:10.1016/j.quascirev.2006.02.004.

Ruddiman, W. F. (2008), The challenge of modeling interglacial CO_2 and CH_4 trends, *Quaternary Sci. Rev.*, *27*(5–6), 445–448, doi:10.1016/j.quascirev.2007.11.007.

Saltzman, B. (2002), *Dynamical Paleoclimatology: Generalized Theory of Global Climate Change*, Academic Press, San Diego.

Sanchez Goñi, M. F., and S. P. Harrison (2010), Millennial-scale climate variability and vegetation changes during the Last Glacial: Concepts and terminology, *Quaternary Sci. Rev.*, *29*(21–22), 2823–2827, doi:10.1016/j.quascirev.2009.11.014.

Schaefer, H., M. J. Whiticar, E. J. Brook, V. V. Petrenko, D. F. Ferretti, and J. P. Severinghaus (2006), Ice record of d^{13}C for atmospheric CH_4 across the Younger Dryas-Preboreal transition, *Science*, *313*(5790), 1109–1112, doi:10.1126/science.1126562.

Schurgers, G., U. Mikolajewicz, M. Gröger, E. Maier-Reimer, M. Vizcaíno, and A. Winguth (2007), The effect of land surface changes on Eemian climate, *Clim. Dynam.*, *29*(4), 357–373.

Sen Gupta, A., and B. McNeil (2011), Variability and change in the ocean, in *The Future of the World's Climate*, edited by A. Henderson-Sellers and K. McGuffie, Elsevier, Amsterdam.

Shafer, S. L., P. J. Bartlein, and C. Whitlock (2005), Understanding the spatial heterogeneity of global environmental change in mountain regions, in *Global Change and Mountain Regions*, edited by U. Huber et al., pp. 21–30, Springer, Dordrecht.

Shakun, J. D., and A. E. Carlson (2010), A global perspective on Last Glacial Maximum to Holocene climate change, *Quaternary Sci. Rev.*, *29*(15–16), 1801–1816, doi:10.1016/j.quascirev.2010.03.016.

Shulmeister, J. (1999), Australasian evidence for mid-Holocene climate change implies precessional control of Walker Circulation in the Pacific, *Quatern. Int.*, *57–58*(1), 81–91, doi:10.1016/S1040-6182(98)00052-4.

Shuman, B., A. K. Henderson, C. Plank, I. Stefanova, and S. S. Ziegler (2009), Woodland-to-forest transition during prolonged drought in Minnesota after ca. AD 1300, *Ecology*, *90*(10), 2792–2807.

Siccha, M., G. Trommer, H. Schulz, C. Hemleben, and M. Kucera (2009), Factors controlling the distribution of planktonic foraminifera in the Red Sea and implications for the development of transfer functions, *Mar. Micropaleontol.*, *72*(1), 146–156.

Singarayer, J. S., P. J. Valdes, P. Friedlingstein, S. Nelson, and D. J. Beerling (2011), Late-Holocene methane rise caused by orbitally controlled increase in tropical sources, *Nature*, *470*(7332), 82–85.

Spahni, R., J. Chappellaz, T. F. Stocker, L. Loulergue, G. Hausammann, K. Kawamura, J. Fluckiger, J. Schwander, D. Raynaud, V. Masson-Delmotte, and J. Jouzel (2005), Atmospheric methane and nitrous oxide of the late Pleistocene from Antarctic ice cores, *Science*, *310*(5752), 1317–1321, doi:10.1126/science.1120132.

Steffensen, J. P., K. K. Andersen, M. Bigler, H. B. Clausen, D. Dahl-Jensen, H. Fischer, K. Goto-Azuma, M. Hansson, S. J. Johnsen, J. Jouzel, V. Masson-Delmotte, T. Popp, S. O. Rasmussen, R. Rothlisberger, U. Ruth, B. Stauffer, M. L. Siggaard-Andersen, A. E. Sveinbjornsdottir, A. Svensson, and J. W. C. White (2008), High-resolution Greenland Ice Core data show abrupt climate change happens in few years, *Science*, *321*(5889), 680–684, doi:10.1126/science.1157707.

Stenni, B., V. Masson-Delmotte, S. Johnsen, J. Jouzel, A. Longinelli, E. Monnin, R. Rothlisberger, and E. Selmo (2001), An oceanic cold reversal during the last deglaciation, *Science*, *293*(5537), 2074–2077, doi:10.1126/science.1059702.

Stott, L., K. Cannariato, R. Thunell, G. H. Haug, A. Koutavas, and S. Lund (2004), Decline of surface temperature and salinity in the western tropical Pacific Ocean in the Holocene Epoch, *Nature*, *431*(7004), 56–59, doi:10.1038/nature02903.

Stouffer, R. J., J. Yin, J. M. Gregory, K. W. Dixon, M. J. Spelman, W. Hurlin, A. J. Weaver, M. Eby, G. M. Flato, H. Hasumi, A. Hu, J. H. Jungclaus, I. V. Kamenkovich, A. Levermann, M. Montoya, S. Murakami, S. Nawrath, A. Oka, W. R. Peltier, D. Y. Robitaille, A. Sokolov, G. Vettoretti, and S. L. Weber (2006), Investigating the causes of the response of the thermohaline circulation to past and future climate changes, *J. Climate*, *19*(8), 1365–1387.

Sutton, R. T., B. Dong, and J. M. Gregory (2007), Land/sea warming ratio in response to climate change: IPCC AR4 model results and comparison with observations, *Geophys. Res. Lett.*, *34*, L02701, doi:10.1029/2006GL028164.

Svensson, A., K. K. Andersen, M. Bigler, H. B. Clausen, D. Dahl-Jensen, S. M. Davies, S. J. Johnsen, R. Muscheler, F. Parrenin, S. O. Rasmussen, R. Roethlisberger, I. Seierstad, J. P. Steffensen, and B. M. Vinther (2008), A 60,000 year Greenland stratigraphic ice core chronology, *Clim. Past*, *4*(1), 47–57.

Thonicke, K., I. C. Prentice, and C. Hewitt (2005), Modeling glacial-interglacial changes in global fire regimes and trace gas emissions, *Glob. Biogeochem. Cy.*, *19*(3), 1-10, doi:10.1029/2004GB002278.

Timm, O., and A. Timmermann (2007), Simulation of the last 21,000 years using accelerated transient boundary conditions, *J. Climate*, *20*(17), 4377–4401.

Tinner, W., and A. F. Lotter (2001), Central European vegetation response to abrupt climate change at 8.2 ka, *Geology*, *29*(6), 551–554.

Tudhope, A. W., C. P. Chilcott, M. T. McCulloch, E. R. Cook, J. Chappell, R. M. Ellam, D. W. Lea, J. M. Lough, and G. B. Shimmield (2001), Variability in the El Niño–Southern oscillation through a glacial-interglacial cycle, *Science*, *291*(5508), 1511–1517, doi:10.1126/science.1057969.

Valdes, P. J., D. J. Beerling, and C. E. Johnson (2005), The Ice Age methane budget, *Geophys. Res. Lett.*, *32*, L02704, doi:10.1029/2004GL021004.

van der Werf, G. R., J. T. Randerson, L. Giglio, N. Gobron, and A. J. Dolman (2008), Climate controls on the variability of fires in the

tropics and subtropics, *Glob. Biogeochem. Cy.*, *22*(3), GB3028, doi:10.1029/2007GB003122.

Voelker, A. H. L. (2002), Global distribution of centennial-scale records for Marine Isotope Stage (MIS): 3. A database, *Quaternary Sci. Rev.*, *21*(10), 1185–1212, doi:10.1016/S0277-3791(01)00139-1.

Vogelsang, E., M. Sarnthein, and U. Pflaumann (2001), *δ18O Stratigraphy, Chronology, and Sea Surface Temperatures of Atlantic Sediment Records (GLAMAPF2000 Kiel)*, Christian-Albrechts Universitat zu Kiel, Germany.

von Storch, H., and F. W. Zwiers (2001), *Statistical Analysis in Climate Research*, Cambridge University Press, Cambridge, UK.

Weldeab, S., D. W. Lea, R. R. Schneider, and N. Andersen (2007), 155,000 years of West African monsoon and ocean thermal evolution, *Science*, *316*(5829), 1303–1307, doi:10.1126/science.1140461.

Werner, M., U. Mikolajewicz, M. Heimann, and G. Hoffmann (2000), Borehole versus isotope temperatures on Greenland: Seasonality does matter, *Geophys. Res. Lett.*, *27*(5), 723–726, doi:10.1029/1999GL006075.

Williams, J., R. G. Barry, and W. M. Washington (1974), Simulation of the atmospheric circulation using the NCAR global circulation model with Ice-Age boundary conditions, *J. Appl. Meteorol.*, *13*(3), 305–317.

Williams, J. W., T. Webb, III, P. H. Richard, and P. Newby (2000), Late Quaternary biomes of Canada and the eastern United States, *J. Biogeogr.*, *27*(3), 585–607, doi:10.1046/j.1365-2699.2000.00428.x.

Williams, J. W., B. Shuman, P. J. Bartlein, N. S. Diffenbaugh, and T. Webb (2010), Rapid, time-transgressive, and variable responses to early-Holocene midcontinental drying in North America, *Geology*, *38*(2), 135–138.

Willis, K. J., and R. J. Whittaker (2000), The refugial debate, *Science*, *287*(5457), 1406–1407.

Willis, K. J., E. Rudner, and P. Sumegi (2000), The full-glacial forests of central and southeastern Europe, *Quaternary Res.*, *53*(2), 203–213, doi:10.1126/science.287.5457.1406.

Wohlfahrt, J., S. P. Harrison, and P. Braconnot (2004), Synergistic feedbacks between ocean and vegetation on mid- and high-latitude climates during the mid-Holocene, *Clim. Dynam.*, *22*(2–3), 223–238, doi:10.1007/s00382-003-0379-4.

Wolff, E. W., J. Chappellaz, T. Blunier, S. O. Rasmussen, and A. Svensson (2010), Millennial-scale variability during the last glacial: The ice core record, *Quaternary Sci. Rev.*, *29*(21–22), 2828–2838, doi:10.1016/j.quascirev.2009.10.013.

Wyrwoll, K. H., and G. H. Miller (2001), Initiation of the Australian summer monsoon 14,000 years ago, *Quatern. Int.*, *83–5*(1), 119–128.

Yu, G. E., and S. P. Harrison (1995), Holocene changes in atmospheric circulation patterns as shown by lake status changes in northern Europe, *Boreas*, *24*(3), 260–268.

Yu, Z., J. Loisel, D. P. Brosseau, D. W. Beilman, and S. J. Hunt (2010), Global peatland dynamics since the Last Glacial Maximum, *Geophys. Res. Lett.*, *37*(13), L13402, doi:10.1029/2010GL043584.

Zachos, J. C., M. Pagani, L. Sloan, E. Thomas, and K. Billups (2001), Trends, rhythms and aberrations in global climate 65 Ma to present, *Science*, *292*(5517), 686–693, doi:10.1126/science.1059412.

Zhao, Y., and S. P. Harrison (2011), Mid-Holocene monsoons: a multi-model analysis of the inter-hemispheric differences in the responses to orbital forcing and ocean feedbacks, *Climate Dynamics* (in press).

Zhuang, Q., J. M. Melillo, D. W. Kicklighter, R. G. Prinn, A. D. McGuire, P. A. Steudler, F. B. S., and S. Hu (2004), Methane fluxes between terrestrial ecosystems and the atmosphere at northern high latitudes during the past century: A retrospective analysis with a process-based biogeochemistry model, *Glob. Biogeochem. Cy.*, *18*(3), GB3010, doi:10.1029/2004GB002239.